UNIVERSITY OF ALBERTA

BIODOSIMETRIC ANALYSIS OF A MEDIUM PRESSURE UV DISINFECTION REACTOR TREATING UNFILTERED SURFACE WATER

by

BRENT LEINAN

A thesis submitted to the Faculty of Graduate Studies and Research in partial fulfillment of the requirements for the degree of MASTER OF SCIENCE

in

ENVIRONMENTAL ENGINEERING

DEPARTMENT OF CIVIL AND ENVIRONMENTAL ENGINEERING

EDMONTON, ALBERTA

SPRING, 2003

National Library of Canada
Acquisitions and Bibliographic Services
395 Wellington Street
Ottawa ON K1A 0N4
Canada

Bibliothèque nationale du Canada
Acquisitions et services bibliographiques
395, rue Wellington
Ottawa ON K1A 0N4
Canada

Your file Votre référence

Our file Notre référence

The author has granted a non-exclusive licence allowing the National Library of Canada to reproduce, loan, distribute or sell copies of this thesis in microform, paper or electronic formats.

L'auteur a accordé une licence non exclusive permettant à la Bibliothèque nationale du Canada de reproduire, prêter, distribuer ou vendre des copies de cette thèse sous la forme de microfiche/film, de reproduction sur papier ou sur format électronique.

The author retains ownership of the copyright in this thesis. Neither the thesis nor substantial extracts from it may be printed or otherwise reproduced without the author's permission.

L'auteur conserve la propriété du droit d'auteur qui protège cette thèse. Ni la thèse ni des extraits substantiels de celle-ci ne doivent être imprimés ou autrement reproduits sans son autorisation.

0-612-82302-4

Canada

UNIVERSITY OF ALBERTA

LIBRARY RELEASE FORM

NAME OF AUTHOR: BRENT LEINAN

TITLE OF THESIS: BIODOSIMETRIC ANALYSIS OF A MEDIUM PRESSURE UV DISINFECTION REACTOR TREATING UNFILTERED SURFACE WATER

DEGREE: MASTER OF SCIENCE

YEAR THIS DEGREE WAS GRANTED: 2003

Permission is hereby granted to THE UNIVERSITY OF ALBERTA LIBRARY to reproduce single copies of this thesis and to lend or sell such copies for private, scholarly or scientific research purposes only.

The author reserves all other publication and other rights in association with the copyright in the thesis, and except herein before provided, neither the thesis nor any substantial portion thereof may be printed or otherwise reproduced in any material form whatever without the author's prior written permission.

PERMANENT ADDRESS:

4611 117a St.

Edmonton AB

T6H 3R9

Dated: Jan 29/03

UNIVERSITY OF ALBERTA

FACULTY OF GRADUATE STUDIES AND RESEARCH

The undersigned certify that they have read, and recommend to the Faculty of Graduate Studies and Research for acceptance, a thesis entitled BIODOSIMETRIC ANALYSIS OF A MEDIUM PRESSURE UV DISINFECTION REACTOR TREATING UNFILTERED SURFACE WATER submitted by BRENT LEINAN in partial fulfillment of the requirements for the degree of MASTER OF SCIENCE in ENVIRONMENTAL ENGINEERING.

Daniel W. Smith

Dr. D. W. Smith – Co-Supervisor

Dr. S. A. Craik – Co-Supervisor

Dr. M. Belosevic – Co-Supervisor

Dr. Tong Yu – Committee Chair and Examiner

Dated: Jan 25, 2003

ABSTRACT

A 304 mm internal diameter, medium pressure, UV reactor was subjected to biodosimetric analysis using the non-pathogenic indicator virus MS2 coliphage and the bacterium *Bacillus subtilis*. Unaltered Lake Okanagan water was used as influent. The objectives of this study were to identify the influence of operational issues such as hydrodynamics, number of lamps in operation, turbidity, UV absorbance and the type of indicator used on microbial inactivation. Each indicator identified different aspects of reactor performance. However, MS2 was shown to be the more valuable biodosimetric indicator. Results from trials performed using MS2 indicated that reactor performance was more consistent when two or more adjacent lamps were in operation relative to running the reactor with one lamp in operation. The presence of particulate in the influent did not inhibit the inactivation of MS2 in the UV reactor, relative to influent with low levels of particulate and the same UV absorbance.

ACKNOWLEDGEMENTS

I would like to thank my supervisors Dr. Stephen A. Craik, Dr. Daniel W. Smith, and Dr. Miodrag Belosevic for their invaluable guidance and support. The technical support provided by Cezary Kucharski, Emmanual Guigard and James Stafford, greatly contributed to the successful completion of this thesis, and is appreciated.

I would also like to acknowledge the agencies that contributed equipment and funding to this project. Calgon Carbon Corporation provided the UV reactor. EPCOR Water designed the UV treatment system installed in Kelowna and assisted in funding. The City of Kelowna provided funding and technical support throughout the course of the study. Additionally, the Natural Sciences and Engineering Research Council of Canada provided partial funding of the project.

DEDICATION

To Steph

for her love and endless patience,

and my family

for their support and understanding.

TABLE OF CONTENTS

1 INTRODUCTION 1

1.1 BACKGROUND 1

1.2 OBJECTIVES 4

1.3 OUTLINE OF THESIS 4

2 BACKGROUND AND LITERATURE REVIEW 6

2.1 UV REDUCTION OF MICROBIAL CONTAMINANTS 6

2.1.1 UV Light Definitions 6

2.1.2 Mechanics of Inactivation 12

2.1.3 UV Dose-Response 14

2.2 UV REACTORS 18

2.2.1 UV Dose Distributions 20

2.2.2 Measurement of UV Dose Delivered 21

2.2.3 Water Quality Considerations 25

2.3 BIODOSIMETRY INDICATOR ORGANISMS 31

2.3.1 *Bacillus subtilis* 33

2.3.2 MS2 phage 40

3 EXPERIMENTAL MATERIALS AND METHODS 46

3.1 EXPERIMENT OVERVIEW 46

3.2 FEED WATER QUALITY 47

3.2.1 Test Site Description and Characterization 47

3.2.2 Feed Water Quality Analysis 48

3.3 DESCRIPTION OF THE UV REACTOR 50

3.4 UV TREATMENT SYSTEM LAYOUT 52

3.5 COLLIMATED BEAM APPARATUS 54

3.6 COLLIMATED BEAM EXPERIMENTS 54

3.6.1 UV Exposure with a Collimated Beam Apparatus 54

3.6.2 UV Irradiance Measurements 54

3.7 FLOW THROUGH UV REACTOR TESTING 56

3.7.1 Preparation of the UV Reactor for Testing 56
3.7.2 Introducing Indicator Organisms into the Influent Stream 56
3.7.3 Sampling 57
3.7.4 Sample Handling and Analysis 57

3.8 MANIPULATION OF INFLUENT TURBIDITY AND UV ABSORBANCE 59
3.8.1 Overview 59
3.8.2 Gravimetric Analysis 61
3.8.3 Grain Size Distribution Analysis 61

3.9 *BACILLUS SUBTILIS* METHODS 62
3.9.1 Spore Production 62
3.9.2 Enumeration 63

3.10 MS2 PHAGE METHODS 63
3.10.1 Coliphage Production 63
3.10.2 *Escherichia Coli* Production 64
3.10.3 Coliphage Enumeration 65

3.11 CALCULATIONS 65
3.11.1 Average UV Dose 65
3.11.2 Microorganism Inactivation 66
3.11.3 Dose-Inactivation Model Parameter Estimation 67
3.11.4 Confidence Intervals for Linear Models 67

3.12 INTERPRETATION OF BIODOSIMETRY RESULTS 68
3.12.1 Mean Residence Time per Lamp 68
3.12.2 Reduction Equivalent Dose 69
3.12.3 Reduction Equivalent Fluence Rate 69
3.12.4 Understanding the Response of UV Reactors 69

4 ANALYSIS OF UV REACTOR PERFORMANCE AT VARIOUS OPERATING CONDITIONS 73

4.1 INTRODUCTION 73

4.2 EXPERIMENTAL DESIGN 74

4.3 FEED WATER QUALITY RESULTS 75

4.4 UV DOSE-INACTIVATION RELATIONSHIPS 76

4.5 INACTIVATION OF MS2 PHAGE IN THE UV REACTOR 81

4.6 INACTIVATION OF *BACILLUS SUBTILIS* SPORES IN THE UV REACTOR 88

4.7 INACTIVATION IN POWER-OFF PROCESS CONTROLS AND TRIP CONTROLS 96

4.8 COMPARISON OF INDICATOR ORGANISMS 98

4.9 SUMMARY OF UV REACTOR EXPERIMENTS 99

5 INFLUENCE OF TURBIDITY AND UV ABSORBANCE ON MS2 PHAGE INACTIVATION 102

5.1 INTRODUCTION 102

5.2 EXPERIMENTAL DESIGN 103

5.3 FEED WATER QUALITY RESULTS 104

5.4 UV DOSE-INACTIVATION RELATIONSHIPS 105

5.5 COMPOSITION OF TURBIDITY AND UV ABSORBING SUBSTANCES 107

5.5.1 Turbidity-UV Transmittance Relationship 112

5.6 INFLUENCE OF TURBIDITY AND UV ABSORBANCE ON MS2 PHAGE INACTIVATION 114

5.7 INACTIVATION IN POWER-OFF PROCESS CONTROLS AND TRIP CONTROLS 122

5.8 SUMMARY OF EXPERIMENTS ADDING TURBIDITY AND UV ABSORBANCE TO FEED WATER 124

6 CONCLUSIONS 127

7 RECOMMENDATIONS 130

8 REFERENCES 132

APPENDIX A: INFORMATION RELATED TO COLLIMATED BEAM UV DOSE-INACTIVATION EXPERIMENTS 144

APPENDIX B: INFORMATION RELATED TO UV REACTOR TRIALS PERFORMED USING MS2 PHAGE (CHAPTER 4 DATA) 156

APPENDIX C: INFORMATION RELATING TO UV REACTOR TRIALS PERFORMED USING *B. SUBTILIS* (CHAPTER 4 DATA) 161

APPENDIX D: INFORMATION FROM UV REACTOR TRIALS INVOLVING MANIPULATED TURBIDITY AND UV ABSORBANCE LEVELS (CHAPTER 5 DATA) 166

APPENDIX E: WATER QUALITY ANALYSIS RESULTS FOR UV REACTOR TRIALS 171

APPENDIX F: DETAILED SCHEMATIC OF UV TREATMENT SYSTEM 179

LIST OF FIGURES

Figure 2-1: Reflection of light.....10

Figure 2-2: Refraction of light. 11

Figure 2-3: UV absorption spectrum of DNA in an aqueous solution.....14

Figure 2-4: Typical collimated beam apparatus setup used in the determination of UV dose-inactivation relationships.....15

Figure 2-5: Common UV dose-inactivation relationships 17

Figure 2-6: Relative emission spectrums for low pressure and medium pressure UV lamps over the 200 nm to 300 nm range. 19

Figure 2-7: Graphical description showing how RED is determined from the UV dose-inactivation relationship and the measured inactivation of an organism due to passage through a UV reactor. 25

Figure 2-8: Life cycle of *B. subtilis*, from vegetative bacteria to free endospore. 34

Figure 3-1: Photograph of an uninstalled, 304 mm internal diameter, Sentinel™ medium pressure UV reactor.....51

Figure 3-2: Two photographs displaying the inside of the Sentinel™ medium pressure UV reactor, with clear views of the lamp and baffle configuration 51

Figure 3-3: Simplified drawing of the treatment system used in biodosimetric analysis of a Sentinel™ UV reactor treating unfiltered surface water. 53

Figure 3-4: Photograph of the system used to hold and mix lake bottom sediment suspensions and tea suspensions that were injected into the influent in phase 3. 60

Figure 3-5: Graphical depiction of UV dose distributions for two reactors. 71

Figure 4-1: UV dose-inactivation relationship of MS2 phage suspended in unaltered lake water and exposed to UV radiation in a collimated beam apparatus (phases 1 and 2). 77

Figure 4-2: UV dose-inactivation relationship of *B. subtilis* spores suspended in unaltered lake water and exposed to UV radiation in a collimated beam apparatus (phases 1 and 2). 80

Figure 4-3: Log inactivation (a), reduction equivalent dose (b), and reduction equivalent fluence rate (c) of MS2 phage as a function of flow rate, calculated from challenge tests performed on the Sentinel™ UV reactor treating unaltered lake water (phase 1). 83

Figure 4-4: Log inactivation (a), reduction equivalent dose (b), and reduction equivalent fluence rate (c) for MS2 phage as a function of flow rate, calculated from challenge tests performed on the Sentinel™ UV reactor treating unaltered lake water (phase 2). 84

Figure 4-5: Log inactivation (a), reduction equivalent dose (b), and reduction equivalent fluence rate (c) for *B. subtilis* spores as a function of flow rate, calculated from challenge tests performed on the Sentinel™ UV reactor treating unaltered lake water (phase 1). Arrows indicate effluent plate counts were beyond quantitation. 89

Figure 4-6: Log inactivation (a), reduction equivalent dose (b), and reduction equivalent fluence rate (c) for *B. subtilis* spores as a function of flow rate, calculated from challenge tests performed on the Sentinel™ UV reactor treating unaltered lake water (phase 2). Arrows indicate effluent plate counts were beyond quantitation. 90

Figure 5-1: UV dose-inactivation relationship for MS2 phage suspended in unaltered lake water and exposed to UV radiation in a collimated beam apparatus (phase 3). 106

Figure 5-2: Grain size distribution of lake bottom sediment used to increase influent turbidity levels in phase 3. 109

Figure 5-3: UV absorbance of tea and lake sediment suspensions added to the feed water in phase 3, relative to unaltered lake water. 111

Figure 5-4: UV absorbance normalized to 254 nm, for unaltered lake water, 84% UVT water prepared by the addition of tea to unaltered lake water, and 5 NTU water prepared by the addition of lake bottom sediment to unaltered lake water. 112

Figure 5-5: Turbidity as a function of UVT, calculated from challenge tests performed on the Sentinel™ UV reactor treating unaltered lake water, lake water with absorbance added, lake water with turbidity added, or lake water with absorbance and turbidity added simultaneously. The linear regression model carried out on data from trials performed using unaltered lake water and trials in which turbidity was added, is plotted alongside the data (phase 3). .113

Figure 5-6: Log inactivation of MS2 phage as a function of UVT, calculated from challenge tests performed on the Sentinel™ UV reactor treating unaltered lake water, lake water with absorbance added, lake water with turbidity added, or lake water with absorbance and turbidity added simultaneously. The linear regression model (equation 25) and its associated 95 percent confidence interval are plotted alongside the data (phase 3). 116

Figure A- 1: UV dose-inactivation relationship determined in collimated beam experiments for MS2 phage showing individual trial data points (phase 1). 145

Figure A- 2: UV dose-inactivation relationship determined in collimated beam experiments for MS2 phage showing individual trial data points (phase 2). 146

Figure A- 3: UV dose-inactivation relationship determined in collimated beam experiments for MS2 phage showing individual trial data points (phase 3). 147

Figure A- 4: UV dose-inactivation relationship determined in collimated beam experiments for *B. subtilis* showing individual trial data points and tailing (phase 1). 148

Figure A- 5: UV dose-inactivation relationship determined in collimated beam experiments for *B. subtilis* showing individual trial data points and tailing (phase 2). 149

Figure F- 1: Detailed drawing of the UV treatment system installed in the City of Kelowna. 180

LIST OF TABLES

Table 2-1: Summary of *B. subtilis* UV dose-inactivation relationships reported in literature, detailing the growth media, exposure device and water matrix used in experimentation. 40

Table 2-2: Summary of MS2 phage UV dose-inactivation experiments in literature, detailing the growth media, exposure device and water matrix used in experimentation. 45

Table 3-1: Summary of the testing plan and operational conditions examined in phases 1, 2, and 3. 47

Table 3-2: Summary of the physical characteristics of Lake Okanagan and the surrounding catchment basin. 48

Table 3-3: Summary of the frequency and methodologies used in testing the influent water quality for all phases of the study. 49

Table 4-1: Operating conditions examined in challenge tests performed on the Sentinel ™ UV reactor treating unfiltered lake water (phases 1 and 2). 74

Table 4-2: Summary of water quality testing of unaltered lake water used as feed water in challenge tests performed on the Sentinel™ UV reactor (phases 1 and 2). 76

Table 4-3: Summary of UV dose-inactivation relationships for MS2 phage suspended in unaltered lake water and exposed to UV radiation in a collimated beam apparatus (phases 1 and 2), accompanied by the dose ranges reported in literature. 78

Table 4-4: Summary of UV dose-inactivation relationships for *B. subtilis* spores suspended in unaltered lake water and exposed to UV radiation in a collimated beam apparatus (phases 1 and 2), accompanied by the dose ranges reported in literature. 80

Table 5-1: Operating conditions examined in challenge tests performed on the Sentinel™ UV reactor in phase 3.....104

Table 5-2: Turbidity and UV absorbance targets for feed water used in challenge tests performed on the Sentinel™ UV reactor in phase 3.....104

Table 5-3: Summary of water quality testing of unaltered lake water used as feed water in challenge tests performed on the Sentinel™ UV reactor in phase 3.....105

Table 5-4: Summary of UV dose-inactivation relationship of MS2 phage suspended in unaltered lake water and exposed to UV radiation in a collimated beam apparatus (phase 3), accompanied by the dose ranges reported in literature.....106

Table 5-5: Summary of the gravimetric analysis performed on the diluted lake bottom sediment suspension injected into the feed water in phase 3.....108

Table A-1: Inactivation of MS2 phage suspended in unaltered Lake Okanagan water and exposed to UV radiation in a collimated beam apparatus (phase 1). 150

Table A- 2: Inactivation of MS2 phage suspended in unaltered Lake Okanagan water and exposed to UV radiation in a collimated beam apparatus (phase 2). 151

Table A- 3: Inactivation of MS2 phage suspended in unaltered Lake Okanagan water and exposed to UV radiation in a collimated beam apparatus (phase 3). 152

Table A- 4: Inactivation of *B. subtilis* spores suspended in unaltered Lake Okanagan water and exposed to UV radiation in a collimated beam apparatus (phase 1). 153

Table A- 5: Inactivation of *B. subtilis* spores suspended in unaltered Lake Okanagan water and exposed to UV radiation in a collimated beam apparatus (phase 2). 154

Table A- 6: Summary of linear regression models performed on data from collimated beam experiments. 155

Table B- 1: Summary of trials examining number of lamps in operation and flow rate using MS2 phage (phase 1). 157

Table B- 2: Summary of trials examining number of lamps in operation and flow rate using MS2 phage (phase 2). 158

Table B- 3: Summary of inactivation data and associated error for trials using MS2 phage (phase 1). 159

Table B- 4: Summary of inactivation data and associated error for trials using MS2 phage (phase 2). 160

Table C- 1: Summary of trials examining the effects of flow rate and number of lamps in operation using *B. subtilis* spores (phase 1). 162

Table C- 2: Summary of trials examining the effects of flow rate and number of lamps in operation using *B. subtilis* spores (phase 2). 163

Table C- 3: Summary of inactivation data and associated error for trials using *B. subtilis* spores (phase 1). 164

Table C- 4: Summary of inactivation data and associated error for trials using *B. subtilis* spores (phase 2). 165

Table D- 1: Summary of grain size distribution analysis performed on lake bottom sediment added to feed water to increase influent turbidity levels in phase 3. 167

Table D- 2: Summary of MS2 phage trials examining the influence of turbidity and UVT on log inactivation measured in challenge tests performed on the Sentinel™ UV reactor (phase 3). 168

Table D- 3: Summary of inactivation data and associated error for MS2 phage trials examining the influence of turbidity on UV reactor performance (phase 3). 170

Table E- 1: Detailed summary of water quality analysis (phase 1). 172

Table E- 2: Detailed summary of water quality analysis (phase 2). 174

Table E- 3: Detailed summary of water quality analysis (phase 3). 176

LIST OF ABBREVIATIONS AND NOMENCLATURE

Abbreviations

ATCC	American Type Culture Collection
CFD	Computational Fluid Dynamics
CFU	Colony Forming Unit
CI	Confidence Interval
DNA	Deoxyribonucleic Acid
HRT	Hydraulic Residence Time
IESWTR	Interim Enhanced Surface Water Treatment Rule
LT2ESWTR	Long Term 2 Enhanced Surface Water Treatment Rule
MCL	Maximum Contaminant Level
MPSS	Multiple Point Source Summation
PFU	Plaque Forming Unit
RED	Reduction Equivalent Dose (mJ/cm^2)
REFR	Reduction Equivalent Fluence Rate (mW/cm^2)
RMS	Root Mean Square
RNA	Ribonucleic Acid
SE	Standard Error
SWTR	Surface Water Treatment Rule
UV	Ultraviolet
UVT	Ultraviolet Transmittance

Abbreviations (Continued)

$UVT_{254\ nm,\ 10\ mm}$	Ultraviolet transmittance measured at 254 nm over a 10 mm path length (%UVT/ 10 mm)

Symbols Used

A_λ	Absorbance at wavelength λ (abs/cm)
c	Speed of light (2.9979×10^8 m/s)
c_i	Molar concentration of an absorbing substance at wavelength λ
D_G	Germicidal UV dose (mW/cm^2)
E	Irradiance (W/m^2)
E'	Depth averaged irradiance
E_G	Germicidal irradiance (mW/cm^2)
E_0	Incident irradiance at the water surface
E_λ	Irradiance at wavelength λ (W/m^2)
h	Planck's constant (6.6261×10^{-34} J-s)
I_C	Inactivation of the challenge organism
I_P	Inactivation of the pathogenic organism
k_C	First order inactivation coefficient for the challenge organism
k_P	First order inactivation coefficient for the pathogenic organism
Ms	Radiant emittance (W/m^2)
N	Number of viable microorganisms after UV exposure
n	Number of measurements
N_O	Number of viable microorganisms before UV exposure
p	Probability of a type I error in a hypothesis test
P_ϕ	Radiant power (W)

Symbols Used (Continued)

Q	Flow rate (L/min or USgpm)
Qe	Radiant energy (J)
R	Reflection of light due to interaction with an interface
$r_{\perp}$	Magnitude of light reflected perpendicular to an interface
$r_{\parallel}$	Magnitude of light reflected parallel to an interface
r^2	Coefficient of determination
$RED_{Normalized}$	Normalized reduction equivalent dose (mJ/cm^2/lamp)
s	Standard deviation
T	Turbidity (ntu)
t	Exposure time (s)
$t_{(v,\alpha/2)}$	Value of the Student t-distribution
u	Energy of one photon (J)
V	Volume (L)
$V_{Total\ Reactor}$	Volume of the entire UV reactor (L)
X_0	Value of the independent variable where the dependent variable is predicted for a linear regression model
$\overline{X}$	Average independent variable for all observations included in the linear regression model
$\hat{Y}_0$	Predicted value for the dependant variable using a linear regression model

Greek Symbols Used

α	Acceptable probability level for hypothesis testing
β_0	y-intercept parameter in a regression model
β_1	Parameter for the first variable in a regression model
λ	Wavelength
$\varepsilon_{\lambda i}$	Molar absorption coefficient at wavelength λ
ν	Degrees of freedom
θ_1	Incident angle onto the reflecting surface
θ_1'	Incident angle onto the refracting surface
θ_2'	Exit angle from the refracting surface

Units

°C	degrees Celsius
g	grams
J	joules
kPa	kilopascals
L/min	litres per minute
m	metres
min	minutes
mg/L	milligrams per litre
mL	millilitres
mm	millimetres
mJ/cm^2	millijoule per square centimetre
mJ/cm^2/lamp	millijoule per square centimetre per lamp operating
m/s	meters per second
M	molar
nm	nanometres
ntu	nephelometric turbidity unit
µg/L	micrograms per litre
µL	microlitres
µm	micrometres
s	seconds

Units(Continued)

mW/cm^2	milliwatt per square centimetre
Pt-Co units	platinum-cobalt units
USgpm	US gallons per minute

1 INTRODUCTION

1.1 BACKGROUND

The advent of filtration and disinfection of drinking water was one of the most significant acts in protection of public health in the twentieth century. The introduction of these processes reduced the threat of deadly waterborne disease outbreaks such as cholera and typhoid. The most widespread and effective water treatment approaches in use today, include chlorination of water.

Although chlorination of potable water supplies greatly reduces the risk of most waterborne disease outbreaks, not all pathogens are rendered harmless and there are some undesirable side effects associated with the process. The most notable problem with chlorine treatment is the reaction of chlorine with organic compounds in the water which produces toxic byproducts, such as chloroform and trihalomethanes. Many of these disinfection by-products have been shown to be, or are suspected carcinogens. Further, pathogens such as *Cryptosporidium parvum* and *Giardia lamblia* have demonstrated a high tolerance to chlorination.

For the reasons outlined above, there is a push in the water treatment industry to develop new methods of disinfection that replace the imperfect practice of chlorination, such as UV technology. UV technology was first developed in 1910, with the advent of the mercury vapor lamp (Malley et al. 1995). It has been used extensively in the microbial reduction of wastewaters, primarily for the deactivation of fecal coliforms. Past studies which attempted microbial reduction of water using low UV doses indicated that it was not a reliable method of disinfecting drinking water supplies because such high UV

doses were thought to be required to deactivate protozoan parasites like *G. lamblia* and *C. parvum* (Rice and Hoff 1981; Ransome et al. 1993). However, recent developments have shown UV irradiation has excellent potential for deactivation of protozoan parasites, which are of concern to potable water production (Clancy et al. 1998; Bukhari et al. 1999; Craik et al. 2000; Craik et al. 2001).

Typical UV doses used for drinking water treatment are around 40 mJ/cm^2, which is approximately one order of magnitude lower than what is required for photo-oxidation byproduct formation. Emissions below 200 nm have the potential to convert nitrate into nitrite, but this is prevented by the use of quartz materials around the lamp, which absorbs wavelengths in that range (von Sonntag and Schuchmann 1992). There are several factors that influence the UV dose delivered to the water. UV dose delivered to a target is a function of exposure time and UV fluence rate. Fluence rate received by microorganisms suspended in water is primarily influenced by the UV absorbance and turbidity of the water. Lamp wattage and spectral power of the lamp also influence fluence rate.

Throughout the world, UV microbial reduction methods are becoming more accepted as a valuable water treatment process. For example, in 1997 Germany and Austria developed a common standard for UV microbial reduction of drinking water. Additionally, a common standard for all of Europe is currently being developed by the European Committee for Standardization (Kolch 1999). Common traits of the standards include: biodosimetric validation; definition of sensor performance and construction; calibration methodologies for UV sensors and collimated beam devices; and definition of water quality with respect to its ability to be disinfected using UV. The US

Environmental Protection Agency is currently developing a guideline addressing the use of UV radiation for microbial reduction of drinking water (Kolch 1999).

Relevant legislation includes the Surface Water Treatment Rule (SWTR) introduced in 1989, the Interim Enhanced Surface Water Treatment Rule (IESWTR) of 1998, and the Long Term 2 Enhanced Surface Water Treatment Rule (LT2ESWTR) scheduled to take effect in 2003. The SWTR requires 3 log reduction of *Giardia* spp. cysts and 4 log reduction of viruses from surface water supplies. The IESWTR recommends a maximum contaminant level goal of zero *Cryptosporidium* spp. in drinking water. The IESWTR requires the use of certain treatment techniques for plants of particular sizes and types. For example, the IESWTR requires 2 log removal by conventional or direct filtration for plants serving more than 10,000 people and use water under the direct influence of surface water supplies. The LT2ESWTR is expected to set removal goals for *Cryptosporidium* spp. based on source water concentrations, using UV radiation and other disinfectants. The LT2ESWTR will likely require pre-filtration before using UV light for microbial reduction of drinking water. However, there may be exceptions where filtration is not required.

It is the role of the scientific community to scrutinize the accepted limits of technology such as UV reactors intended for use in microbial reduction of drinking water. Only by testing these limits can they be verified or potentially expanded. Currently there are few studies addressing the use of UV reactors to treat unfiltered surface water for the production of drinking water. This thesis is a case study intended to provide insight into the performance of a commercially available UV reactor design used in treating an unfiltered water for the production of potable water. It is a research study and should not

be interpreted as a recommendation for future water treatment facilities in the City of Kelowna or any other community.

1.2 OBJECTIVES

1. The primary objective of this study was to analyze the performance of a model R-110 Sentinel™ 304 mm internal diameter medium pressure UV reactor, with respect to microbial reduction, in treating unfiltered lake water. The key factor setting this study apart from existing studies is that unfiltered water was used as feed water instead of filtered water. This is important, because the upcoming LTSWTR2 may require filtration before UV treatment of drinking water. To investigate the performance of the reactor, the effects of indicator organism type, hydrodynamics, number of lamps operating, and feed water quality on the reduction equivalent dose (RED) were determined.
2. Another fundamental objective of this study was to investigate the effect of influent turbidity and influent UV absorbance on microbe inactivation and the associated RED. The focus of this experimentation was to develop some basic operational guidelines for the unit, with respect to influent quality.
3. The final objective of this study was to identify the strengths and weaknesses of using MS2 phage and *B. subtilis* as biodosimetric indicators for testing the performance of a UV reactor treating unfiltered surface water.

1.3 OUTLINE OF THESIS

This thesis was organized according to traditional format. The document is divided into six chapters. The literature review (Chapter 2) examines UV radiation, its

mechanisms for inactivating microorganisms, biodosimetry and the characteristics of two biodosimetric indicators. The indicators analyzed were MS2 phage and *Bacillus subtilis*. MS2 phage is a virus that infects and reproduces in *Escherichia coli*, while *B. subtilis* is a spore forming bacterium. Experimental materials and methods are detailed in Chapter 3. The results and discussion are broken up into two sections (Chapters 4 and 5). Chapter 4 examines the influence of flow rate, number of lamps in operation and the type of biodosimetric organism used on the determination of reduction equivalent dose (RED) and overall microorganism inactivation due to passage through the reactor. Chapter 5 examines the influence of variations in feed water UV absorbance and turbidity on microorganism inactivation within the reactor. The conclusions of the study are outlined in Chapter 6, while recommendations are presented in Chapter 7. Appendices contain additional information on collimated beam trials (Appendix A), MS2 phage inactivation in the UV reactor (Appendix B), *B. subtilis* inactivation in the UV reactor (Appendix C), and the influence of UV absorbance and turbidity on MS2 phage inactivation in the UV reactor (Appendix D). Water quality test results on reactor feed water (Appendix E), and a detailed drawing of the UV treatment system installed in the City of Kelowna (Appendix F) were also included.

2 BACKGROUND AND LITERATURE REVIEW

2.1 UV REDUCTION OF MICROBIAL CONTAMINANTS

2.1.1 UV Light Definitions

This section summarizes the nature and behavior of UV radiation as described by Bolton (1999; 2000). Only a small portion of electromagnetic radiation is visible to the human eye. Photochemical reactions can be driven by light wavelengths ranging from 100 to 1000 nanometers (nm). Within this range lies UV (100 to 400 nm) and the visible light spectrum (400 to 700 nm). One of the most recognizable examples of a photochemical reaction is photosynthesis.

The energy carried by light is described by Planck's Law of Radiation:

$$u = \frac{hc}{\lambda} \qquad (1)$$

where u is the energy of one photon (J), h is Planck's constant (6.6261×10^{-34} J-s), c is the speed of light (2.9979×10^{8} m/s) and λ is wavelength (m). The energy of a photon increases as its wavelength decreases. For this reason, UV light is the most studied spectrum for the investigation of photochemical reactions.

UV light can be classified into 4 ranges based on its effect on human skin: UVA (315 to 400 nm), UVB (280 to 315 nm), UVC (200 to 280 nm) and vacuum UV (100 to 200 nm) (Bolton 1999). UVA light is the least harmful of the four UV ranges and is

responsible for what is commonly known as sun tanning. UVB light causes sun burns and has been shown to have carcinogenic properties (Bolton 1999). UVC is the most dangerous range because it is not completely absorbed by the atmosphere and absorbs to RNA, DNA and proteins, which can result in cell mutations and death. Vacuum UV is readily absorbed by air, water and most other substances and therefore can only be transmitted in a vacuum (Bolton 1999). UV radiation is good for microbial reduction of water because UV photons have a high energy state, which promotes the occurrence of photochemical reactions in the nucleic acids of microorganisms. Also important is UV's ability to propagate through media such as air and water, both of which exist in typical UV reactors.

It is useful to define some basic parameters of light emission, reception and measurement before examining the propagation of UV radiation. The radiant power of a source can be calculated by dividing the total radiant energy emitted in all directions from a source with respect to time:

$$P_{\Phi} = \frac{dQ_e}{dt} \qquad (2)$$

where P_{Φ} is radiant power (W), Q_e is radiant energy (J), and t is time (s). The radiant emittance (M_S) is the radiant power emitted from an infinitesimal area (dA) on the surface of a source and is determined as follows:

$$M_S = \frac{P_{\Phi}}{dA} \qquad (3)$$

Fluence rate is the radiant power passing through a sphere of cross-section dA in all directions, divided by dA. The irradiance is a special case of fluence rate, where light energy is only passed through the target from one direction, and is an essential parameter in UV biodosimetry. It is defined as the total radiant power of each wavelength incident to an element of surface area dS, divided by dS. The irradiance at a distance r (m), from a point source is calculated as:

$$E = \frac{P_{\Phi}}{4\pi r^2} \qquad (4)$$

where E is the irradiance (W/m^2). Irradiance and fluence rate are commonly confused. In simple terms, fluence rate accounts for radiation incident on a particle from all directions, whereas irradiance only considers incident radiation from one direction.

Propagation through, and interfaces between different media cause filtering and redirection of electromagnetic radiation, which in turn influences the spatial irradiance patterns in a UV reactor. Critical considerations when using UV for microbial reduction include absorption by the water, scattering by particles, refraction and reflection at media interfaces. Light in a UV reactor travels from the lamp, through the quartz sheath, through the water, where it is intercepted by particulate matter, UV absorbing compounds, and microbes, and then is absorbed and reflected off the reactor walls.

UV transmittance (UVT) of unfiltered water is a measure of the energy loss and redirection of UV light passed though a solution due to absorption, reflection, refraction

and scatter (Bolton 1999). Absorbed light is transformed into other forms of energy, which is the basis of photochemical reactions. Absorption is dependent on the wavelength of light. Further, transmittance and absorption are only meaningful when accompanied by the path length over which the measurement was taken. Absorbance, transmittance and their relationship with each other follow the Beer-Lambert Law:

$$A_\lambda = \sum_i \varepsilon_{\lambda i}\, c_i\, l = \log\left(\frac{E_{\lambda(O)}}{E_{\lambda(t)}}\right) = -\log UV T_\lambda \qquad (5)$$

where $\varepsilon_{\lambda i}$ is the molar absorption coefficient at wavelength λ (1/M-cm), c_i is the molar concentration of the absorbing substance at wavelength λ (M) and l is path length. $E_{\lambda(O)}$ and $E_{\lambda(t)}$ are the incident spectral irradiance, and the spectral irradiance of transmitted radiation at wavelength λ, respectively. A_λ is absorbance (unitless) and UVT_λ is UV transmittance (unitless) at wavelength λ.

Reflection is the deflection of light due to interaction with an interface (Figure 2-1). At an interface, a portion of the light will be deflected back into the same medium and the remainder passes through the interface into the new medium. Reflection is governed by Fresnel's Law:

$$R = \frac{1}{2}\left(r_{||}^{\,2} + r_{\perp}^{\,2}\right) \qquad (6)$$

$$r_{||} = \frac{n_2 \cos\theta_1' - n_1 \cos\theta_2'}{n_1 \cos\theta_2' + n_2 \cos\theta_1'} \qquad (7)$$

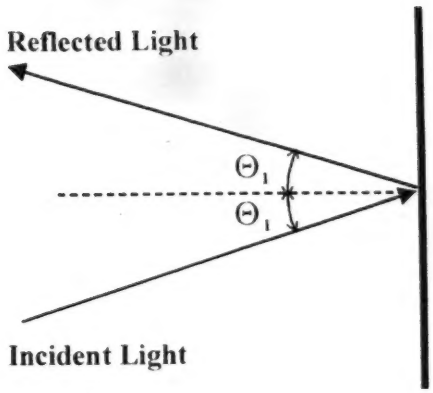

Figure 2-1: Reflection of light.

$$r_{\perp} = \frac{n_1 \cos\theta_1' - n_2 \cos\theta_2'}{n_1 \cos\theta_1' + n_2 \cos\theta_2'} \qquad (8)$$

where $r_{||}$ is the magnitude of light reflected parallel to the interface and $r_{\perp}$ is the magnitude of light reflected perpendicular to the interface. The parameters n_1 and n_2 are the index of refraction of the first and second media, respectively. The incident angle onto the interface is defined as θ_1', while the exit angle from the interface is θ_2'.

Refraction occurs when the direction of light changes upon passing through an interface between mediums (Figure 2-2). Refraction follows Snell's Law:

$$n_1 \sin\theta_1' = n_2 \sin\theta_2', \qquad (9)$$

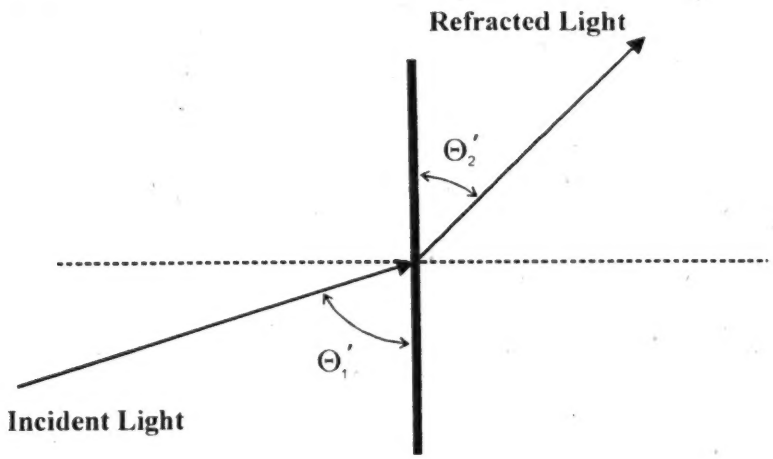

Figure 2-2: Refraction of light.

Scattering is the interaction of light with particles, causing direction, phase or wavelength changes in the light. The two main types to consider are Rayleigh and Mie scattering. Rayleigh scattering is due to particles smaller than the radiation wavelength and is dependant on the incident light's wavelength with respect to the size of the intercepting particle (Reese 2000). This type of scattering is of increasing significance as wavelength decreases. The relative intensity of light scattered in any direction is proportional to the inverse of the fourth power of the incident light wavelength, resulting in short wavelengths being scattered more efficiently than longer wavelengths (Reese 2000). With particles slightly smaller than the light wavelength, more forward scattering occurs. Mie scattering is due to interaction with particles larger or near the wavelength of the incident light. As the particle size increases, scattering effects approach that of diffuse reflection. Longer wavelengths are scattered more efficiently than shorter ones with Mie scattering, which is the opposite of Rayleigh scattering (Reese 2000). Mie scattering

increases the influence of backscattering. In drinking water treatment, Mie scatter would tend be the more important of the two scattering types, as a substantial percentage of the particulate in the water is larger than UV radiation wavelengths. Treating unfiltered water would tend to increase the amount of large suspended matter relative to filtered water, which would increase the importance of mie scattering.

It is possible to manipulate light emissions from a source to produce a single collimated beam of light. Collimated light is a light beam where all light travels in a parallel path. This can be done by placing the source in the focal point of a parabolic or spherical reflector, or the focal point of a lens. It is also possible to collimate light by passing it through a long collimating tube with a non-reflective coating, which often contains baffles to intercept light not parallel with the axis of the tube. Collimated light is required for accurately determining UV dose-inactivation relationships for microorganisms.

2.1.2 Mechanics of Inactivation

All living cells contain either deoxyribonucleic acid (DNA), ribonucleic acid (RNA), or both. DNA is comprised of two nucleotide chains which further contain nucleotide bases of the two purines, adenine and guanine, pairing with the two pyrimidines, thymine and cytosine, respectively. These sequences of nucleotide bases in a DNA chain form the genetic makeup of an organism. The genetic makeup of an organism is responsible for encoding the products required for development, reproduction, and other metabolic processes. Bacteria and protozoa contain double stranded DNA as well as RNA, while viruses and bacteriophage can contain either DNA, or single or double

stranded RNA. The main structural distinction between DNA and RNA is that in RNA, thymine is substituted with uracil.

Common disinfection chemicals like chlorine and ozone inactivate microorganisms by oxidiation of cellular material (Haas 1999). UV microbial reduction relies on an entirely different mechanism. The UV light is absorbed by cell nucleic acid, which is believed to cause dimerization of adjacent pyrimidine nucleobases (von Sonntag and Schuchmann 1992). Both purine and pyrimidine bases undergo significant UV absorption, but the rate of damage is much larger in pyrimidines. In DNA, thymine-thymine dimer formation dominates, because thymine has higher absorbance than cytosine in the germicidal range (Harm 1980). The formation of both uracil-uracil and cytosine-cytosine dimers are common in RNA. Dimer formation prevents DNA and RNA replication. Without replication, the microorganism cannot reproduce and therefore cannot infect.

The amount of UV light absorbed by DNA is a function of wavelength (Figure 2-3). Nucleotides absorb light between 200 and 310 nm, with a maximum at about 260 nm and a local minimum at approximately 230 nm (Jagger 1967). Maximum microbiocidal effect occurs close to DNA's absorption maximum (Gates 1930).

Some organisms have natural defenses against mutations in their nucleic acid. Photoreactivation is an enzyme based repair mechanism that allows microorganisms to mend minor damage to DNA. When the damaged organism is exposed to light between 310 and 490 nm, the enzyme DNA photolyase becomes activated and cleaves the dimers from the DNA. RNA viruses cannot photorepair in a host cell (Rauth 1965). Light-independent repair mechanisms are also enzyme based. The presence of DNA repair

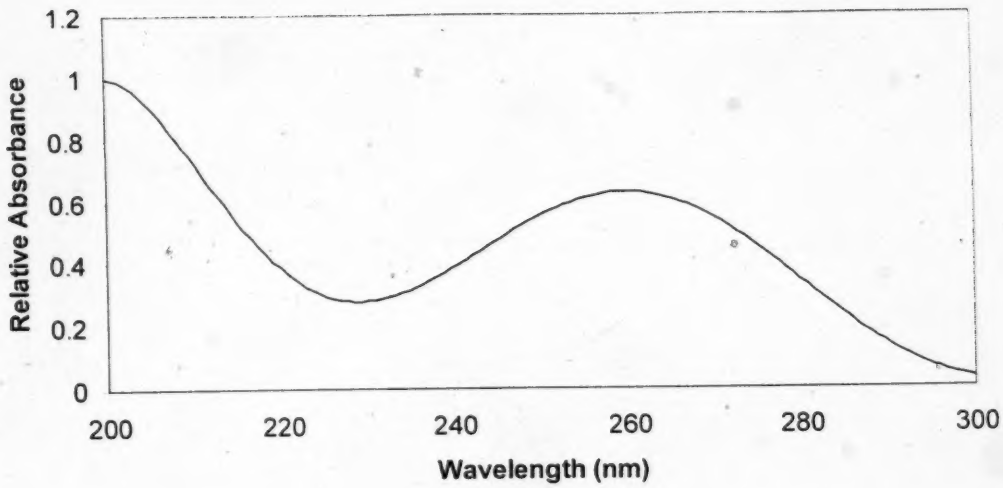

Figure 2-3: UV absorption spectrum of DNA in an aqueous solution.

(adapted from von Sonntag and Schuchmann 1992)

mechanisms increase the minimum UV dose required to achieve a given level of microbial inactivation. The goal of microbial reduction using UV light is to damage the organism to a degree that DNA repair will not occur. High UV doses can directly cause cell death, but lower doses are adequate because replication is prevented.

2.1.3 UV Dose-Response

Dose-inactivation relationships are determined in laboratory batch experiments. Use of a collimated beam apparatus provides the simplest and most accurate means of applying a predetermined UV dose (Figure 2-4). A low or medium pressure UV lamp is mounted horizontal to the sample being irradiated. A long collimating tube, often containing internal baffles is used to ensure that the light path is perpendicular to the sample surface. Some setups use a lens or reflector to improve the collimation of UV

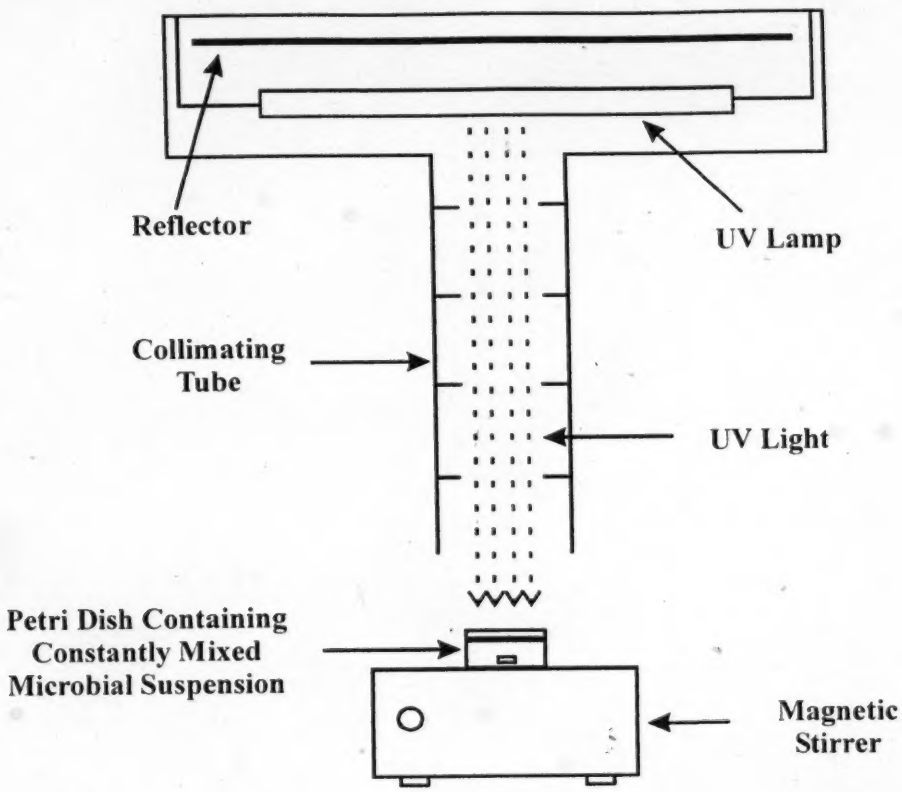

Figure 2-4: Typical collimated beam apparatus setup used in the determination of UV dose-inactivation relationships.

light. The sample to be exposed is placed beneath the collimating tube. If UV transmittance is low, the sample should be continuously mixed to ensure uniform UV exposure. The applied UV dose is adjusted by changing the distance between the sample and the lamp or altering the exposure time. Samples are seeded with the desired microorganism and enumerated before and after exposure in order to determine the survival ratio.

Typically, UV dose-response relationships are presented as plots of the microorganism survival ratio expressed in log units versus the unweighted or germicidal

UV dose applied. Low pressure lamps emit nearly all radiation at 254 nm, which is near the local maximum of DNA's absorption spectrum (260 nm). Therefore, radiation emitted from low pressure lamps is treated as 100% germicidal. However, lamps that emit radiation over a broad spectrum, such as medium pressure lamps, can be adjusted to account for germicidal effectiveness by weighting their output spectra with the absorbance spectrum of DNA. Germicidal UV dose (D_G) is calculated as the average germicidal fluence rate (FR_G) multiplied by the exposure time (t).

$$D_G = FR_G\, t \qquad (10)$$

The fluence rate a sample is subjected to can be determined by modeling, or by direct measurement with a radiometer if the incident radiation is well collimated. Calculation of average germicidal fluence rate and germicidal UV dose should account for the output spectrum of the lamp, absorbance of the water, reflection at the sample surface, radial variation in the fluence rate of the collimated beam, depth of the sample, and the UV absorbance spectra of the microorganism's nucleic acid.

Three common dose-inactivation relationships are given in Figure 2-5. Microbe inactivation often follows Chick's law, which yields linear increase in log inactivation as applied UV dose is increased:

$$N = N_O e^{-k D_G} \qquad (11)$$

where N is the number of viable microorganisms after UV exposure, N_O is the initial number of microorganisms and k is an inactivation rate constant (cm^2/mJ).

Some organisms demonstrate a shouldering effect where limited inactivation occurs at low UV doses. Shouldering has been attributed to poor mixing and to multi-hit or series-event kinetics (Jagger 1967). The multi-hit theory states that an organism contains a number of critical targets which all must be hit before full inactivation occurs.

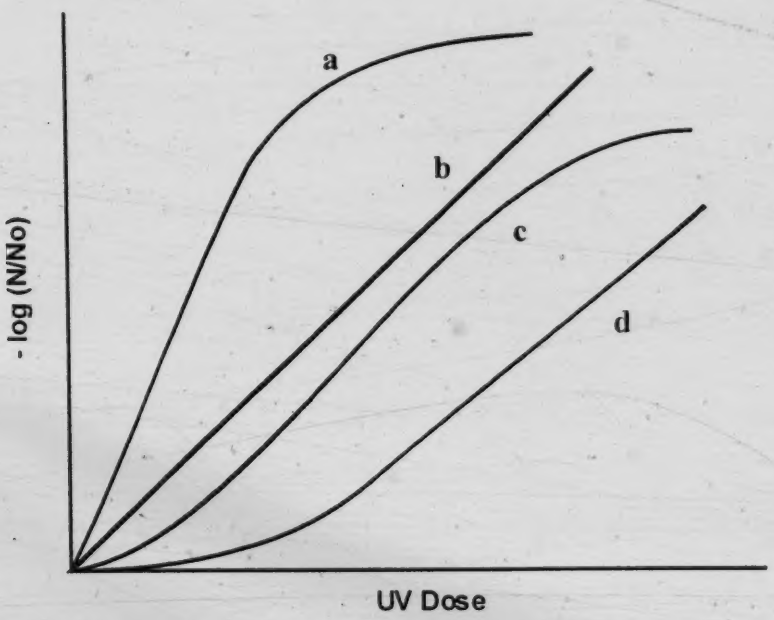

Figure 2-5: Common UV dose-inactivation relationships

(a) presence of tailing

(b) linear (follows Chick-Watson rate law)

(c) presence of a shoulder and tailing

(d) presence of a shoulder

The multi-hit kinetic model simplifies to first order kinetics when only one "hit" is required to cause inactivation. *E. coli B* follows one-hit kinetics, where one hit consists of the formation of roughly 800 thymine dimers which cause inactivation (Jagger 1967). The series-event kinetic model is based on the target organism undergoing a series of distinct reactions that cause damage to the organism, where an event is a unit of damage. An organism is inactivated once it reaches an event level above its threshold (Severin et al. 1983). Shouldering has also been connected with dark repair in *E. coli* (Morton and Haynes 1969). At higher doses a tailing effect is sometimes seen, where inactivation becomes independent of UV dose. Tailing has been attributed to shading of microorganisms by particles (Oliver and Cosgrove 1975; Qualls et al. 1983; Emerick et al. 2000), microorganism clumping, error in enumerating survivors, and sub-populations of microorganisms with increased resistance to UV irradiation (Cerf 1977).

2.2 UV REACTORS

For the purposes of this thesis, the term UV reactor refers to a flow through system, where water is continuously passed by an arrangement of UV lamps. These reactors can be used for microbial reduction of water in water or wastewater treatment plants.

The technology necessary for UV microbial reduction has existed for nearly a century. The fluorescent lights that dominate office and industrial lighting are very similar in design to the lamps used to produce UV light for microbial reduction. Lamps currently being studied for water treatment applications include low pressure and medium pressure lamps, both mercury based, and flash lamps, which are typically xenon based. When the gas pressure in a mercury lamp is low (<10 torr) the emission spectrum is

narrow, but maximum power usage is low as well (Bolton 1999). As the vapor pressure is increased, the same lamp can use more power, but the emission spectrum broadens. The increased pressure in medium pressure lamps results in higher intensity UV output, with the majority of the light emitted between 200 nm and 300 nm. Low pressure lamps emit 85 to 90 percent of their light at 254 nm (von Sonntag and Schuchmann 1992). Figure 2-6 shows the differences in relative intensity and spectral output for low and medium pressure lamps. The higher intensity of medium pressure units allows for designs with fewer lamps and makes automated cleaning systems a viable option. This results in a less

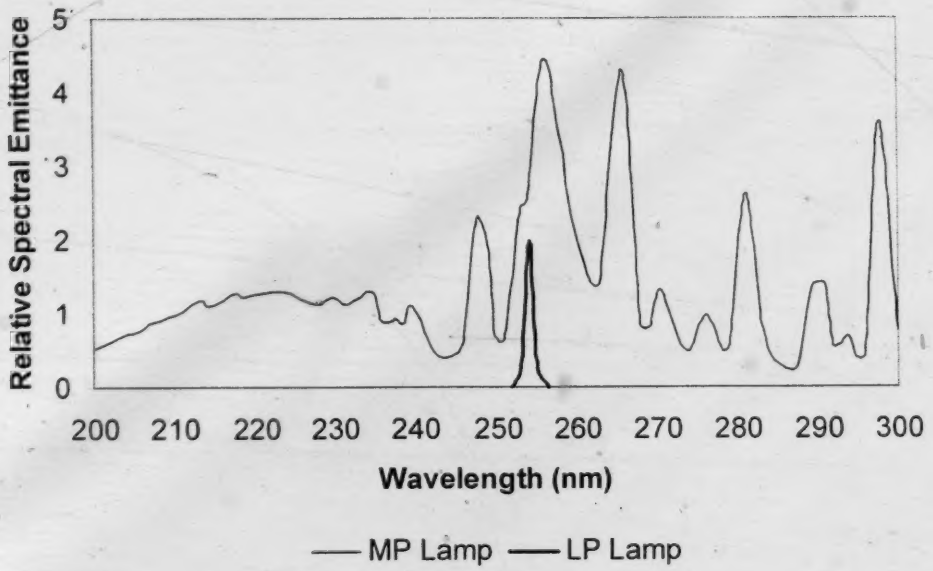

Figure 2-6: Relative emission spectrums for low pressure and medium pressure UV lamps over the 200 nm to 300 nm range.

(adapted from Bolton 1999)

labor intensive treatment system with a smaller footprint. Flash lamps are similar to the continuous emission lamps previously mentioned, but repeatedly discharge high energy bursts instead of continuous low-level energy (Bolton 1999).

2.2.1 UV Dose Distributions

The concept of dose distribution can be illustrated by following a single microorganism as it travels through a reactor. If a microorganism travels along the reactor walls, it will only travel through low fluence rate zones and will receive a UV dose far lower than the average. A microbe traveling close to the lamps will be subjected to high fluence rate levels and will receive a higher than average UV dose. Therefore, the dose delivered by a UV reactor is best described using a dose distribution. Factors such as reactor geometry, hydraulics, water quality, lamp type, age and orientation all influence the dose distribution for a UV treatment system.

An ideal UV reactor has perfect radial mixing with plug flow. In this case, fluence rate gradient has no effect on inactivation, because all microbes receive the same exposure to UV irradiation and have identical exposure times. Any factor resulting in deviation from perfect radial mixing with plug flow will result in non-homogeneous UV dosing to microorganisms passing through their chambers. In UV water treatment this effect is called a dose distribution. The presence of a fluence rate gradient, combined with imperfect radial mixing, causes a dose distribution because not all microbes are exposed to the same fluence rate as they pass through the reactor. Axial dispersion within a reactor also induces a dose distribution, as not all microbes have the same retention time within the irradiation zone.

2.2.2 Measurement of UV Dose Delivered

The lack of a simple method of measuring UV dose delivered in a reactor is a primary obstacle in the widespread implementation of UV technology for the purpose of microbial reduction of drinking water supplies. Chemical disinfection methods typically provide a residual in the water, which can be easily measured on location. UV leaves no chemical residual, so more complex methodologies must be used to confirm performance. Numerical modeling, actinometry and biodosimetry are three methods that can be used to measure the UV dose delivered.

2.2.2.1 Modeling

Estimating UV dose in a reactor requires the coupling of UV fluence rate modeling with a description of the hydrodynamics. This allows estimation of the dose for an individual particle traveling through the reactor or the average dose. Average viable microorganism effluent concentrations can be estimated by most models if the following data is available: target microorganism influent concentration; average fluence rate; residence time distribution; and a dose-inactivation curve. Empirical methods can also be used to estimate dose.

Multiple point source summation (MPSS) is the current standard for approximating spatial fluence rate patterns in a reactor. The lamp output is approximated by summing the effects of a series of imaginary point sources with spherical emission, equally spaced along the lamp's axis. A volume of influence for each lamp can be defined by physical barriers such as reactor walls or by the distance from the lamp where transmittance falls below a preset negligible level. Microorganisms traveling through the reactor are 3 dimensional targets that can absorb UV radiation from all directions.

However, because fluence rates are spatially additive, it is simple to include the effects of multiple lamps into a model (Bolton 2000). The use of a UV fluence rate model in combination with the assumptions of perfect radial mixing and plug flow can be used to determine the ideal dose for a reactor. The ideal dose can then be compared to the measured dose from biodosimetry or actinometry to provide an assessment of reactor mixing efficiency (Bolton 2000).

The hydrodynamics of a reactor can be accounted for in several different ways. The simplest methodology is to assume reactor flow is that of an ideal reactor such as plug flow with perfect radial mixing, or a number of continuous flow stirred tank reactors (CFSTRs) in series. Accuracy may be improved by accounting for factors such as residence time distributions or the time for a certain percentage of a slug injection to pass through the reactor. One of the most accurate means of estimating reactor hydrodynamics is by use of computational fluid dynamic (CFD) modeling. CFD modeling attempts to mimic flow patterns in a reactor.

UV fluence rate within a reactor has been successfully estimated using point-source summation models and alternatively by use of biodosimetry methods (Qualls and Johnson 1983). Mathematical models will always result in simplifications of the actual processes occurring within a reactor. For this reason, a simple model verified for specific conditions may not provide accurate predictions outside of the field tested range. A benefit of using mathematical modeling is that once the model is developed, it is possible to quickly examine a wide variety of operating conditions and changes in reactor design. There is limited literature detailing the use of CFD models to predict UV microbial reduction in drinking water reactors. Models incorporating both MPSS and CFD have

been used to accurately predict scale-up and allowed for improvement of existing reactor designs (Petri and Olsen 2002). Modeling may prove to be an efficient means of predicting UV dose in reactors.

2.2.2.2 Actinometry

Actinometry is a field testing procedure reliant on chemicals to determine UV dose in a reactor. It involves injecting a photosensitive chemical into a water sample and subjecting it to UV irradiation. The chemical undergoes photochemical decomposition of a known quantum yield. The quantity of product produced by the reaction is then used to estimate the dose (Harris et al. 1987).

An ideal chemical actinometer has a known quantum yield when it is exposed to UV radiation and the photoproduct is stable and easily measured. Photochemicals used in previous studies include potassium ferrioxalate (Harris et al. 1987) and uridine (von Sonntag and Schuchmann 1992).

Actinometry accounts for most factors influencing actual UV dose and quickly estimates the UV dose delivered. However, results can be sensitive to procedural variation and the relatively high cost of chemicals may make the method impractical for regular use in field situations (Harris et al. 1987).

2.2.2.3 Biodosimetry

Biodosimetry involves matching UV dose-inactivation relationships for the target microorganism, with measured inactivation from challenge tests performed on a UV reactor. The dose-inactivation relationship for a microorganism is determined in a laboratory batch UV reactor that delivers the same dose to all microorganisms (Wright

2001). The collimated beam apparatus described in this thesis (Figure 2-4) has become the unofficial standard UV batch reactor for this purpose, but past studies often used novel devices in its place (Wiedenmann et al. 1993; Nieuwstad and Havelaar 1994; Sommer et al. 1995). Challenge tests on UV reactors involve injection of an appropriate indicator organism into reactor influent and the collection of samples of the seeded water before and after passage through the UV reactor. The most common indicators used in biodosimetry studies for microbial reduction of potable water are MS2 phage (Havelaar et al. 1990; Nieuwstad and Havelaar 1994), and *B. subtilis* (Qualls and Johnson 1983; Qualls et al. 1989; Sommer and Cabaj 1993; Sommer et al. 1997; Leuker 1999). Indicator viability is assessed for both samples and an inactivation ratio is calculated. The log inactivation is compared to the UV dose-inactivation curve and the corresponding dose is termed reduction equivalent dose (RED). RED is a function of the dose distribution and therefore is subject to change as reactor operating conditions are altered. A graphical depiction of how RED is determined from measured inactivation and the UV dose-inactivation relationship is given by Figure 2-7.

Biodosimetry has been extensively studied and is the current UV reactor validation standard in existing European regulations and upcoming North American guidelines (Kolch 1999). Bioassay methods inherently account for most factors that influence UV dose in a reactor (Harris et al. 1987).

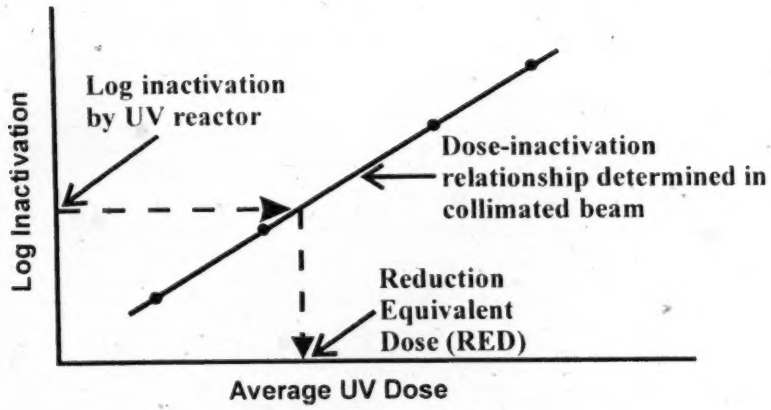

Figure 2-7: Graphical description showing how RED is determined from the UV dose-inactivation relationship and the measured inactivation of an organism due to passage through a UV reactor.

2.2.3 Water Quality Considerations

UV microbial reduction has been shown to be relatively independent of many water quality parameters. The effectiveness of UV microbial reduction is not impeded by variations in temperature (Yip and Konasewich 1972; Severin et al. 1983) or pH (Malley et al. 1995). This is a major advantage over chemical microbial reduction techniques.

Turbidity and UV absorbance are useful in relating the influence of water quality on UV microbial reduction effectiveness. Turbidity partially accounts for harboring of pathogens within particulate matter, and blocking and scattering of UV light. UV absorbance aids in accounting for photochemical reactions of substances in the water due to exposure to UV.

2.2.3.1 Turbidity

Turbidity is an optical property measuring visible light scattering by suspended particulate and colloidal matter. Turbidity is measured by recording the intensity of light scattered at one or more angles from the incident beam. Turbidity cannot be directly related to the amount, number, or concentration of suspended particles for several reasons. White particles will reflect more light than similarly shaped dark particles, and the higher surface area to volume ratio of small particles results in a disproportional amount of light to be reflected from small particles than larger particles of similar shape and composition. Additionally, scattering of light is dependant on particle size. Therefore, turbidity is highly dependant on the properties of particulate and colloidal matter suspended in the water.

Both natural and anthropogenic sources can significantly influence water turbidity. The type of light scattering material introduced varies by its origin. Particles in unaltered lake water contributing to turbidity can consist of inorganic materials such as silt or minerals, live and dead organic matter, and microorganisms.

Natural influences on turbidity include watershed characteristics such as geology, catchment area size, turbulence and size of the water body and climatic factors such as precipitation, wind, seasonal temperature changes and stratification (Hroncich 1999). Water may be drawn from the ground, rivers, streams or large water bodies. Groundwater is naturally filtered through rock and soil, resulting in high dissolved solids and mineral content, but low suspended solids content and therefore low turbidity. Rivers tend to have high turbidities due to the erosive potential of moving water and the reduced ability to settle particles out of suspension as water turbulence increases. Turbidity is created by the

erosion of clay, silt, and rock from the riverbed or the catchment area, and from natural organic matter (NOM) from decaying vegetation. Large water bodies such as lakes and reservoirs tend to have low turbidity due to long detention times and quiescent conditions that allow for settlement of larger particles. Lake Okanagan, the water source in this study, typically has low turbidity.

Anthropogenic sources include agricultural runoff, mining runoff, industrial discharges, urban effluent discharges and storm runoff. Crop operations will primarily contribute eroded soil, fertilizer, pesticides and organics. Intensive livestock operations will tend to introduce high organic solids rich in nutrients such as nitrogen and phosphorus, and microorganisms, many of which are pathogenic to humans. Mining runoff typically contributes high suspended solids to water bodies and is often acidic in nature. Industrial operations can contribute a wide variety of chemicals and toxins. Forestry is of special note, because it encourages soil erosion in logged areas, thus magnifying the influence of natural turbidity sources. Mining, forestry and agricultural operations all exist in the Lake Okanagan watershed, and have the potential to increase the turbidity of the water.

2.2.3.2 UV Absorbance

UV absorbance is a measure of the transformation of UV radiation into other forms of energy. It is measured by comparing transmission of radiation at 254 nm through a suspension to transmission through purified water over the same distance. The light not transmitted through the solution will have been reflected, scattered or absorbed. This measurement is often made on filtered water to eliminate the effect of reflection and scattering due to particles. In UV treatment of drinking water, the water sample is not

filtered in order to give a more realistic view of how much light is actually reaching target microorganisms. UV absorbance has a large impact on the average fluence rate a pathogen is exposed to in a UV reactor.

Compounds that may be present in water that absorb UV light include iron, sulfites, nitrites, phenols, ozone and dissolved organics. The presence of iron, hardness or hydrogen sulfide may lead to scaling on the lamp quartz sleeve, which can reduce transmission of light to water. Scaling problems can be alleviated by frequent cleaning of lamp surfaces.

The doses required to inactivate pathogens of concern in drinking water treatment have not been found to cause significant formation of byproducts in studies conducted to date. No significant change in groundwater turbidity, pH, non-purgeable dissolved organic carbon, UV absorbance at 254 nm, nitrate, nitrite, bromide, iron or manganese concentrations was observed for doses as high as 200 mJ/cm^2 (Malley et al. 1995). UV irradiation from a medium pressure lamp displayed minimal effect on the formation of low molecular weight organic by-products, such as phenols, aldehydes and organic acids (Peldszus et al. 2000).

2.2.3.3 Water Quality Related Obstacles to UV Disinfection

Water quality influences both chemical and UV microbial reduction effectiveness. The primary obstacles to UV microbial reduction that can be related to water quality issues are:

- physical blocking of light, which includes:
    - scattering of light,
    - protection of microorganisms by embedment within particles,
- absorption of UV light,
- encouragement of microorganism clumping or aggregation by adsorption to particle surface, and
- formation of chemical and biological films on the surface of UV lamps.

As UV absorbance increases, the fluence rate gradient within a reactor increases. A steeper gradient has the potential to intensify the effect of any variation from ideal flow conditions on microorganism inactivation and widen the dose distribution. As the dose distribution of a reactor widens, microbial reduction due to passage through the reactor decreases. The fluence rate gradient may also be increased due to scattering and physical blocking of light. Unfiltered surface water, such as the feed water used in this study, generally has lower UV transmittance than filtered water.

The presence of particles in the water causes some of the light to be scattered, decreasing fluence rate levels far away from the lamp. This increases the probability that a particle can travel through the reactor and only be exposed to low UV fluence rate levels, thus widening the dose distribution. Particles may also be present directly between the target microbe and the lamp, reducing the fluence rate or completely blocking the passage of light to the microbe. The short retention time in UV reactors magnifies the importance of scattering and physical blocking of light.

A large number of studies have demonstrated that particle associated microorganisms require higher UV doses to achieve inactivation than discrete microorganisms (Oliver and Cosgrove 1975; Qualls et al. 1983; Parker and Darby 1995; Emerick et al. 2000). The characteristics of the particles and dissolved compounds in a natural water influence the degree to which each potential interference mechanism will hinder microorganism inactivation. In some cases solids association related mechanisms will be prevalent and, in others, simple blocking and absorption of UV will dominate. The size and composition of particles in water vary by source and time of year. The significance of each parameter is site specific and best determined by testing the natural water in question.

Clumping and particle association of organisms threatens the accuracy and reliability of standard enumeration methodologies. When enumerating microorganisms, a particle with multiple microorganisms adsorbed to it, or a clump solely consisting of organisms is counted as a single colony or plaque forming unit. Clumping in sufficient numbers has the potential to cause reduced inactivation levels, because some microbes may be partially protected from the radiation. This is because light must first pass through the other microorganisms surrounding the protected microbe before irradiating the organism. The degree of clumping and particle association is dependent on the characteristics of the solids, and the tendencies of each organism in question.

Microorganisms can be found on the solid-liquid interface of a particle with a direct pathway to the water, and thus directly exposed to UV radiation, or on a solid liquid interface within a particle pore with no direct UV exposure pathway. Microorganisms can also be sheltered deep within solid material with no direct pathway

to the water or UV radiation. Locations with no direct pathway to UV radiation may have increased resistance to inactivation, because light can not reach the organism without first passing through solid material (Loge et al. 1999).

Fouling at the quartz-water interface can occur due to inorganic and organic sources. Organic films quickly form on the quartz sheath with the lamp turned off, but are rapidly diminished in the presence of UV radiation (Lin et al. 1999). Inorganic fouling tends to be a thermally induced precipitation and impaction of inorganic colloidal matter. Iron, aluminum, and calcium are the most common cations, while carbonate, sulfate, hydroxide, chloride and phosphate are primary anions contributing to fouling (Lin et al. 1999). Though pH does not interfere with UV microbial reduction directly, higher pH often associated with unfiltered surface waters can encourage precipitation and scaling.

The influence of many water quality parameters are site specific. UV microbial reduction of untreated surface water is more susceptible to natural swings in water quality then pre-treated water. Therefore, generalized UV dosing rules or guidelines set out for pre-treated water should not be applied to systems dependant on natural water supplies. Site-specific evaluations should be carried out to determine local requirements and appropriate UV doses to ensure public health protection.

2.3 BIODOSIMETRY INDICATOR ORGANISMS

There are usually insufficient numbers of pathogens or suitable indicator organisms naturally present in the source water to allow measurement of inactivation efficiency. In biodosimetry, the reactor influent is often seeded with a suitable indicator organism in sufficient numbers to observe the desired inactivation levels. The ideal indicator for UV microbial reduction of potable water has the following properties:

1. the indicator should be non-pathogenic,
2. the indicator should be present in natural waters in high numbers or readily produced using laboratory procedures,
3. the indicator organism should have a consistent response to UV light,
4. the indicator response to UV light should have a direct relationship with the pathogen of concern,
5. the testing procedure should be straight forward and easy to perform,
6. the indicator should not reproduce in the water,
7. other microorganisms should not give positive results for the enumeration procedure,
8. the enumeration procedure should be able to detect low levels of the indicator,
9. the enumeration procedure should have high reproducibility, and
10. the procedure should be inexpensive.

It has been shown that germicidal efficiencies for one species of bacteria or virus can be used to represent the relative response to UV light for all bacteria and viruses (Giese and Darby 2000). However, correction factors must be applied to account for differences in dose-inactivation relationships. No correction is required for indicators with lower UV resistance than the target pathogen, but overly conservative estimates of target pathogen inactivation may result.

Current water treatment regulations encourage the use of multi-treatment processes to achieve target reductions. UV microbial reduction is not ideal as a sole

means of treatment due to its lack of disinfection residual, but is very complimentary when used in conjunction with other disinfectants such as chlorine. Protozoan parasites are highly resistant to chlorine disinfection (Haas 1999), but are susceptible to inactivation by low doses of UV (Bukhari et al. 1999), whereas the reverse is true for some pathogenic viruses (Battigelli et al. 1993; Cohn et al. 1999; Wright et al. 1999). The use of UV can also allow reductions in chlorine concentrations, thus reducing the formation of toxic chlorine related by-products. The protozoan parasite *C. parvum* requires a UV dose of 19 mJ/cm^2 to achieve 3.9 log inactivation, which is within the capabilities of most commercially available UV reactors intended for microbial reduction of potable water (Bukhari et al. 1999).

2.3.1 *Bacillus subtilis*

2.3.1.1 Biology

B. subtilis is a gram-positive, rod shaped, endospore forming bacterium (Kobayashi 1989). The ability to form resistant spores gives the species an advantage in surviving periods of dryness and nutrient deprivation. The spores have high resistance to chemical degradation, heat, radiation, UV light and dry conditions (Kobayashi 1989). *B. subtilis* have a spore coat, cortex, and inner spore membrane surrounding the protoplast and they can remain dormant and viable for very long periods (Prescott et al. 1996). Sporulation is triggered when the organism is deprived of nutrients, usually carbon, nitrogen or phosphorus (Kobayashi 1989). Vegetative cells form ellipsoidal endospores in a complex developmental process lasting approximately 8 hours (Prescott et al. 1996).

Sporulation consists of seven distinct steps as seen in Figure 2-8 (Kobayashi 1989). Stage 0 is the vegetative cell. In stage I, axial filaments are formed within the vegetative cell. Stage II is characterized by the appearance of a septum dividing the cell into a large mother cell and a smaller prespore cell. In stage IIIa the mother cell engulfs the prespore and then the prespore becomes a spore protoplast or forespore in Stage IIIb. After this stage, the cell is committed to completion of the sporulation and the process cannot be reversed even if environmental conditions become favorable again (Doi 1989). Stage IV sees the development of the cortex between the inner and outer forespore membranes. In stage V the spore coat is formed by deposition of proteins on the forespore membrane. The spore matures and becomes resistant to adverse environmental

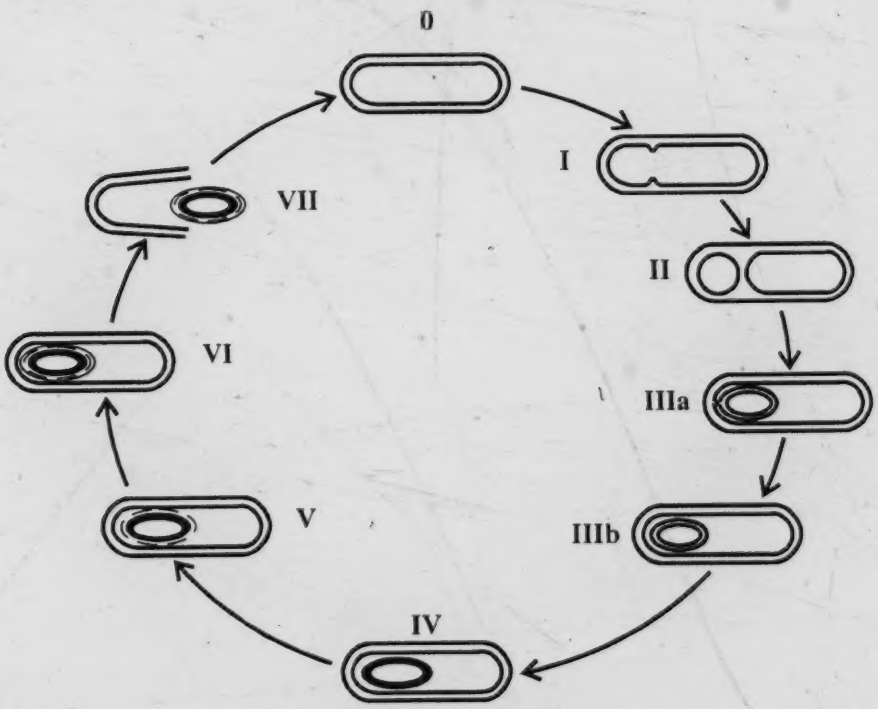

Figure 2-8: Life cycle of *B. subtilis*, from vegetative bacteria to free endospore.

conditions in stage VI. In the final stage (Stage VII) the spore is released from the mother cell. Endospores quickly germinate to form vegetative cells when in the presence of a germinant such as glucose or L-alanine (Kobayashi 1989). The generation time of vegetative cells is approximately 0.43 hours at 40 °C in a nutrient rich medium (Prescott et al. 1996).

Endospore formation is most efficient when the vegetative cells have grown for at least six or seven generations in a nutrient rich medium before the onset of sporulation (Doi 1989). The spores can be detected by heating at 70 to 80°C for 10 minutes and incubating on an appropriate growth medium. Only endospores and some thermophiles will survive this treatment (Prescott et al. 1996).

The benefits of using *B. subtilis* as a biodosimetric indicator are as follows:

- the spores have high resistance to UV light,
- spores remain viable for long periods of time,
- they are non-pathogenic,
- spores do not reproduce in samples, and
- very few other organisms existing in natural water will return a false positive in the enumeration of viable spores (Prescott et al. 1996).

2.3.1.2 UV Reactor Evaluation Studies Using Spores

Bacillus subtilis spores have been examined in numerous laboratory and pilot scale UV reactor studies. In the early eighties their potential as biodosimetric indicators was first recognized (Qualls and Johnson 1983). Early research was plagued by a lack of

a standard procedure, which inhibited direct comparison of results. UV dose-inactivation relationships were often determined using non-collimated UV light or novel collimation devices. The majority of early literature neglected to fully describe the methodologies used. The literature often does not make clear whether factors such as non-uniformity of the UV light beam, lamp age and wavelength dependant UV sensitivity of the target microorganism were accounted for. Many studies did not even explicitly state whether low pressure or medium pressure UV lamps were used. UV light has been used to disinfect wastewater for decades, whereas its use for microbial reduction of surface water is still in its infancy. As a result, many of the best and most relevant studies focused on wastewater and did not address all of the issues relevant to drinking water.

Qualls et al. (1989) examined the use of *B. subtilis* (strain 6633), purchased from the American Type Culture Collection (ATCC), for evaluation of two small scale and two pilot scale, continuous flow UV wastewater treatment systems. UV doses ranged from 64 mJ/cm^2 to 118 mJ/cm^2. Focus was on comparison of the various methods to calculate intensity and spore survival rates were not explicitly reported. The objectives were to develop methods to measure fluence rate and residence time distribution in multiple lamp reactors, to validate a method of calculating fluence rate patterns in a reactor, and measure capacity and efficiency in a way that allows comparison to other UV reactors. One lot of spores was grown on Schaeffer's medium, while another was generated on the surface of BBL A-K Agar. The spores grown on agar were much more resistant to UV than the Schaeffer's medium collection. Using a collimated beam apparatus, agar spores underwent 1 log inactivation at 90 mJ/cm^2. Spores grown on Schaeffer's medium

underwent 1 log inactivation at 36 mJ/cm^2 and approximately 4 log inactivation at 80 mJ/cm^2.

It was found that flow was retarded substantially along the sides of the unit. Insufficient mixing across fluence rate gradients caused microorganisms passing through low fluence rate zones to contribute disproportionally to the number of viable microorganisms. This resulted in a broad and skewed dose distribution and low inactivation. As absorbance of the solution increased, the fluence rate gradient became more severe. The results from the slug injection and continuous flow assays corresponded well, suggesting that either are appropriate methodologies.

This study provided valuable information on spore UV resistance dependency on generation methods, and outlined a biodosimetric procedure that many subsequent studies were based on. This study identified that reactor doses determined by biodosimetry are not the average UV doses if there is insufficient mixing across fluence rate gradients. Also, it was observed that the majority of surviving microbes that passed through the reactor had retention times less than the average, compared to the total number of spores injected into the reactor influent stream. Due to the linear UV dose-log inactivation relationship, the shorter retention times resulted in reduced inactivation and lower UV doses relative to microbes with exposure times greater than the average. In other words a UV dose cannot be assigned to a reactor without recognizing the influence of the dose distribution characteristic of reactor operation for a given set of conditions. Qualls et al. (1989) was a very thorough study which paved the way for current biodosimetry research.

Sommer and Cabaj (1993) investigated the use of *B. subtilis* (ATCC 6633) spores to evaluate a continuous flow, UV drinking water reactor. The dose-inactivation curve displayed both shouldering and tailing, with linear log inactivation in between. The UV reactor was the commercially available, model U 1 reactor (Katadyn Products Inc., Wallisellen, Switzerland). It was not explicitly stated what type of UV lamp was used in the reactor. UV doses tested ranged from approximately 5 mJ/cm^2 to 120 mJ/cm^2. Spores were generated using three different methods. Method of generation influenced the spore sensitivity to inactivation by UV light, similar to the study performed by Qualls et al. (1989). The dose-inactivation curves show that the least resistant spores exhibited greater than 4 log inactivation at a UV dose of roughly 32 mJ/cm^2. At the same dose, the most resistant spores underwent approximately 1.8 log inactivation. Another significant finding was that operating time of the UV lamps had a significant effect on the effective dose in the reactor. A lamp with 7000 hours experienced a 30% decrease in output. The investigators recommend future testing needs to be performed on lamps near the end of their recommended operating time.

The study performed by Sommer and Cabaj (1993) is relevant because it investigated the influence of indicator type, flow rate, lamp operating parameters and UV absorbance on the efficiency of a commercially available UV reactor treating drinking water. UV dose-inactivation relationships reported confirm the observation by Qualls and Johnson (1989) that UV resistance of *B. subtilis* spores is dependent on the cultivation methods used. As UVT decreases, at the lower flows tested in the reactor the reduction in log inactivation was nearly linear. There was insufficient information on the pilot plant installation and testing methodologies. No mention was made of static mixers or other

inline mixing devices used before sampling ports to ensure homogeneous flow through the reactor and therefore representative samples. Otherwise, this study provided a good biodosimetric procedure that could be applied to further research in the area. Additionally, *B. subtilis* was confirmed to be a suitable biodosimetric indicator for UV reactors treating potable water.

A summary of UV dose-inactivation relationships determined for several studies involving *B. subtilis* spores is given in Table 2-1. All studies examined found some degree of shouldering at lower UV doses. Tailing was also displayed when high log inactivations were measured. UV susceptibility for the species was very broad, and was shown to be highly dependant on the method of cultivation (Qualls et al. 1989; Sommer and Cabaj 1993). For all cases, the UV resistance of the spores (minimum 30 mJ/cm^2 required for 4 log inactivation (Qualls and Johnson 1983)) was higher than that reported for *C. parvum* by Bukhari (1999) (19 mJ/cm^2 for 3.9 log inactivation). Therefore, *B. subtilis* spores are a suitable biodosimetric indicator organism for the protozoan parasite, but caution must be used when preparing the organisms using a non-standard method. Additionally, the UV dose-inactivation relationship of the spores must be carefully determined using collimated beam methods.

Table 2-1: Summary of *B. subtilis* UV dose-inactivation relationships reported in literature, detailing the growth media, exposure device and water matrix used in experimentation.

Log Inactivation				Growth Media[a]	Exposure Device[b]	Water Matrix[c]	Source
1	2	3	4				
UV Dose (mJ/cm^2)							
36	49	61	78	SB	CB	FWW	(Chang et al. 1985)
16	22	27	33	NA	CB	DI	(Harris et al. 1987)
19	30	48	61	CA	CB	P	(Sommer and Cabaj 1993)
11	19	26	32	SA			
22	35	40	54	SB			
12	18	24	30		CB	BDI	(Qualls and Johnson 1983)
36	62	67		SM	CB	BDI	(Qualls et al. 1989)
90				BA			

[a] Exposure Device Key: CB = collimated beam apparatus;

[b] Growth Media Key: BA = BBL AK agar; CA = Columbia agar; NA = nutrient agar; SA = Schaeffer's agar; SB = Schaeffer's broth; SM = Schaeffer's medium;

[c] Water Matrix Key: BDI = buffered deionized water; DI = deionized water; FWW = filtered wastewater; P = potable water.

2.3.2 MS2 phage

2.3.2.1 Biology

MS2 coliphage are small, icosahedral, non-enveloped, F-specific, single stranded RNA viruses in the *Leviviridae* morphological group (van Duin 1988; Prescott et al. 1996). The phage diameter is typically 26.0 to 26.6 nm (van Duin 1988). The phage can only reproduce in actively metabolizing *E. coli* bacteria. They attach to the F-pili of their host and enter the cell by an unidentified mechanism (van Duin 1988).

Having only three or four genes, genetically it is one of the simplest known phages. Single stranded RNA phage are among the smallest things that carry the necessary information for self-replication and transmission (van Duin 1988). One protein is involved in phage adsorption to the host cell and possibly also in virion construction and maturation. The other three genes code for a coat protein, an RNA replicase, and a protein needed for cell lysis (Prescott et al. 1996).

The life cycle of the phage consists of four phases. First the virus adsorbs to the host cell and injects it with genetic material. In phase II the host cell stops production of its own nucleic acids and protein and is forced to synthesize virus RNA. The assembly of complete virions occurs in phase III. Finally, the new phage particles are released from the host cell in phase IV (Prescott et al. 1996).

The benefits of using MS2 phage as a biodosimetric indicator include the following:

- the virus does not have photoreactivation capabilities,
- its UV dose-inactivation relationship is reproducible and follows first order kinetics (Harm 1980),
- it has a high resistance to UV relative to bacterial spores (Harm 1980),
- it is non pathogenic, and
- MS2 is easily generated in large numbers up to 10^{12} pfu/mL (Havelaar et al. 1990), whereas *B. subtilis* spores can only be cultured up to roughly 10^{8} cfu/mL (Qualls and Johnson 1983).

2.3.2.2 UV Inactivation of MS2 phage

The inactivation of MS2 phage has been examined in many bench scale and pilot scale UV reactor experiments. In general, the coliphage has been found to be suitable for use as a biodosimetric indicator for both wastewater and drinking water applications.

Nieuwstad and Havelaar (1994) performed an experiment extremely relevant to this thesis. They investigated the inactivation kinetics of MS2 phage and used it as a biodosimetric indicator to calibrate a low pressure ultraviolet pilot plant treating wastewater effluent. The pilot plant consisted of 6 MSA4 units (manufactured by Berson Milieutechniek, Nuenen, Holland) connected in series. Each unit contained four low pressure UV lamps. UV doses were manipulated by altering the flow rate and turning lamps on or off. UV doses administered ranged from 25.8 to 287.3 mJ/cm^2. $UVT_{254,\ 10\ mm}$ was between 45.6 and 47.5 percent, which is lower than what would be encountered in drinking water treatment. Log inactivations ranging from 3.4 to greater than 12.7 were recorded from pilot plant samples. The laboratory batch exposures were performed using a novel light collimation device.

Non-linear regression was used to calculate UV doses because it best accounted for the tailing effects observed at higher doses. Calculations treated the reactors as a number of completely mixed reactors in series. The study concluded that when the kinetic constants of MS2 were determined from laboratory batch experiments, the hydraulic characteristics of a UV pilot plant could be found for different operational conditions by relating MS2 inactivation in the UV pilot plant to MS2 inactivation achieved in laboratory batch experiments.

There are several positive and negative aspects of the study. The use of a novel collimation device is a major shortcoming of this experiment, as it makes direct comparison of results to other studies questionable. Unfortunately, this is a common occurrence in much of the related literature. A positive aspect of the study was the broad range of doses and inactivation levels examined, which is much larger than is presented in other studies that examined MS2 inactivation within UV reactors. Measured log inactivations were greater than 12.7 log units in some trials, which is well beyond the probable required range for drinking water treatment. The study provided valuable insight into MS2 phage behavior at high UV doses. It was concluded that MS2 phage inactivation did not follow first or second order kinetics. Both models were assumed to have a y-intercept of zero and included a tailing region observed at high UV doses in the kinetic modeling data set. Tailing can be a product of the testing methodology, and assuming identical causes for tailing in a pilot scale flow-through UV reactor relative to a collimated beam batch reactor may not be valid.

There are several issues with the pilot plant itself. There was no reference to upstream piping conditions. Also, the article made no mention of static mixers or other inline devices to ensure samples were representative of average microbe concentrations in the flow stream. However, this study did manage to correlate the UV dose-inactivation relationship with a pilot scale UV reactor and identify hydraulic effects. The study confirmed the potential of MS2 phage as a biodosimetric indicator.

Mackey et al. (2002) carried out *C. parvum* and MS2 phage bioassays in order to directly link inactivation of the two organisms due to exposure to UV radiation. The study involved biodosimetric analysis of a flow through UV reactor treating drinking

water, measuring the inactivation of both *C. parvum* and MS2 phage. The reactor contained six, low pressure-high output lamps mounted perpendicular to the flow. UV dose-inactivation relationships were determined by suspending the target microorganisms in feed water used in the flow through reactor trials and exposing the suspensions to UV radiation in a collimated beam apparatus.

The study concluded that MS2 phage can reliably serve as a surrogate test organism for pathogenic microorganisms in the assessment of UV reactor performance. However, the use of MS2 would result in conservative inactivation estimates for a UV sensitive organism such as *C. parvum*. Use of an organism with UV resistance closer to the target organism would allow for a more precise determination of the log inactivation that the target organism would undergo.

Table 2-2 summarizes dose-inactivation relationships for MS2 phage determined in existing literature. The dose-inactivation relationships reviewed display a wide range of UV susceptibility, but it is generally more predictable and more resistant to UV light than *B. subtilis* spores. UV doses typically required for 4 log inactivation are in the 60 to 70 mJ/cm^2 range, which is much higher than the 19 mJ/cm^2 required to provide roughly the same inactivation in *C. parvum* (Bukhari et al. 1999). Conservative inactivation estimates will likely result when using MS2 phage as a biodosimetric surrogate for protozoan parasites such as *C. parvum* and *G. lamblia*. However, there is potential for other appropriate biodosimetric applications for MS2 phage to be identified in the future, due to its high UV resistance, non-pathogenic properties and reproducible UV dose-inactivation relationship.

Table 2-2: Summary of MS2 phage UV dose-inactivation experiments in literature, detailing the growth media, exposure device and water matrix used in experimentation.

Log Inactivation				Growth Media[a]	Exposure Device[b]	Water Matrix[c]	Source
1	2	3	4				
UV Dose (mJ/cm^2)							
22	43	65		TYGEB	CB	M9	(Havelaar et al. 1990)
22	44	65		TYGEB	CB	M9	(Havelaar et al. 1991)
25	50	75	100	TSB	CB	P	(Mackey et al. 2002)
14	29	45	62	TSA	CB	P	(Meng and Gerba 1996)
7	13	21	29	TYGEB	N	M9	(Nieuwstad and Havelaar 1994)
17	34			Broth	N	PBS	(Rauth 1965)
12	30			TYGEB	CB	SWW	(Tree et al. 1997)
16	34	52	71	TYEA	CB	Water	(Wilson et al. 1992)
4	16	38	68	Broth	N	NaCl solution	(Wiedenmann et al. 1993)

[a] Growth Media Key: TSA = tryptic soy agar; TSB = trypticase soy broth; TYEA = tryptone yeast extract agar; TYGEB = tryptone yeast extract glucose broth;

[b] Exposure Device Key: CB = collimated beam apparatus; N = novel device;

[c] Water Matrix Key: M9 = M9 buffer; P = potable water; PBS = phosphate buffered saline solution; SWW = secondary wastewater effluent.

3 EXPERIMENTAL MATERIALS AND METHODS

3.1 EXPERIMENT OVERVIEW

Reactor performance was analyzed using biodosimetry. Field testing in the City of Kelowna occurred in three phases. Phase 1 was conducted in July, 2001, phase 2 in October, 2001, and phase 3 in February, 2002. The objectives of phase 1 tests were to explore the operational limits of the reactor at various operating conditions and correlate indicator organism inactivation with operating settings. Phase 2 examined reactor performance in greater detail and with increased precision than phase 1. Phase 3 examined the influence of turbidity and absorbance on the measured microorganism inactivation due to exposure to UV radiation in the reactor. Table 3-1 summarizes basic information pertaining to the 3 phases.

Both physical operation parameters and water quality parameters were closely monitored during the operation of the unit. Unit operation items examined were: flow rate; number of active lamps; lamp voltages; lamp current; cumulative lamp hours; and sensor readings. Environmental variables measured on site were: water temperature; pH; and turbidity. Daily water samples were taken to the lab and tested for: total alkalinity; total hardness; pH; absorbance at 254 nm; turbidity; colour; sulfate; and chloride.

Table 3-1: Summary of the testing plan and operational conditions examined in phases 1, 2, and 3.

Issue	Phase 1	Phase 2	Phase 3
Testing date	July 2001	October 2001	February 2002
Indicators used	MS2 phage *B. subtilis*	MS2 phage *B. subtilis*	MS2 phage
Flow rates tested (L/min)	380, 1900	380, 760, 1140	1140
# of lamps operated during testing	1, 4	1, 2	2
Feed water tested[a]	U	U	U, A, T, AT
Number of replicate trials	2	3	3

[a]U = unaltered lake water; A = lake water with absorbance added; T = lake water with turbidity added; AT = lake water with absorbance and turbidity added

3.2 FEED WATER QUALITY

3.2.1 Test Site Description and Characterization

The City of Kelowna draws raw water from Lake Okanagan, adds free chlorine as the sole method of treatment, and then distributes the water throughout the municipality. The city system serves approximately 100,000 people.

Lake Okanagan is the largest of the five main interconnected lakes in the Okanagan Valley. In the north, the lake is fed by Kalamalka Lake and Vernon Creek and at the south end drains into Skaha Lake by way of the Okanagan River. It has a volume of 24.6 km^3 and a catchment area of approximately 6200 km^2. The theoretical residence time in the lake is roughly 52.8 years. Other physical characteristics of the lake are summarized in Table 3-2.

Table 3-2: Summary of the physical characteristics of Lake Okanagan and the surrounding catchment basin.

Parameter	Value
Volume	24.64 km^3
Surface Area	351 km
Shoreline	270 km
Maximum Depth	230 km
Average Depth	76 m
Catchment Area	6188 km^2
Theoretical Residence Time	52.8 yr

Vernon, Kelowna and Penticton are the three major communities on the lake's shore. Vernon is in the north, Kelowna is near the middle and Penticton is at the south end. Major anthropogenic influences on lake water quality are municipal sewage discharges from Vernon and Kelowna, agricultural and forestry related runoff, and a copper mine located within the catchment basin. The importance of tourism to the region's economy has made the maintenance of high lake water quality a priority for area residents.

3.2.2 Feed Water Quality Analysis

Temperature, pH, and turbidity were measured on-site immediately preceding each trial. Additional laboratory testing was performed on daily grab samples. On-line turbidity measurements were taken using a Great Lakes Instruments (GLI International Inc., Loveland, CO) model 8320, Accu4 low range turbidimeter. On-site equipment was calibrated semi-weekly. A summary of the frequency and methodologies employed for water analysis is given in Table 3-3.

Table 3-3: Summary of the frequency and methodologies used in testing the influent water quality for all phases of the study.

Parameter	Frequency	Testing Location	Method
Temperature	Each run/daily	On-site	
pH	Each run/daily	On-site & lab	HACH 8156
Turbidity	Each run/daily	On-site & lab	Standard Method 2130 B
Unfiltered UV Absorbance at 254 nm	Daily	Lab	Standard Method 5910
Total Alkalinity	Daily	Lab	Standard Method 2320 B
Total Hardness	Daily	Lab	Standard Method 2340 C
Apparent Colour	Daily	Lab	Hach 8025
Chloride	Daily	Lab	Hach 8113
Sulfate	Daily	Lab	Hach 8051
Total Coliforms	Semi-weekly	Lab	Colisure
Enterococci	Semi-weekly	Lab	Enterolert
Heterotrophic Plate Counts	Semi-weekly	Lab	SimPlate

Water quality testing was performed in the drinking water lab at the City of Kelowna wastewater treatment plant. Laboratory equipment was calibrated daily. Turbidity was measured using a flow through HACH 2100AN (Hach Co., Loveland, CO) turbidimeter. The pH was measured using a HACH EC30 pH meter. The HACH model DR/4000U spectrophotometer with a flow through cell was used in determination of apparent colour, chloride, sulfate and UV absorbance at 254 nm. Apparent colour was measured using HACH method 8025. Chloride was measured using the HACH mercuric thiocyanate method 8113. Sulfate was measured using the HACH Sulfa Ver 4 Method 8051. Total hardness was measured according to standard method 2340 C, titration using

ethylenediamineteraacetic acid (EDTA) (Greenberg et al. 1992). Total alkalinity was determined by titration with sulfuric acid according to standard method 2320 B (Greenberg et al. 1992).

Total coliforms and *E. coli* were measured using the Colisure test kits manufactured by IDEXX Laboratories Inc. (Westbrook, ME). Enterococci levels were measured using the Enterolert test kit. SimPlate, was used for quantifying the concentration of heterotrophic bacteria in water samples. IDEXX manufactures both Enterolert and SimPlate.

3.3 DESCRIPTION OF THE UV REACTOR

The Sentinel™ UV model R-110 unit is a 304 mm (12 in) internal diameter, continuous flow, medium pressure UV reactor. Sentinel™ reactors are produced by Calgon Carbon Corporation of Pittsburgh, PA. The unit was supplied with a control panel, monitoring controls and transformer. Lamp hours, current, voltage and sensor output for each lamp are automatically logged and can be transmitted to an off-site monitoring computer.

The reactor is a stainless steel, flow through reactor with 4 x 1 kW medium pressure UV lamps mounted perpendicular to the flow (Figure 3-1). Each lamp is enclosed in a protective quartz sheath. Baffles are located on the reactor wall, upstream of each UV lamp, perpendicular to the flow (Figure 3-2). The lamp/baffle arrangement creates four distinct fluence rate zones, arranged in series with the flow. An automatic lamp cleaning system allows the time interval between cleaning phases to be altered to adjust for variable lamp fouling as water quality changes. The lamp cleaning system consists of circular, wire brushes that pass over the surface of the quartz sheath and

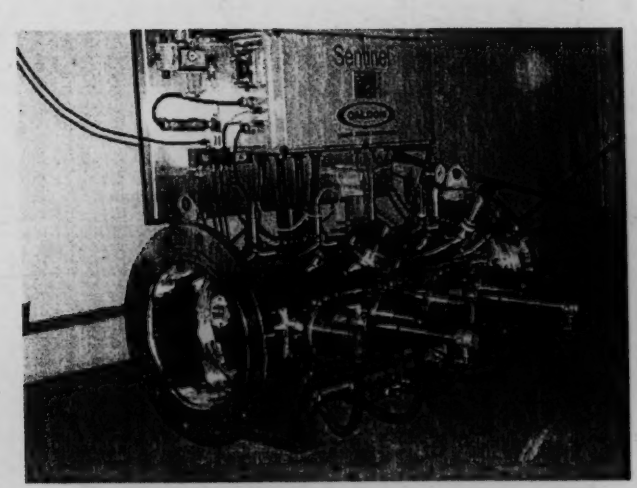

Figure 3-1: Photograph of an uninstalled, 304 mm internal diameter, Sentinel™ medium pressure UV reactor.

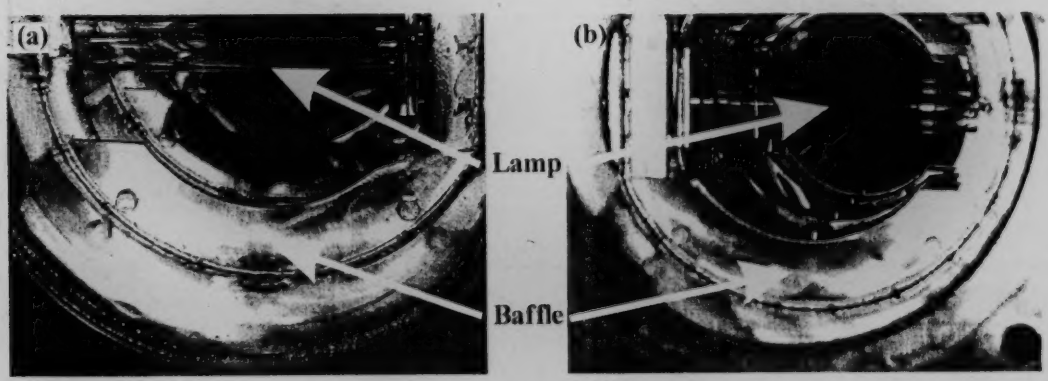

Figure 3-2: Two photographs displaying the inside of the Sentinel™ medium pressure UV reactor, with clear views of the lamp and baffle configuration .

remove any deposits or growths, which may interfere with UV light propagation. The wire brush is pushed over the entire length of the quartz sheath by a stainless steel push rod activated by compressed air.

One UV sensor is placed in close proximity to each lamp. The sensor window is approximately 90 mm from the reactor longitudinal axis and the actual sensor 100 mm from the longitudinal axis of the reactor. The sensor output is measured as a percentage relative to the maximum lamp output.

3.4 UV TREATMENT SYSTEM LAYOUT

A biodosimetric test facility was constructed in the El Dorado pump house operated by the City of Kelowna. A detailed schematic of the facility is located in APPENDIX F, and a simplified drawing is given in Figure 3-3. Unaltered lake water was pumped into a storage reservoir from an intake pipe with origins approximately 100 metres from shore and 20 metres below the surface. The unaltered lake water was then drawn from the storage reservoir and pumped through the UV treatment system. The installation included:

- a port for indicator injection,
- a bypass loop to allow gradual dilution of indicator organisms,
- a port for injection of solutions to increase the UV absorbance and turbidity of reactor influent,
- influent and effluent sampling ports,
- static mixers immediately upstream of sampling ports,

- flow measurement and control, and
- a pipe expansion 1500 mm upstream of the UV reactor.

The bypass loop was located upstream of the first static mixer. Indicator organisms were injected into the bypass loop and introduced in the center of the primary flow stream. Static mixers ensured uniform distribution of indicator organisms and homogeneous composition of water flowing through the reactor. The 1500 mm of straight pipe between the reactor and the pipe expansion, ensured an even flow distribution existed at the reactor inlet.

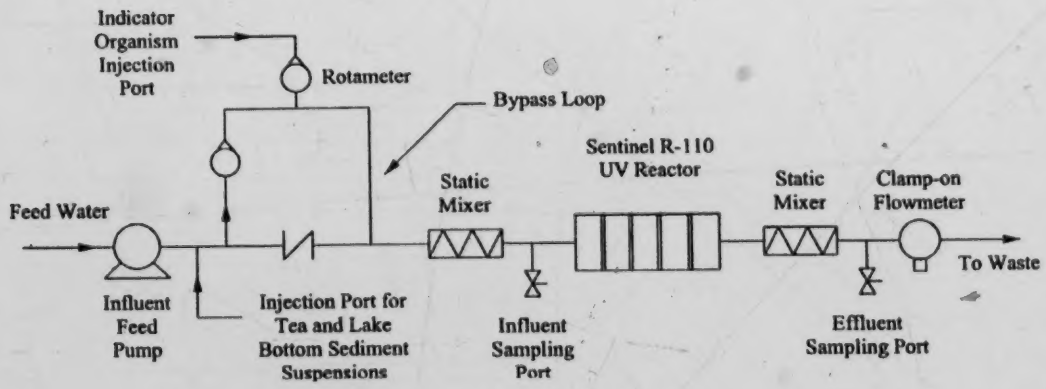

Figure 3-3: Simplified drawing of the treatment system used in biodosimetric analysis of a Sentinel™ UV reactor treating unfiltered surface water.

3.5 COLLIMATED BEAM APPARATUS

The UV dose-inactivation relationships were determined using a collimated beam apparatus (model PSI-1-120, Calgon Carbon Corporation, Pittsburgh, PA). The collimated beam contained a 1 kW medium pressure bulb (model QC-1000-45000071, HNG, Germany). Below the bulb was a 60 mm diameter, 930 mm long collimating tube, with a non-reflective black coating inside, which collimated the UV radiation. A manual pneumatic shutter located at the top of the collimating tube allows control of UV exposure duration. Exposure times were measured using a stopwatch.

3.6 COLLIMATED BEAM EXPERIMENTS

3.6.1 UV Exposure with a Collimated Beam Apparatus

UV dose-inactivation curves were prepared using the collimated beam apparatus, unaltered Lake Okanagan water, and microorganisms from the same batch of indicator organisms used in the UV reactor challenge test. Glass Petri dishes (56 mm internal diameter x 12 mm high) were filled with 20 mL of sample suspensions containing known concentrations of indicator organisms. The samples were placed 280 mm directly below the collimating tube and exposed to UV radiation for set exposure times. Samples were gently stirred during exposures using a 10 mm x 3 mm Teflon® coated stir bar.

3.6.2 UV Irradiance Measurements

UV irradiance measurements were made at the center of the petri dish, at the liquid surface, using an International Light Model IL1400A Radiometer equipped with an

SED240 UV detector. The calculation of average UV irradiance was determined by the methods outlined in previous studies (Bukhari et al. 1999; Craik et al. 2000; Craik et al. 2001). The weighted germicidal UV dose was calculated to account for radial variation in the irradiance of the collimated beam, output spectrum of the lamp, reflection at the surface, absorbance of the water and the UV absorbance spectrum of DNA. The radial variation in irradiance was determined by taking measurements at 5 mm intervals across two perpendicular lines passing through the center point of the beam. The average irradiance at the liquid surface was calculated as 79% of the irradiance measured at the center of the beam. The liquid surface was estimated to reflect 2.5% of radiation based on the refractive indices of air and water. An integrated form of Beer's law was used to calculate the depth averaged irradiance (E') of the water samples:

$$\frac{E'}{E_0} = \frac{(1-10^{-A})}{\ln(10)A} \qquad (12)$$

where A is the absorbance of the water and E_0 is the average incident irradiance at the water surface.

The average germicidal irradiance (E_G) was calculated as the measured irradiance multiplied by the sum of the transmitted irradiance, the normalized lamp output, a germicidal factor, a sensor factor, a reflection factor (0.975) and a radial variation factor (0.79). The transmitted irradiance, normalized lamp output and the germicidal factor were determined at 5 nm increments over the 200 to 300 nm range. The absorbance spectrum of the water sample was determined by measuring the absorbance through a 10 mm

quartz cell over the 200 to 300 nm range, in a model HP 8452A (Hewlett Packard Co., Palo Alto, CA) UV-vis spectrophotometer. The output spectrum of the lamp was provided by the manufacturer. The germicidal factor was determined based on the UV absorbance spectrum of DNA. A sensor factor of 1.286 was used account for the spectral sensitivity of the radiometer, as recommended by the manufacturer.

3.7 FLOW THROUGH UV REACTOR TESTING

3.7.1 Preparation of the UV Reactor for Testing

Several things were done to prepare the Sentinel reactor for testing in order to ensure representative performance. The reactor was shut down between experimental phases, reducing the potential for decreased performance due to aging of system components and lamp fouling. Flow through the reactor was maintained for 48 hours before experimental trials, to ensure all trapped air bubbles and sediment remaining from previous trials were purged from the system. This was done because air bubbles and particulate matter could potentially influence UV intensity and impact microbe inactivation. Lamps were turned on at least 15 minutes prior to executing any trials, ensuring all lamps were operating at maximum radiant intensity during testing.

3.7.2 Introducing Indicator Organisms into the Influent Stream

Concentrated microorganism stock was diluted three times before being added to the UV reactor. This staged dilution was done to promote uniform dispersion of the microbes in the reactor flow stream. The static mixer downstream of the microorganism injection point further promoted dispersion. First, the concentrated microorganism stock was mixed with influent water in an 8 litre plastic jug on a magnetic mixing plate. The

diluted microorganism suspension was pumped from the continuously stirred jug into the bypass loop at a rate of 1.52 L/min, where it was diluted a second time and then reintroduced into the primary flow stream, diluting the third and final time.

The resulting flow through concentration for the first phase of tests was $2x10^5$ cfu/L for *B. subtilis* and $1x10^9$ pfu/L for MS2 phage. For the second round of tests the concentrations were $5x10^6$ cfu/L for *B. subtilis* and $1x10^9$ pfu/L for MS2 phage. The phase 3 target concentration for MS2 phage was $2x10^9$ pfu/L. MS2 phage and *B. subtilis* were tested independently, so that only one of the two indicator species was added to the influent stream for any one trial.

3.7.3 Sampling

Sampling ports for both the influent and effluent were located directly after the static mixers to ensure representative, well mixed samples, with respect to microorganism concentration. Sampling ports were left partially open during testing to maintain steady state sampling conditions. At the beginning of each trial, the two pumps were turned on and a stopwatch started. Three hydraulic retention times (measured between the microorganism inlet and the downstream effluent sample point) elapsed and then two 150 mL influent samples and three 150 mL samples of effluent were collected over a period of approximately one to three minutes.

3.7.4 Sample Handling and Analysis

Upon completion of a trial, sample bottles were sealed inside Ziploc bags and placed in a cooler with ice. One or two times a day, the samples were brought back to the City of Kelowna's potable water lab and stored at 4°C. After all trials were completed for

a particular experimental phase, samples were repacked in coolers with cold packs and shipped back to Edmonton via two day courier service. Concentrated indicator stock solutions were also transported between Kelowna and Edmonton in coolers using two day courier service.

Sample viability for both indicator organisms was determined at University of Alberta laboratories. All samples were stored at 4°C prior to analysis. MS2 phage samples were enumerated before any *B. subtilis* samples were analyzed. This was because the spores remain viable for long periods of time whereas coliphage viability decreases rapidly with time. A trip control was performed to ensure no detrimental impacts on sample viability occurred due to transportation between Kelowna and Edmonton. The trip control consisted of microorganism stock suspension samples transported to and from the test site, with sample viability determined before and after transporting the samples. If the viability of the two samples was the same, then no degradation of the samples occurred as a result of the trip. Matching influent and effluent samples were prepared and plated at the same time to minimize any time-associated testing uncertainties that could potentially impact the measured survival ratio. Individual trials were tested randomly.

In analyzing MS2 phage trials, one influent sample and three effluent samples were tested for the concentration of viable MS2 phage. Three replicates were plated for the influent sample in all phases. Each effluent sample was tested in triplicate for the first experimental phase and in duplicate for the second and third phases of the study.

In *B. subtilis* trials, one influent sample and three effluent samples were tested to determine the concentration of viable *B. subtilis* spores. For both phase 1 and 2, influent

sample were tested in triplicate, while effluent samples were each tested with a single dilution series.

3.8 MANIPULATION OF INFLUENT TURBIDITY AND UV ABSORBANCE

3.8.1 Overview

Phase 3 trials involved manipulation of feed water turbidity and UV absorbance to determine their effect on RED. Turbidity causing or UV absorbing substances were mixed with unaltered lake water and maintained in suspension in a 700 L carboy. The suspension was injected into the feed water upstream of the first static mixer.

Turbidity levels were raised by injecting lake bottom sediment into the influent. Sediment was manually collected in the vicinity of the pipe intake of the Poplar Point pump house (City of Kelowna), by divers employed by the City of Kelowna. High turbidity events at Kelowna are thought to be due to storm events that change the currents in the lake and bring low quality water to the water intakes. The storm currents have the potential to resuspend lake sediment, which may contribute to the high turbidity of the water entering the intake. Therefore, the material settling out of the lake should be similar in composition and behavior to material that raises turbidity levels during storm events.

Red Rose orange pekoe brand tea was used to artificially raise the UV absorbance. Tea was prepared by heating unaltered lake water containing approximately 1.4 tea bags per liter of water. The $UVT_{254,\ 10\ mm}$ of the tea preparation was measured and this was used to estimate the required dilution of tea suspension to achieve the desired UV absorbance.

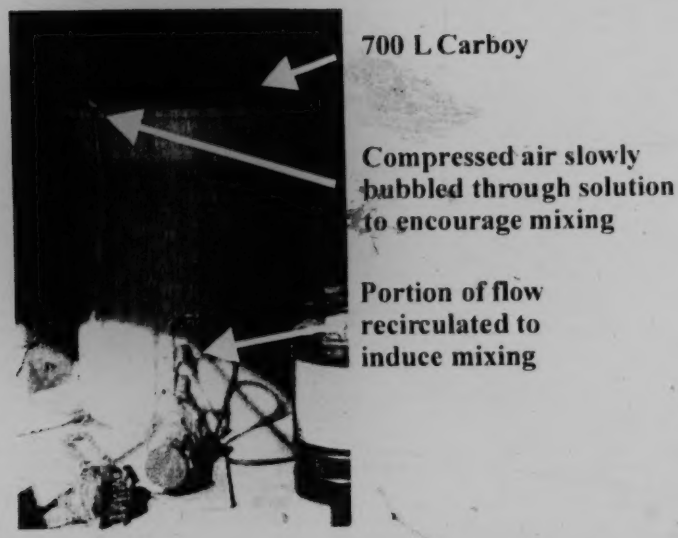
700 L Carboy
Compressed air slowly bubbled through solution to encourage mixing
Portion of flow recirculated to induce mixing

Figure 3-4: Photograph of the system used to hold and mix lake bottom sediment suspensions and tea suspensions that were injected into the influent in phase 3.

The suspensions were mixed using two methods (Figure 3-4). A recirculation pump was installed at the bottom of the carboy to promote mixing of the suspension. The recirculation loop was incapable of providing sufficient mixing alone, so compressed air was gently bubbled through the tank. This permitted large, heavy particles such as sand and grit to settle at the tank bottom while maintaining a near homogeneous suspension of the fine lake sediment particles. The premise for this methodology is that larger particles would settle rapidly, and would not enter the intake during a storm event.

3.8.2 Gravimetric Analysis

It is essential to properly characterize the feed water and additive substances to fully understand the mechanisms interfering with UV microbial reduction in the reactor. Standard Methods 2540 B, D and E (Greenberg et al. 1992) were used for the gravimetric analysis of diluted lake sediment injected into the influent stream. Dissolved solids are defined as the portion of solids that pass through a 2.0 μm or smaller nominal pore size, glass filter (Greenberg et al. 1992). Suspended solids are defined as the material remaining on the filter after drying. In this study, samples were dried at 103 to 105°C. Fixed solids are defined as the residue of total, suspended or dissolved solids after being ignited at 550°C.

3.8.3 Grain Size Distribution Analysis

The lake bottom sediment used in phase 3 was analyzed using a mechanical grain size analysis methodology. A three litre sample of the diluted lake sediment was dried at 103 to 105°C until a constant weight was obtained. The dry solids were resuspended in ELGA water on a magnetic stir plate and a water softening agent (Somat, manufactured by Henkel KGaA, Dusseldorf, Germany) was added in order to disperse smaller particles. The sediment suspension containing water softening agent was then washed through a #400 (38 μm) nylon mesh sieve using distilled water. This was done to prevent smaller particles from adhering to large particles as dust and subsequently being retained on larger sieves, thus skewing the grain size distribution. The retained solids were again dried at 103 to 105°C until a constant weight was obtained. The dried sample was then

passed through a series of sieves and the retained weight was recorded. The sieve progression used in this analysis was as follows:

- # 25 (710 μm)
- # 30 (600 μm)
- # 100 (150 μm)
- #400 (38 μm)

3.9 *BACILLUS SUBTILIS* METHODS

3.9.1 Spore Production

The procedure used to produce *Bacillus subtilis* spores is a modified version of that described by Craik (2001). *B. subtilis* strain 6633 was purchased from the American Type Culture Collection (ATCC, Manassas, VA). Part of the purchased stock was added to BBL nutrient broth (Becton Dickinson 11479) and incubated for 2 days at 35°C. Incubation in high nutrient broth produces the vegetative form of the bacterium. To promote sporulation, 1 mL of vegetative cell suspension and 15 mL of sterile, 0.05 M, pH 6.0, phosphate buffer was spread over solid media. The media consisted of approximately 275 mL of R2A agar in a 1 L flask. The flasks were incubated for 14 days at 35°C and then the spores were collected. Harvesting of the spores consisted of centrifuging the suspension 3 times in 0.05 M, pH 6.0 phosphate buffer (4500 x g, 15 min). The supernatant was removed after each centrifuge cycle and the remaining solids were resuspended in fresh buffer. Next, the suspension was maintained at 75°C in a water bath

for 1 hour and then centrifuged in phosphate buffer a final time. The resulting spore suspension was stored at 4°C and maintained as a mother stock. Spores used in biodosimetry testing were produced using the above process, but using the mother stock as starting material instead of the stock purchased from ATCC.

3.9.2 Enumeration

The viability of spores was assessed using a membrane filtration method (Barbeau et al. 1997; Craik 2001). Water sample dilutions were prepared by adding 10 mL of sample to 90 mL of sterile peptone dilution water (Greenberg et al. 1992). For bench scale experiments, the initial dilution was prepared by placing 5 mL of sample into 90 mL of dilution water, but all subsequent samples were prepared using 10 mL aliquots into 90 mL of dilution water. Using a vacuum filtration apparatus, the dilutions were filtered through pre-sterilized 47 mm x 0.45 µm membrane filters (part no. 66586, Gelman Sciences, Ann Arbor, MI). Filters were placed on tripticase soy broth saturated pads in Petri dishes. The dishes were maintained at 70 to 76°C for 20 minutes in an oven. This was done to kill all vegetative cells present on the filter. The filters were then incubated at 35°C for 22 to 24 hours. Each colony formed on the plate was counted as one viable spore in the original sample, and designated a colony forming unit (cfu).

3.10 MS2 PHAGE METHODS

3.10.1 Coliphage Production

MS2 phage strain 15597-B was purchased from the American Type Culture Collection (ATCC, Manassas, VA). An actively growing broth culture of the *E. coli* host was prepared 18 to 24 hours before propagating the coliphage. Approximately 1.0 mL of

ATCC 271 broth was added to a freeze dried phage vial. ATCC 271 bottom agar 100 mm diameter plates were then overlain with 2.2 mL of a top agar/MS2 phage broth mixture. The top agar was the same composition as the ATCC 271 bottom agar, but contained 5 g/L instead of 15 g/L of granulated agar. Approximately 10 drops of *E. coli* host broth was added to every litre of top agar and was maintained at 43 to 45°C until plates were ready to be poured. At a ratio of 10 to 1, top agar was added to the broth suspension containing MS2 phage, mixed and spread over the hardened surface of the bottom agar. Plates were incubated upside down for 18 to 24 hours at 37°C.

To harvest the MS2 phage from the plates, approximately 2 mL of phosphate buffered saline solution was added to each plate and then the top agar was harvested from the plate surface. The top agar was centrifuged at 1000 rpm for 25 minutes at 4°C, and the supernatant was passed through a presterilized, 0.22 μm membrane filter (part no. SVGSB1010, Millipore Corporation, Bedford, MA). The phage suspension produced from the freeze dried vial was termed the mother stock and was stored at 4°C. MS2 phage stock used in biodosimetry testing was produced using the same procedure as stated above, but using the mother stock as starting material, instead of the stock purchased from ATCC.

3.10.2 *Escherichia Coli* Production

Escherichia coli strain 15597 was purchased from the American Type Culture Collection (ATCC, Manassas, VA). This bacteria was used as the host for generating and enumerating MS2 coliphage. Approximately 0.5 to 1.0 mL of ATCC 271 broth was added to the dehydrated pellet. The rehydrated pellet was then transferred into a tube containing 5 to 6 mL of the broth medium and mixed. The suspension was then incubated

at 37°C on a shaker table for 24 hours. Subsequent *E. coli* suspensions were prepared by adding one drop of previously grown *E. coli* broth to a test tube containing 10 mL of ATCC 271 broth. The tube was mixed and incubated in the same manner as stated above.

3.10.3 Coliphage Enumeration

MS2 phage was enumerated in a procedure nearly identical to the method used for production. Cooled 100 mm diameter plates with hardened ATCC 271 bottom agar were warmed to room temperature and 2.2 mL of top agar combined with MS2 phage ATCC 271 broth suspension was poured on top. This mixture was prepared in the same manner described in the MS2 phage production procedure. The plates were incubated upside down at 37°C for 18 hours. Each plaque formed on the *E. coli* lawn was counted as one viable MS2 phage and designated as a plaque forming unit (pfu).

Water samples containing MS2 phage from biodosimetry tests, were diluted by adding 100 µL of the sample to a tube containing 900 µL of ATCC 271 broth and mixed, producing a phage concentration one tenth of the original sample concentration. To continue the dilution series, a 100 µL aliquot of diluted suspension was added to another tube containing 900 µL of ATCC 271 broth and mixed, reducing the concentration by a factor of ten. The process was repeated until the desired phage concentrations were achieved.

3.11 CALCULATIONS

3.11.1 Average UV Dose

The average germicidal UV dose in collimated beam exposures is referred to as "average UV dose" for the purposes of this thesis. This parameter was calculated by

multiplying the average germicidal irradiance (E_G) as calculated in section 3.6.2, by the exposure time (t):

$$\text{Average UV Dose} = E_G\, t \qquad (13)$$

3.11.2 Microorganism Inactivation

Microorganism inactivation in both collimated beam experiments and in the flow through UV reactor was examined as the log inactivation ratio, calculated as:

$$\textit{Log Inactivation} = -\log\left(\frac{N}{N_O}\right) = -(\log N - \log N_O) \qquad (14)$$

where N_0 was the average viable microorganism concentration before exposure to UV radiation and N was the average viable microorganism concentration after exposure to UV radiation. The value of log N was determined by the following equation:

$$\log N = \frac{1}{n}\left(\sum_{i=1}^{n} \log N_i\right) \qquad (15)$$

where N_i was the viability determined for the i^{th} replicate sample, and n was the number of replicate samples.

Standard error for the inactivation ratio was determined according to the following equations:

$$SE = \frac{s}{\sqrt{n}} \qquad (16)$$

$$SE\left(-\log\frac{N}{N_O}\right) = SE(\log N_O) + SE(\log N) \qquad (17)$$

where SE was the standard error, and s was the standard deviation for the inactivation ratio. The standard error was used for the error bars located on UV dose-inactivation plots referred to in subsequent sections.

3.11.3 Dose-Inactivation Model Parameter Estimation

Linear regression was performed using the Microsoft EXCEL™ 2000 regression analysis tool. Models were tested for statistical significance using residual analysis, normal probability plots and lack of fit testing according to standard statistical procedures (Draper and Smith 1998).

3.11.4 Confidence Intervals for Linear Models

The confidence interval (CI) for linear models was calculated according to the following equation:

$$95\%\ CI = \hat{Y}_0 \pm t(\upsilon, 0.975)\left\{1 + \frac{1}{n} + \frac{(X_0 - \bar{X})^2}{\Sigma(X_i - \bar{X})^2}\right\}^{\frac{1}{2}} s \qquad (18)$$

where $\hat{Y}_0$ is a value predicted using the model at point X_0, t is the critical value for a two tailed student t distribution for the specified degrees of freedom (υ) of the standard deviation, n is the number of observations the model is based on, $\bar{X}$ is the average independent variable value for all observations, and s is the standard deviation of the prediction errors (Draper and Smith 1998).

3.12 INTERPRETATION OF BIODOSIMETRY RESULTS

3.12.1 Mean Residence Time per Lamp

Residence time was calculated based on the volumetric flow rate and volume of the reactor. By defining the fluence rate zone for a single lamp as one quarter of the total reactor volume ($V_{Total\ Reactor}$), the hydraulic retention time for the fluence rate zone of 1 lamp ($HRT_{1\ Zone}$) was calculated by dividing the 1 lamp fluence rate zone volume by the flow rate (Q). Assuming the reactor was composed of four identical fluence rate zones arranged in series with the flow, the $HRT_{1\ Zone}$ was calculated as follows:

$$HRT_{1\ Zone} = \frac{V_{Total\ Reactor}}{Q \bullet 4} \qquad (19)$$

3.12.2 Reduction Equivalent Dose

Reduction Equivalent dose was determined by correlating the inactivation measured due to passage of microorganisms through the reactor to the UV dose-inactivation relationship determined in collimated beam experiments (Figure 2-7). In order to examine the influence of the number of lamps in operation during treatment, a normalized RED was calculated.

$$RED_{Normalized} = \frac{RED}{\#\ Lamps\ Operating} \qquad (20)$$

3.12.3 Reduction Equivalent Fluence Rate

Reduction equivalent fluence rate (REFR) is a useful parameter for examination of a reactor's hydrodynamic properties. It eliminates the influence of average exposure time due to changes in flow rate. This helps to isolate the effects of changing flow patterns on indicator inactivation. REFR was calculated as follows:

$$REFR = \frac{RED_{Normalized}}{HRT_{1\ Zone}} \qquad (21)$$

3.12.4 Understanding the Response of UV Reactors

There is currently no practical method of measuring the dose distribution of a UV reactor. However, it is possible to describe a reactor's dose distribution by relating the

information obtained using biodosimetry and comparing it to the extreme theoretical possibilities. The performance of a UV reactor is bounded by the behavior of ideal and worst case reactors (Wright 2001).

A worst case reactor delivers an infinite dose to a fraction of the water and a zero dose to the remaining fraction (Wright 2001). In such a reactor, the inactivation of the pathogen and surrogate organism is the same. Therefore, inactivation of the pathogen is calculated as:

$$- \log I_P = - \log I_C \qquad (22)$$

where I_P is the estimated inactivation ratio of the pathogen, and I_C is the measured inactivation ratio of the challenge organism (Wright 2001). However, if the UV dose-inactivation relationship of the pathogen and challenge organisms are not identical, they would result in different RED values. As the relative difference in UV resistance increases between a target and surrogate organism, the difference between RED values grows. A high resistance to UV will result in a higher RED than an organism with a low UV resistance.

In an ideal UV reactor, the hydraulic conditions consist of plug flow with perfect radial mixing. All microbes passing through the reactor receive the same UV dose (Wright 2001). Therefore, the dose delivered to the pathogen and the surrogate is the same, so the inactivation of the pathogen can be calculated as:

$$-\log I_P = -\log I_C \left(\frac{k_P}{k_C} \right) \quad (23)$$

where k_P is the first order inactivation coefficient for the pathogen, and k_C is the first order inactivation coefficient of the challenge organism (Wright 2001). The dose distribution of a reactor is a plot of the probability of occurrence that microorganisms receive a certain UV dose as depicted in Figure 3-5 (Wright 2001). Since all microorganisms have a 100 percent probability of receiving the same dose in an ideal reactor, no dose distribution exists.

In an ideal reactor, the RED of an organism is identical to the average dose in the reactor. This also results in the REFR of the reactor being identical to the average fluence rate in the reactor, as REFR is a mathematical transformation of the RED. All organisms,

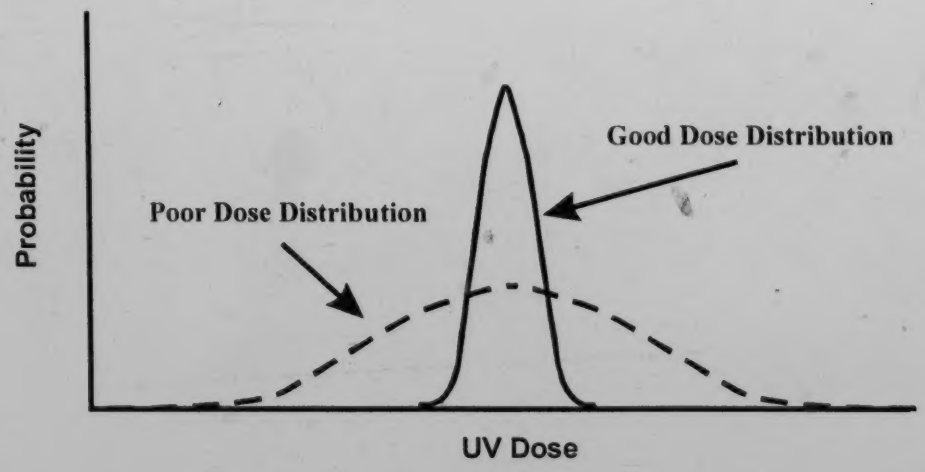

Figure 3-5: Graphical depiction of UV dose distributions for two reactors.

regardless of their respective UV resistances, will yield the same RED and REFR. The RED will change as either the average fluence rate, or the average exposure time in the reactor is altered. However, the REFR is independent of average exposure time, therefore it only responds to changes in the average fluence rate.

In an ideal reactor, the REFR is independent of flow rate and the number of lamps operating in the reactor. REFR is independent of flow rate, because average exposure time and the constant hydrodynamics of an ideal reactor ensure that an organism has a 100 percent probability of having the average exposure time. The REFR is independent of the number of lamps in operation, because the probability of an organism being exposed to the average fluence rate is 100 percent. This results in the plot of REFR versus flow rate being a horizontal line at the average fluence rate. If the plot for a non-ideal reactor deviates from this horizontal line as either flow rate or number of lamps in operation are altered, this indicates a change in the efficiency of the reactor with respect to the microbial reduction being achieved. Changes in reactor hydrodynamics or spatial fluence rate patterns have the potential to dramatically change the REFR, and therefore change the overall microbial reduction efficiency occurring in the reactor.

4 ANALYSIS OF UV REACTOR PERFORMANCE AT VARIOUS OPERATING CONDITIONS

4.1 INTRODUCTION

Biodosimetry is likely to become the standard method used for verifying the UV dose delivered in UV reactors to satisfy regulatory requirements. However, there are few published studies involving biodosimetric analysis of UV reactors using unfiltered surface water in the production of drinking water. Unfiltered surface water has the potential for high natural absorbance, high suspended solids, and increased variability of overall water quality relative to filtered water. These factors have the capacity to negatively influence reactor performance and therefore merit further research. This thesis was a case study, that provided insight into the performance of a commercially available UV reactor design used in treating unfiltered surface water for the production of potable water.

This chapter examines overall reactor performance as flow rate, number of lamps in operation, and type of indicator organism were varied. The objective was to identify operational conditions that produce less than optimal microbial inactivation and, from this, determine how RED could be increased most efficiently for unaltered Lake Okanagan feed water. In turn, this allowed for the development of some basic guidelines that can be applied during standard operation and maintenance of the reactor for feed waters with similar characteristics.

4.2 EXPERIMENTAL DESIGN

MS2 phage and *B. subtilis* were used as indicator organisms in phase 1 and phase 2 of this study. Different operating conditions were examined in each of the experimental phases (Table 4-1). The first phase was performed at high (1900 L/min) and low (380 L/min) flow rates. The number of lamps operating during the trials for phase 1 was set to the minimum (1 lamp) and maximum (4 lamps) number of operational lamps possible for the unit. In phase 2, the experiment was designed to examine a broader range of flow conditions with more precision than the first phase. Flow rates were set at 380, 760 or 1140 L/min and either 1 or 2 lamps were in operation. The number of lamps in operation for phase 2 was chosen based on the desired UV dose, as predicted by interpolation of results from phase 1 of the study.

Table 4-1: Operating conditions examined in challenge tests performed on the Sentinel ™ UV reactor treating unfiltered lake water (phases 1 and 2).

Phase	Flow		# of Lamps Operating	Target Turbidity (ntu)	Target UVT (%)
	(L/min)	(USgpm)			
1	380	100	1 or 4	ua[a]	ua
	1900	500	1 or 4	ua	ua
2	380	100	1 or 2	ua	ua
	760	200	1 or 2	ua	ua
	1140	300	1 or 2	ua	ua

[a]ua: denotes unaltered lake water

Power-off process controls for the study consisted of seeding the reactor with indicator organisms when no lamps were in operation. The purpose of the power off process controls was to determine if there were any sources of reduction in cfu or pfu, other than UV light exposure that would contribute to the determination of inactivation. Potential concerns included adsorption of indicator organisms to equipment surfaces, and clumping or agglomeration of organisms between influent and effluent sampling ports. Adsorption would result in physical microbial removal from the flow stream, inflating the measured log inactivation. Clumping of organisms between the sampling ports would not change microbe concentrations, but clumps containing more than one organism would be counted as one colony or plaque, artificially deflating the cfu or pfu counts. In phase 1, two controls were performed at each flow rate examined for each biodosimetric indicator. In phase 2, one control was performed for each biodosimetric indicator at all three flow rates investigated.

4.3 FEED WATER QUALITY RESULTS

The water quality experienced during the two testing periods was stable and typical of summer and fall unaltered Kelowna water. Water samples were taken daily during the testing period. Daily tests included pH, total alkalinity, total hardness, turbidity, UV absorbance at 254 nm, colour, sulphate and chloride (Table 4-2). Turbidity remained below 0.55 ntu for all trials. The $UVT_{254\ nm,\ 10\ mm}$ of the water, ranged from 86.7% to 87.5% for phase 1 and from 87.5% to 88.3% for phase 2.

Table 4-2: Summary of water quality testing of unaltered lake water used as feed water in challenge tests performed on the Sentinel™ UV reactor (phases 1 and 2).

Parameter	Phase 1	Phase 2
pH	8.40 to 8.60	8.43 to 8.52
Alkalinity-Total (mg/L as $CaCO_3$)	110 to 113	110 to 114
Hardness-Total (mg/L as $CaCO_3$)	119 to 122	120 to 122
Turbidity (ntu)	0.282 to 0.379	0.343 to 0.547
UV absorbance at 254nm (abs/10 mm)	0.058 to 0.062	0.054 to 0.058
$UVT_{254\ nm,\ 10\ mm}$ (%/10 mm)	87.5 to 86.7	88.3 to 87.5
Colour (Pt-Co units)	7 to 10	7 to 9
Sulphate (mg/L SO_4^-)	33.8 to 35.4	32.5 to 34.4
Chloride (mg/L Cl^-)	3.20 to 3.93	4.96 to 5.41

4.4 UV DOSE-INACTIVATION RELATIONSHIPS

A standard curve was prepared for each set of trials. The UV dose-inactivation relationship was determined by applying linear regression to plots of the log inactivation ratio versus average germicidal UV dose. At high log inactivation levels, some collimated beam experiments displayed a tendency for little to no additional inactivation to occur as the UV dose was increased. This effect is known as tailing. Data displaying tailing effects were not included in the models.

MS2 phage is a single stranded RNA virus and therefore its UV dose–inactivation curve should follow first order kinetics (Harm 1980). Figure 4-1 shows the average germicidal UV dose plotted against log inactivation and the associated standard error observed for MS2 phage in both experimental phases. The β_0 and β_1 values for MS2 phage in phase 1 were 0.115 and 0.0365 ($p=2.5\times10^{-7}$), respectively. The β_0 and β_1 values for MS2 phage in phase 2 were 0.333 and 0.0390 ($p= 5.5\times10^{-7}$), respectively. The models

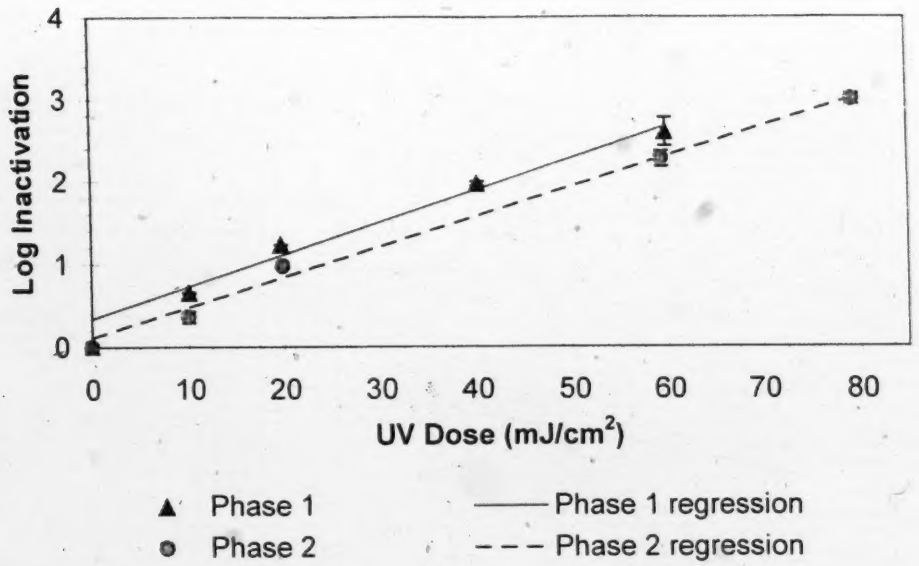

Figure 4-1: UV dose-inactivation relationship of MS2 phage suspended in unaltered lake water and exposed to UV radiation in a collimated beam apparatus (phases 1 and 2).

for both phases have positive y intercepts and were linear for doses up to 60 mJ/cm^2 for phase 1 data, and up to 80 mJ/cm^2 for phase 2 data. The r^2 values for the models were 0.95 for phase 1 and 0.99 for phase 2. In phase 1, no tailing was detected for the dose range examined, while in phase 2 tailing was observed at doses of 120 mJ/cm^2 and higher (Figures A-1 and A-2). Both models were statistically significant. Table 4-3 presents the UV dose-inactivation relationships in tabular form along side data from relationships found in literature. The UV dose-inactivation relationships determined in this study were comparable to relationships reported in the reviewed literature (Table 4-3).

Table 4-3: Summary of UV dose-inactivation relationships for MS2 phage suspended in unaltered lake water and exposed to UV radiation in a collimated beam apparatus (phases 1 and 2), accompanied by the dose ranges reported in literature.

Log Inactivation				Source
1	2	3	4	
UV Dose (mJ/cm^2)				
17	43	68		Phase 1
24	52	79		Phase 2
4 to 25	13 to 50	21 to 75	29 to 100	Range from literature reviewed in Table 2-2

MS2 phage inactivation typically follows the Chick-Watson model. However, models determined in this thesis were not forced through zero as was done in some other biodosimetry studies involving MS2 phage (Havelaar et al. 1991; Nieuwstad and Havelaar 1994). Giving freedom to the y-intercept demonstrates the error due to the testing methodology itself.

Other studies have also displayed a tendency of MS2 phage UV dose-inactivation curves to return positive y-intercepts (Havelaar et al. 1990). There are several possible reasons why this occurs. One explanation is that the suspensions were subjected to inhomogeneous irradiance distributions (Havelaar et al. 1990). However, in this study, radial variations in the collimated UV beam were accounted for by the germicidal irradiance calculation. Additionally, microbial suspensions were constantly mixed during exposure to UV radiation. Another possibility is that the phage suspension may have contained sufficient organic matter to allow some particle association such that the

viruses had different degrees of protection from the UV radiation (Havelaar et al. 1990). Absorption of phage onto the stir bar, Petri dish or other items used in testing and enumeration could also contribute to positive y intercepts. However, UV exposed and control samples were treated identically to correct for the impact of absorption on testing supplies.

The UV resistance of *B. subtilis* was highly variable between the two phases. The average germicidal UV dose was plotted against the log inactivation ratio and the associated standard error observed in phases 1 and 2 (Figure 4-2). It has been shown that *B. subtilis* frequently displays a shoulder at low UV doses (< 5 mJ/cm^2), due to multi-hit or series event kinetics and also undergoes linear log inactivation at higher doses (Severin et al. 1983; Sommer and Cabaj 1993). In phase 1, the *B. subtilis* β_0 and β_1 values were 0.128 and 0.131 ($p=1.1x10^{-5}$), respectively, and in phase 2, the β_0 and β_1 values were -0.675 and 0.279 ($p= 3.1x10^{-7}$), respectively. The r^2 values for the models were 0.90 for phase 1 and 0.98 for phase 2. The higher precision of the phase 2 model is attributable to the practical experience gained in working with the spores in phase 1. Table 4-4 presents the UV dose-inactivation relationship in tabular form alongside the UV dose-inactivation relationships encountered in literature. The spores used in this experiment were slightly less resistant to UV light than those used the previous studies examined. However, the dependency of UV resistance on generation methods reported in other studies, may explain why this occurred (Qualls et al. 1989; Sommer and Cabaj 1993).

A tailing effect was observed with *B. subtilis* at log inactivation levels of approximately 5.9 and 4.2 for phases 1 and 2, respectively (Figures A-3 and A-4). Only

Table 4-4: Summary of UV dose-inactivation relationships for *B. subtilis* spores suspended in unaltered lake water and exposed to UV radiation in a collimated beam apparatus (phases 1 and 2), accompanied by the dose ranges reported in literature.

Log Inactivation				Source
1	2	3	4	
UV Dose (mJ/cm^2)				
7	14	22	29	Phase 1
6	10	13		Phase 2
11 to 90	18 to > 90	24 to >90	30 to >90	Range from literature reviewed in Table 2-1

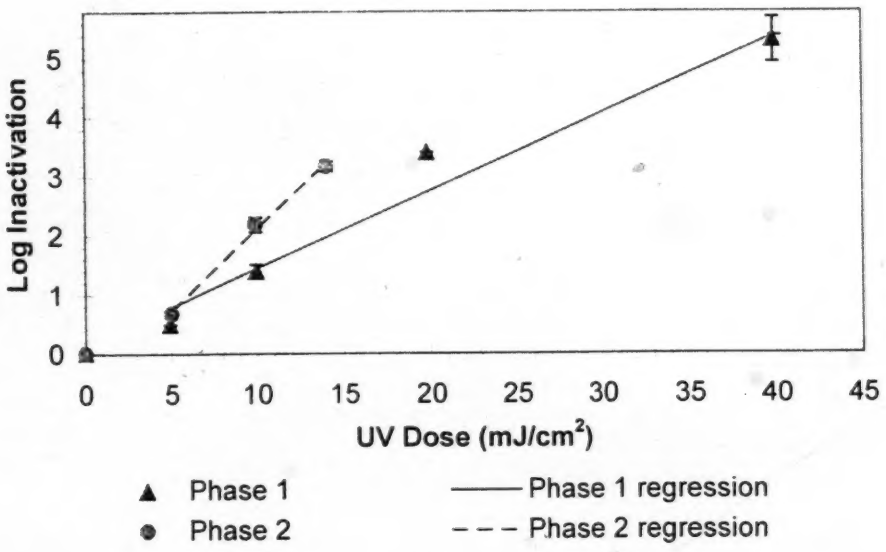

Figure 4-2: UV dose-inactivation relationship of *B. subtilis* spores suspended in unaltered lake water and exposed to UV radiation in a collimated beam apparatus (phases 1 and 2).

the linear portions of the UV dose-inactivation curves were used to determine RED values in this study. However, the presence of tailing requires further explanation. The tailing may be due to the presence of a small sub-population of indicator organisms that are highly resistant to UV radiation, or it may be an artifact of the experimental procedure used which allowed some organisms to escape exposure to UV (Cerf 1977). Sub-populations could develop high resistance to UV radiation due to genetic or morphological variations (Cerf 1977). This could be in the form of UV resistant spore or oocyst coats, or strong repair mechanisms. Additionally, microorganisms could theoretically avoid UV exposure because of incomplete mixing in the reaction vessel, shielding of organisms by the stir bar, shielding due to clumping and high microbe densities, and shielding due to adsorption to, or blocking by, particulate matter in the suspension.

Tailing has been observed in studies involving *C. parvum* and *G. muris* (Craik et al. 2000; Craik et al. 2001). If tailing is characteristic of parasites in natural waters and not simply an effect of testing procedures, it will be difficult to achieve inactivation levels above the tailing levels using UV radiation alone. Additional studies need to be performed relating tailing effects of indicator organisms and pathogens before the non-linear portion of UV dose-inactivation curves can be used confidently to determine REDs for biodosimetry.

4.5 INACTIVATION OF MS2 PHAGE IN THE UV REACTOR

Biodosimetry trials performed using MS2 phage as the indicator organism revealed several important operational issues for the Sentinel™ UV reactor. Figure 4-3 shows log inactivation, RED, and REFR plotted against flow rate for phase 1. Phase 2

plots of log inactivation, RED and REFR versus flow rate are given by Figure 4-4. Detailed information from trials using MS2 phage is given by Tables B-1 to B-4.

The analysis process can be visualized by examining the change in data values and patterns as one progresses from the inactivation plot to the RED and finally to the REFR figure. As expected, inactivation and RED decreased as flow rate was increased. This result was due to the reduction in exposure time as flow rate increases, which results in a lower average UV dose applied and therefore, decreased inactivation. Of note are the two data points at 380 L/min and 4.9 log inactivation (Figure 4-3 a). These two points fall above the confirmed linear range of the UV dose-inactivation curve and therefore were not included in subsequent plots. The effect of having a positive y-intercept is also demonstrated by the data point for one lamp in operation at 1900 L/min with 0.32 log inactivation (Figure 4-3 a). The positive log inactivation was converted to an RED of -0.4 mJ/cm^2, because the UV dose-inactivation y-intercept was 0.33 log units (Figure 4-3 b). A negative RED value implies an increase in the number of viable microbes upon passage through the reactor. It may not be appropriate to correlate log inactivations below the y-intercept of the dose-inactivation relationship determined in collimated beam experiments. The correlation is inappropriate because negative RED values result, which are not an accurate measure of the microbial reduction occurring in the UV reactor. Conversely, if that correlation is made, more conservative values result, which are acceptable from a public health stand point.

RED is subsequently converted into REFR. Conversion to REFR is useful, because it allows simple identification of changes in the dose distribution. Trends are easier to identify using REFR than using log inactivation or RED, because REFR is

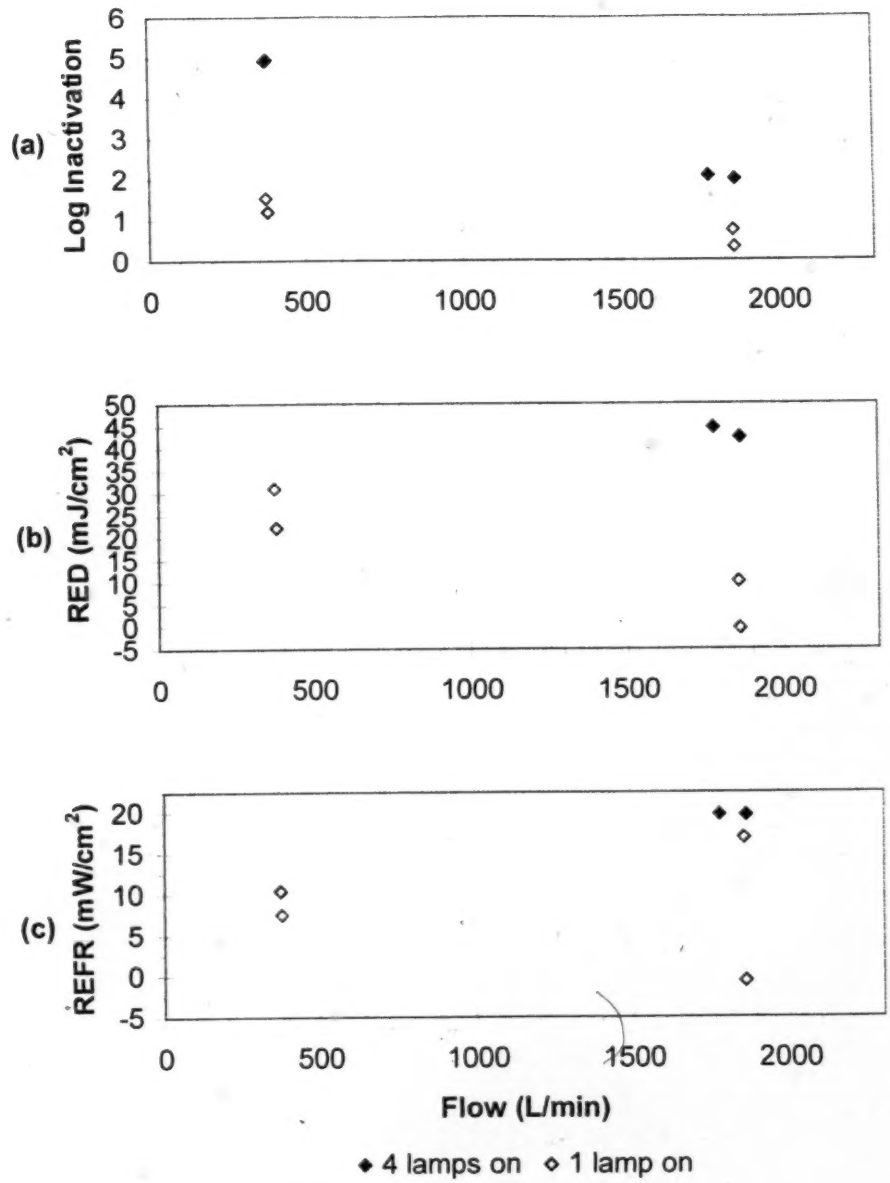

Figure 4-3: Log inactivation (a), reduction equivalent dose (b), and reduction equivalent fluence rate (c) of MS2 phage as a function of flow rate, calculated from challenge tests performed on the Sentinel™ UV reactor treating unaltered lake water (phase 1).

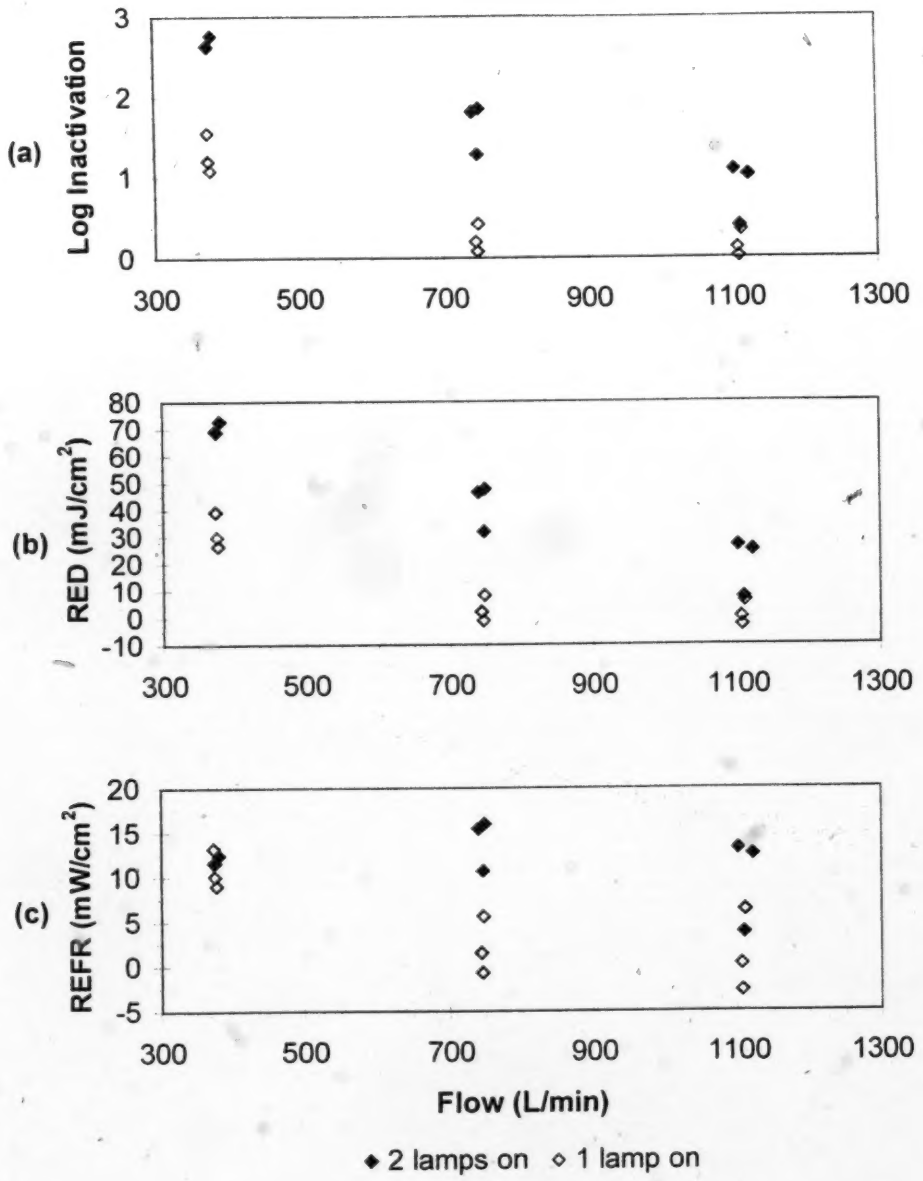

Figure 4-4: Log inactivation (a), reduction equivalent dose (b), and reduction equivalent fluence rate (c) for MS2 phage as a function of flow rate, calculated from challenge tests performed on the Sentinel™ UV reactor treating unaltered lake water (phase 2).

independent of changes in the number of lamps in operation and the average exposure time. In a plot of REFR versus flow rate a deviation from a horizontal line indicates a change in the reactor's dose distribution, as discussed in section 3.12.4. Nevertheless, when the range of log inactivations for replicate trials includes the value calculated to be the y-intercept of the UV dose-inactivation curve, the variability of challenge test replicate trials tends to be inflated as was observed for RED (Figure 4-3). At a flow rate of 1900 L/min with 1 lamp in operation, the REFR was equal to the RED divided by an exposure time of approximately 0.6 seconds. At these operating conditions, an RED of -0.4 (Figure 4-3 b) translates to a REFR of -0.6 mW/cm^2 (Figure 4-3 c).

All log survival ratios determined were greater than zero for both phase 1 and phase 2. However, log inactivation values near zero translate to negative RED and REFR values, due to the positive y intercepts returned from linear modeling of the UV dose-inactivation relationships. The small number of data points available made it difficult to identify any trends for the phase 1 data, but REFR proved invaluable for phase 2, where more data was available.

REFR tended to increase when the number of lamps in operation was increased. This effect was magnified when flow rate was increased. In phase 2 when two or more adjacent lamps were in operation, the REFR was nearly independent of flow rate (Figure 4-4 c). On the other hand, in phase 2 when 1 lamp was in operation, the REFR decreased as flow rate was increased (Figure 4-4 c). In phase 2, at a flow rate of 1140 L/min with 2 lamps in operation, the average REFR was 9.9 mW/cm^2, while it was only 1.3 mW/cm^2 with 1 lamp in operation (Figure 4-4 c). A reduction in REFR indicates a widening of the reactor's dose distribution. This suggests that the dose distribution in the reactor remained

relatively constant when 2 or more adjacent lamps were in operation, while the dose distribution tended to widen when flow rate was increased when 1 lamp was in operation. More consistent microbial reduction was achieved when 2 or more adjacent lamps were operated in the reactor, relative to operation with 1 lamp on. Additionally, the results suggest that the dose distribution narrowed as the number of lamps in operation increased. No strong trends regarding REFR behavior with flow rate could be derived from the phase 1 results, due to the limited number of data points.

Effects such as short circuiting, axial dispersion and imperfect radial mixing could potentially have affected the efficiency of microbial inactivation occurring in the reactor. The potential for reducing process efficiency is related to the number of lamps in operation. This is best explained by following the path of a single microbe traveling through the reactor. With one lamp in operation, it may be possible for a microorganism to predominantly travel through low fluence rate zones along the reactor wall. Particles taking this path would only be exposed to low fluence rate zones and receive a UV dose lower than the average. As more microbes take this pathway, the dose distribution of the reactor would widen and overall inactivation would decrease. The baffles located between the lamps, in combination with operating 2 or more adjacent lamps, appeared to decrease the likelihood of this pathway. A microbe traveling near the reactor wall past the first lamp will encounter the baffle before passing into the fluence rate zone of the second lamp. The baffle tends to redirect microorganisms skirting along the wall towards the center of the reactor, exposing the microorganism to the high fluence rate levels that occur closer to the lamp. Having two adjacent fluence rate zones separated by baffles, reduces the probability of a microbe passing through the reactor and only being exposed

to low fluence rate levels, therefore narrowing the dose distribution and improving the performance of the reactor.

Previous studies have found that the effects of poor mixing across fluence rate gradients can be minimized by adding baffles to encourage mixing, directing flow perpendicular to lamp axes, or making the distance across the gradients very small relative to the fluence rate zone length (Qualls and Johnson 1985). Increasing the number of adjacent lamps in operation increases the fluence rate zone length relative to the distance across fluence rate gradients and also increases the number of baffles actively encouraging radial mixing in the fluence rate zone.

For a given set of operating conditions, the consistency of hydraulic conditions and spatial fluence rate patterns occurring in the UV reactor can be examined by comparing the reproducibility achieved in collimated beam experiments and that achieved in biodosimetry tests. For MS2 phage replicate trials performed using the collimated beam apparatus in phase 2, the standard error ranged from 0.01 to 0.17 log inactivation units (Figure 4-1). For replicate MS2 phage trials from biodosimetry challenge tests in phase 2, performed using the UV reactor, the minimum and maximum standard errors observed were 0.03 and 0.22 log inactivation units, respectively (Figure 4-4 a). The variation in collimated beam experiments was comparable to that observed in challenge tests performed on the UV reactor. Since low standard error in collimated beam experiments translates to repeatability, the low standard error observed in UV reactor experiments suggests that spatial fluence rate patterns and hydrodynamics for a given set of operating conditions were also repeatable.

4.6 INACTIVATION OF *BACILLUS SUBTILIS* SPORES IN THE UV REACTOR

B. subtilis trials yielded different results than MS2 phage trials. Unfortunately, there was less data available for analysis than with MS2 phage trials, due to factors relating to the large difference in UV resistance of the spores used in phases 1 and 2. Log inactivation, RED, and REFR were plotted against flow rate in Figure 4-5 (phase 1) and in Figure 4-6 (phase 2). Detailed information from trials using *B. subtilis* is given by Tables C-1 to C-4.

Many of the *B. subtilis* trials resulted in log inactivation levels that were greater than the linear portion of the UV dose-inactivation curve and, for this reason, were not included in the graphical analysis of reactor performance. For phase 1, in two of the eight trials with *B. subtilis* the log inactivation measured in the UV reactor was above the linear portion of the UV dose-inactivation curve for this batch of spores. These were due to operation with 4 lamps on at the lowest flow condition (380 L/min), which resulted in the highest UV doses recorded. Unfortunately, the UV resistance of the spore batch used in phase 2 was much lower than in phase 1, resulting in much of the data being excluded from analysis (Figures A-4 and A-5). UV resistance of *B. subtilis* spores have been shown to be dependant on the methodology used in their cultivation (Qualls et al. 1989; Sommer and Cabaj 1993). In phase 2, all three trials performed at the lowest flow (380 L/min), with 2 lamps in operation showed plate counts that were beyond quantitation and not included in the plots. Samples from one trial at 780 L/min and one at 1140 L/min with 2 lamps in operation were contaminated and therefore these trials were excluded

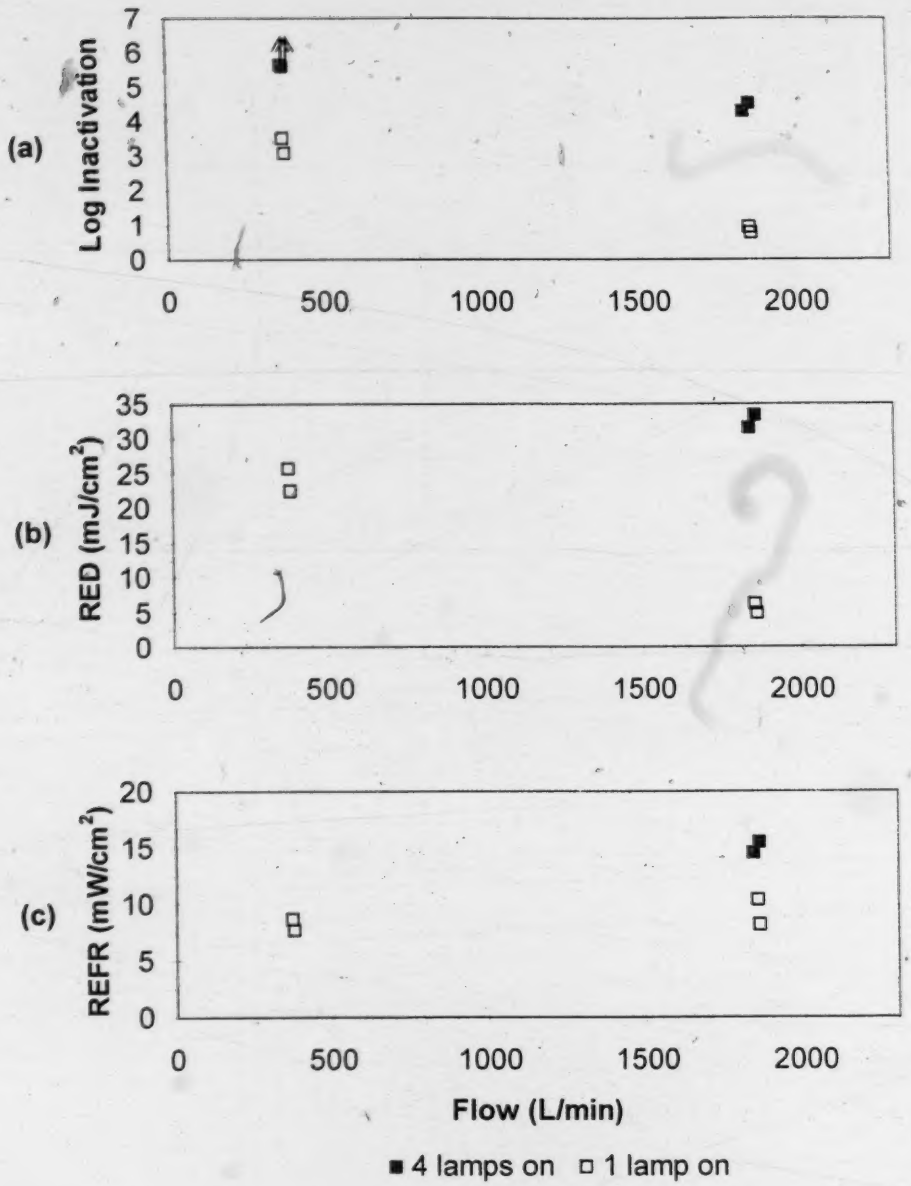

Figure 4-5: Log inactivation (a), reduction equivalent dose (b), and reduction equivalent fluence rate (c) for *B. subtilis* spores as a function of flow rate, calculated from challenge tests performed on the Sentinel™ UV reactor treating unaltered lake water (phase 1). Arrows indicate effluent plate counts were beyond quantitation.

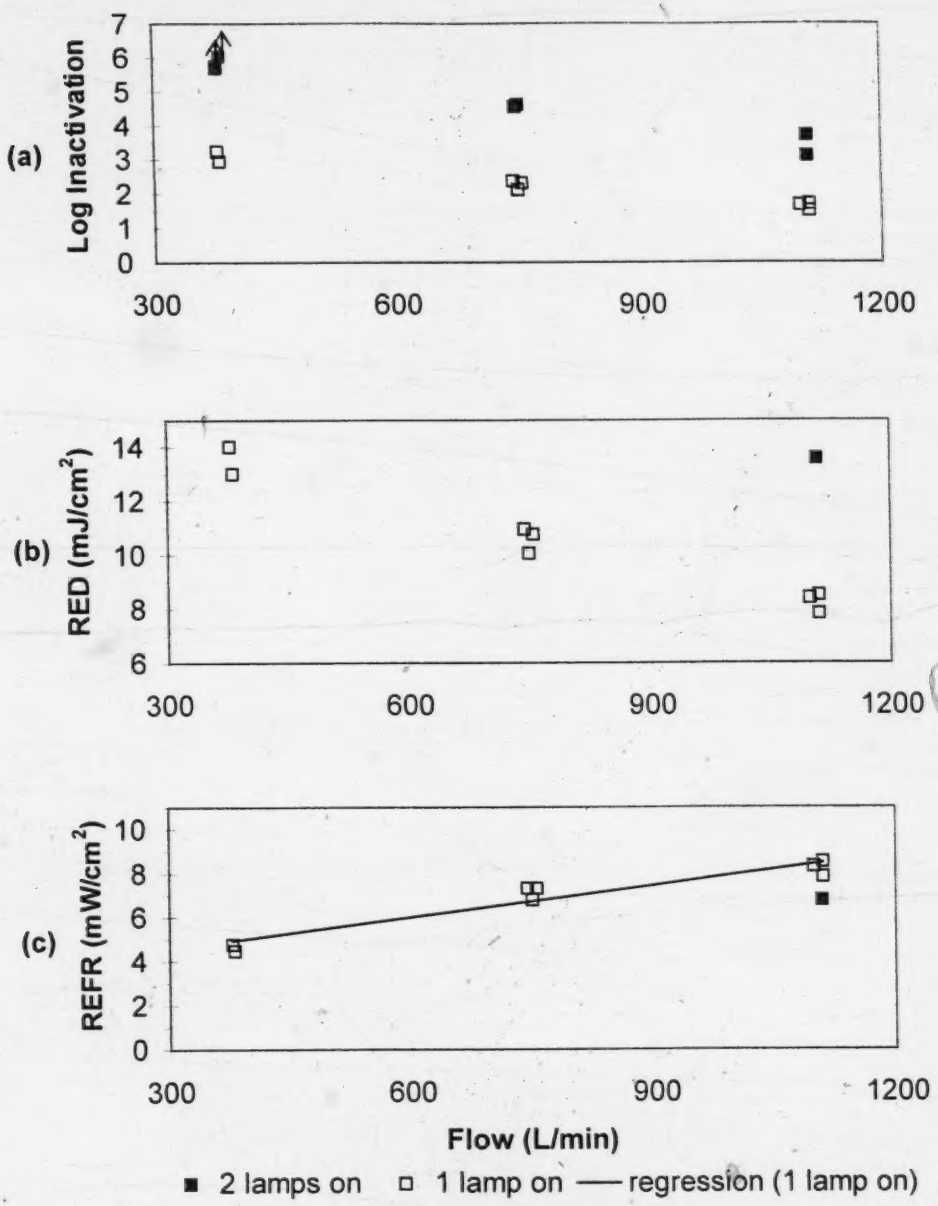

Figure 4-6: Log inactivation (a), reduction equivalent dose (b), and reduction equivalent fluence rate (c) for *B. subtilis* spores as a function of flow rate, calculated from challenge tests performed on the Sentinel™ UV reactor treating unaltered lake water (phase 2). Arrows indicate effluent plate counts were beyond quantitation.

from the analysis. Four of the remaining 13 trials in phase 2, resulted in log inactivation levels above the linear portion of the UV dose-inactivation curve.

In phases 1 and 2, inactivation and RED decreased as the flow rate was increased. This was expected, because the average exposure time within the reactor decreases as flow rate increases, thus lowering the average UV dose delivered. In phase 1 with one lamp in operation, the average REFR increased marginally from 8.2 mW/cm^2 at 380 L/min, to 9.3 mW/cm^2 at 1900 L/min (Figure 4-5 c). However, it is difficult to draw statistically significant conclusions from only four data points. In phase 2 with 1 lamp in operation, the REFR increased linearly with flow rate (Figure 4-6 c). Replicate trials were tightly grouped around the average values. Linear regression on the phase 2, 1 lamp in operation data, showed a statistically significant REFR increase ($r^2 = 0.92$) of 74% (3.6 mW/cm^2) over the flow range examined. According to this data the reactor performance, with respect to microbial reduction, improved with increasing flow rate.

Operation with 1 lamp on did not have the same effect on *B. subtilis* as it did with MS2 phage. It does not appear that operation with two lamps on resulted in a larger REFR for *B. subtilis*. In phase 1, operation with 4 lamps in operation as opposed to 1 lamp in operation resulted in a 62% increase in REFR (5.8 mW/cm^2) as demonstrated by Figure 4-5 c, but this effect was not duplicated with 2 lamps in operation in phase 2 (Figure 4-6 c). The large number of trials with *B. subtilis* that resulted in log inactivations that were greater than the linear portion of the UV dose-inactivation curve, occurred at the high end of UV doses tested, which in most cases had multiple lamps in operation. As a result, there is a limited amount of useable data for trials using *B. subtilis*, with 2 or more lamps in operation.

Response of MS2 phage and the different response by *B. subtilis* to operation of the unit with one lamp on is the opposite of what theory would predict. The results for *B. subtilis* with 1 lamp in operation are exactly opposite to those obtained with MS2 phage. *B. subtilis* has a steeper UV dose-inactivation relationship than MS2 phage and, therefore, should be more sensitive to imperfect mixing across fluence rate gradients and changes in the dose distribution of the reactor. However, the exact cause of this departure from theory cannot be adequately explained without further experimentation.

One possible explanation as to why the REFR increased with flow rate for *B. subtilis* trials with 1 lamp in operation relates to the presence of spore clumps during exposure to UV radiation in the UV reactor. It may be possible that *B. subtilis* spores were clumped together upon entering the reactor and as flow rate was increased, the resulting increase in particle shearing separated some of the clumps. Clumped microorganisms have the potential to partially shield microbes deep within the clump, because UV light must first pass through solid material before reaching the microbe. As flow rate was increased, the percentage of spores entering the reactor as part of a clump may have decreased, resulting in a smaller percentage of microbes being protected from UV light. The presence of clumped spores at low flow rates and a reduction in the number of clumps as flow rate was increased could potentially result in an increase in REFR as flow rate was increased. The enumeration procedure involved vigorous vortexing which potentially broke up all existing clumps in water samples, such that each enumerated colony originated from a single spore. However, the experimental apparatus and testing procedure were designed to discourage the passage of clumped microorganisms and increase the likelihood of only discrete microorganisms passing

through the reactor. The spore stock was vortexed for 2 minutes to brake up existing clumps. Next, the concentrated spore stock was diluted three times to encourage uniform dispersion in the reactor influent. Immediately preceding the UV reactor, the influent passed through a static mixer, which further encouraged the passage of discrete spores and reduced the probability of microorganisms entering the reactor as clumps. Further experimentation is required to determine the viability of this explanation.

The increased REFR with increased flow rate observed in phase 2 could be explained by reactor hydraulics becoming closer to plug flow with perfect radial mixing (Figure 4-6 c). More complete radial mixing, approaching plug flow conditions, and minimization of short circuiting all have the potential to make the distribution of doses delivered to indicator organisms narrower. Narrowing the dose distribution of a reactor generally results in an increase in the overall efficiency of the microbial reduction process. However, this explanation does not explain why *B. subtilis* responded differently to running the UV reactor with 1 lamp in operation, relative to MS2 phage.

To further illustrate the influence of dose distribution on the microbial reduction efficiency, consider a UV reactor operating so that the average UV dose delivered was equal to the UV dose required to cause 3 log inactivation of a particular microorganism. If 1,000,000 microbes receive a dose sufficient for 2 log inactivation, 10,000 of these microbes would remain viable. Three log inactivation of 1,000,000 microbes would result in 1,000 microbes remaining viable, while 4 log inactivation would result in 100 microbes remaining viable. Reduction of the UV dose from 3 log to 2 log would result in an additional 9,000 microbes remaining viable. On the other hand, increasing the log inactivation from 3 log to 4 log would result in an additional 900 microbes inactivated.

The portion of microorganisms exposed to lower than average UV doses will have a larger impact on the overall inactivation achieved than the microbes exposed to UV doses higher than the average. Operating a UV reactor at a wide dose distribution exposes a larger percentage of microorganisms to low UV doses than occurs when operating at a narrow dose distribution. If both dose distributions have the same average UV dose, the operation of a UV reactor at a wide dose distribution will generally result in decreased inactivation relative to operation at a narrow dose distribution.

The limited number of data points for *B. subtilis* trials where 2 or more lamps were in operation made it difficult to make strong comparisons regarding the affect of number of lamps in operation on the REFR. In phase 1, the *B. subtilis* REFR was 5.8 mW/cm^2 larger when 4 lamps were operated versus 1 (Figure 4-5 c). The increase in REFR was potentially due to enhanced radial mixing induced by the baffles between operating lamps, which would theoretically narrow the dose distribution of the reactor. However, these observations are only based on 4 data points. For *B. subtilis* in phase 2, at a flow of 1140 L/min the REFR with 2 adjacent lamps in operation was 1.5 mW/cm^2 less than observed for trials performed at the same flow rate with 1 lamp in operation (Figure 4-6 c). However, there was only one data point available for analysis for trials performed with *B. subtilis* with two lamps in operation. The limited data makes it difficult to make meaningful conclusions on the effect of number of lamps in operation using data from *B. subtilis* trials.

As the UV resistance of the microorganism increases, the measured RED will increase (Cabaj et al. 1996). In phase 1, the REFR determined for *B. subtilis* was approximately 15 mW/cm^2 at 1900 L/min with 4 lamps in operation, and roughly 20

mW/cm^2 for MS2 phage at the same operating conditions. In phase 2, the REFR determined using *B. subtilis* was approximately 5 mW/cm^2 at 380 L/min with 1 lamp in operation, and about 12 mW/cm^2 for MS2 phage for the same operating conditions. MS2 is more resistant to UV radiation than *B. subtilis*. The microorganism with the lower resistance to UV will be more susceptible to wide dose distributions in a reactor, and will subsequently yield a lower REFR. Comparing the spore data to MS2 phage with multiple lamps in operation, the spores returned lower REFRs than MS2 phage, which is consistent with the theory (Wright 2001).

The differences between the reproducibility achieved in collimated beam experiments and that achieved in biodosimetry tests helps to describe the consistency of hydraulic conditions and spatial fluence rate patterns occurring in the UV reactor for a given set of operating conditions. For replicate trial data in the *B. subtilis* phase 2 linear model performed using a collimated beam apparatus, the observed standard errors were between 0.08 and 0.12 log inactivation units (Figure 4-2). For replicate data from *B. subtilis* biodosimetry challenge tests performed on the UV reactor in phase 2, the standard errors were between 0.06 and 0.30 log inactivation units (Figure 4-6 a). The variation in collimated beam experiments was comparable to that observed in challenge tests performed on the UV reactor. Since low standard error in collimated beam experiments translates to repeatability, the low standard error observed in UV reactor experiments suggests that spatial fluence rate patterns and hydrodynamics for a given set of operating conditions were also repeatable. This observation is in agreement with findings from MS2 phage experiments.

4.7 INACTIVATION IN POWER-OFF PROCESS CONTROLS AND TRIP CONTROLS

Process controls were performed in phase 1 and phase 2 using both MS2 phage and *B. subtilis* spores. The purpose of the process controls was to confirm that there were no other factors other than exposure to UV light that was influencing measured microorganism viability. Ideally, there would be no measurable change in viability between influent and effluent samples, with only random variability centered about zero.

The process controls conducted for MS2 phage showed mixed results. In phase 1, the average inactivation was 0.03 with a standard error of 0.08. Phase 2 process controls yielded average log inactivation of 0.18 with a standard error of 0.06. Standard t-tests showed that the mean log inactivation was statistically equivalent to zero in phase 1, but not in phase 2. Though not necessarily statistically equal to zero, the power-off process control inactivations were relatively low when compared to the variability of MS2 phage inactivations induced by exposure to UV light in the UV reactor when 1 or more lamps were in operation. The process controls suggest that there were no major factors other than the action of UV light, which caused MS2 phage reduction between the influent and effluent sampling ports.

For both phase 1 and 2 trials performed using *B. subtilis* spores, the deviation from ideal control behavior was small and thus acceptable. Process controls conducted for phase 1 showed an average log inactivation of 0.0 with a standard error of 0.054. Phase 2 process controls had an average log inactivation of -0.14 and a standard error of 0.11. Standard t-tests show that both these mean log inactivations were statistically equivalent to zero. The process controls for both phases suggest that there were no major

factors other than the impact of UV light that caused microbial reduction of *B. subtilis* spores.

Trip controls were performed in phase 1 and phase 2 using both MS2 phage and *B. subtilis* spores. The purpose of the trip controls was to confirm that transportation and handling of the indicators was not detrimental to test results. Ideally there would be no difference in the viability of the microorganism stock solution for tests performed before and after the trip. Unfortunately, practical considerations prevented the immediate determination of sample viability. As expected, a decrease in the viability of MS2 phage was observed between the time of the UV reactor challenge tests and microorganism enumeration. The viability of *B. subtilis* spores remained relatively stable over the same period. Additional study should be performed to determine the influence of time lag between generation of the indicator organisms and the experimental determination of UV dose-inactivation of MS2 phage and *B. subtilis*, on inactivation relationships. However, inactivation for a trial was determined by comparing the relative concentrations in influent and effluent samples. Additionally, the viability of influent and effluent water samples for a given trial were always tested concurrently. This was done to ensure any reduction in viability occurred proportionally in influent and effluent samples so that measured inactivation would not be affected. The power-off process controls for both indicators returned inactivation values of approximately zero, which indicates that any viability loss due to transportation and handling was the same in influent and effluent samples and thus did not influence inactivation results.

4.8 COMPARISON OF INDICATOR ORGANISMS

The two biodosimetric indicators highlighted different aspects of reactor performance. Data from MS2 phage trials suggested that there was improved efficiency with respect to microbial reduction when running the unit with 2 or more adjacent lamps in operation, relative to operation with a single lamp. *B. subtilis* data suggested there was improved efficiency, with respect to microbial reduction, when flow rate was increased with 1 lamp in operation.

The stability of the indicator over time is an important factor to consider when choosing an indicator organism. MS2 phage has a high rate of natural decrease in viability with time, and enumeration must be performed as soon after sampling as possible. *B. subtilis*, on the other hand, can be stored for several weeks without significant reduction in its viability.

The resistance of *B. subtilis* to UV radiation varied significantly between phase 1 and 2 for reasons that were not clear. Previous studies have shown that the conditions under which the spores are grown and harvested can alter their resistance to UV (Qualls et al. 1989; Sommer and Cabaj 1993). In this study, the UV resistance of *B. subtilis* varied widely between spore batches, even though identical generation and harvesting procedures were used in both cases. This suggests that even small deviations in procedure may have the potential to influence UV resistance. Changes in the slope of the dose-inactivation relationship have the potential to influence RED values determined in testing.

It is important to consider the UV resistance of a biodosimetric indicator relative to the pathogen of concern. The majority of research dealing with microbial reduction of

drinking water using UV radiation has focused on *C. parvum* as the primary pathogenic target organism. MS2 phage has a higher UV resistance to *B. subtilis* spores, which in turn is more resistant to UV than *C. parvum*. Although organisms with higher UV resistances than a target organism can be used as biodosimetric surrogates, there are potential drawbacks. Biodosimetry results must be interpreted conservatively to ensure the protection of public health. If an indicator has a lower resistance to UV than the target pathogen, the indicator must demonstrate an RED equal to or higher than the dose required for the pathogen (Wright 2001). As the dose distribution widens in a UV reactor, the difference between the RED of a UV sensitive and UV resistant organism also widens. Since REFR is calculated by dividing the RED by number of lamps in operation and the average exposure time, REFR responds in the same manner as RED. If comparing the indicator with a pathogen, an indicator with a higher resistance to UV must demonstrate an REFR equal to or higher than the REFR required for the pathogen. However, using an indicator with higher resistance to UV radiation than the target pathogen, the indicator must demonstrate an inactivation greater than or equal to the pathogen (Wright 2001). Consequently, the use of MS2 phage will yield more conservative results than use of *B. subtilis* for use as biodosimetric surrogates for *C. parvum*.

4.9 SUMMARY OF UV REACTOR EXPERIMENTS

The recent increase in usage of UV reactors for microbial reduction of potable water has encouraged research that investigates the practical issues of widespread application of this technology. The main conclusions that can be drawn from phases 1 and 2 of this study are as follows:

1. Results from trials conducted using MS2 phage suggested that operation of the UV reactor with 2 or more adjacent lamps in operation resulted in an increased REFR, relative to operation with a single lamp in operation. The elevated REFR suggests a narrower dose distribution exists in the reactor for this operating condition, and therefore there was an increase in the overall efficiency of the microbial reduction process. With only 1 lamp in operation, the probability of a microbe passing through the reactor and receiving a low UV dose was higher. More consistent treatment was achieved when two or more adjacent lamps were operated. When two or more adjacent lamps were in operation, the REFR returned using MS2 phage was nearly independent of flow rate, suggesting the hydraulics of the reactor in combination with the spatial fluence rate pattern were providing a narrow dose distribution.
2. The results from trials performed using *B. subtilis*, displayed a statistically significant increase in REFR as flow rate increased while running the reactor with 1 lamp in operation. Insufficient data was available to draw solid conclusions about reactor performance with 2 or more lamps in operation, using *B. subtilis*.
3. MS2 phage and *B. subtilis* responded differently to running of the reactor with 1 lamp in operation. As flow rate was increased when 1 lamp was in operation, the REFR of MS2 phage decreased, while the REFR of *B. subtilis* increased. Based on the UV dose-inactivation relationships of the two indicators, this is opposite of what theory would predict. The exact cause of

this departure from theory cannot be adequately explained without further experimentation.

4. MS2 phage was found to be the superior of the two biodosimetric indicators for various reasons. It has a high resistance to UV radiation and it is possible to cultivate large titers of the organism over short periods of time. These traits allow for identification of a wide range of UV doses occurring in a reactor. MS2 phage's major limitation as an indicator is that its viability rapidly decreases over time and must be enumerated quickly after testing. Both indicators are conservative biodosimetric indicators for *C. parvum*, which is acceptable from a public heath standpoint.
5. MS2 phage resulted in larger RED values than *B. subtilis*, in accordance with theory. MS2 phage is more resistant to UV radiation than *B. subtilis*, which theoretically makes MS2 phage more resistant to wide dose distributions in the reactor. As the UV resistance of an indicator increases, its RED will increase, for a given UV reactor operating under a fixed set of conditions. The difference between RED values returned by UV sensitive and UV resistant organisms tends to increase as the dose distribution in a reactor widens.

5 INFLUENCE OF TURBIDITY AND UV ABSORBANCE ON MS2 PHAGE INACTIVATION

5.1 INTRODUCTION

Turbidity is a measure of how light is scattered as it passes through water. It is dependant on the wavelength of the light and properties of particles contained in the water, such as their composition, size and shape (Sethi et al. 1997). During storm events, excessively turbid water sometimes enters the Kelowna distribution system, with the historical high being 15 ntu (Weaden 2002). Turbidity has the potential to shield pathogens from chemical disinfectants, such as the free chlorine employed by the City of Kelowna for its water treatment. Turbidity may also result in a reduction in the effectiveness of UV microbial reduction of potable water. Particles can shield pathogens from receiving the desired UV dose, or simply scatter and absorb light within the reactor, reducing the average fluence rate microbes are exposed to. As turbidity increases in the irradiated water, the UV fluence rate gradient within the reactor has the potential to increase, which tends to widen the UV reactor's dose distribution. Dissolved compounds also have the ability to absorb UV light, but would not display any of the particle association effects that can limit reactor effectiveness. However, if a particle was to travel along the outer edge of the reactor where the fluence rate was lowest, the particle may not receive a sufficient dose to inactivate the pathogens associated with that particle. This chapter investigates the effect of turbidity and UV absorbance on microbial reduction in a

Sentinel™ medium pressure UV reactor using the biodosimetric indicator organism MS2 phage.

5.2 EXPERIMENTAL DESIGN

The influence of turbidity and absorbance on microbial inactivation in the UV reactor was investigated in phase 3, carried out in February 2002. Operational conditions tested are summarized in Tables 5-1 and 5-2. Turbidity goals were met by the addition of lake sediment, while absorbance goals were met by the addition of tea to the water. All trials were performed at a constant flow rate of 1140 L/min (300 USgpm). Trials were performed at low (≤0.55 ntu), medium (5 ntu) and high (10 ntu) turbidity levels. Additional trials in which tea was added to influent to alter UV absorbance at 254 nm (measured through a 10 mm quartz cell) were performed at 0.053 absorbance units/10mm (unaltered lake water, $UVT_{254\ nm,\ 10\ mm}$ = 89%), 0.076 absorbance units/10 mm ($UVT_{254\ nm,\ 10\ mm}$ = 84%) and 0.097 absorbance units/10 mm ($UVT_{254\ nm,\ 10\ mm}$ = 80%), respectively. For trials in which both lake sediment and tea were simultaneously added to the feed water, the target turbidity levels were 5 ntu and 10 ntu (Table 5-2). The UV treatment installation was set up so that the lake bottom sediment and tea suspensions were mixed together before injection into the influent. Practical consideration prevented achieving targets for both turbidity and UV absorbance simultaneously. Therefore, no target UV absorbance was set for trials in which both lake sediment and tea were simultaneously added to the feed water.

Table 5-1: Operating conditions examined in challenge tests performed on the Sentinel™ UV reactor in phase 3.

Flow		# of Lamps Operating	Target Turbidity (ntu)	Target UVT (%)
(L/min)	(USgpm)			
1140	300	2	ua[a], 5 and 10	ua, 84 and 80

[a]ua: denotes unaltered lake water

Table 5-2: Turbidity and UV absorbance targets for feed water used in challenge tests performed on the Sentinel™ UV reactor in phase 3.

Test Water Setting	Manipulated Parameter		
	Turbidity	UV Absorbance (abs/10 mm)	Turbidity and UV Absorbance
Low	Unaltered Lake Water	Unaltered Lake Water	Unaltered Lake Water
Medium	5 ntu	0.076 (84% UVT)	5 ntu
High	10 ntu	0.097 (80% UVT)	10 ntu

5.3 FEED WATER QUALITY RESULTS

The water quality experienced during the two testing periods was stable and typical of winter, unaltered Kelowna water. Unaltered lake water samples were taken daily during the testing period. Daily tests included pH, total alkalinity, total hardness, turbidity, UV absorbance at 254 nm, colour, sulphate and chloride (Table 5-3). Detailed information from daily water tests is given by Table E-3.

Table 5-3: Summary of water quality testing of unaltered lake water used as feed water in challenge tests performed on the Sentinel™ UV reactor in phase 3.

Parameter	Phase 3
pH	7.99 to 8.18
Alkalinity-Total (mg/L as $CaCO_3$)	108 to 113
Hardness-Total (mg/L as $CaCO_3$)	120 to 124
Turbidity (ntu)	0.248 to 0.488
UV absorbance at 254nm (abs/10 mm)	0.052 to 0.055
$UVT_{254\ nm,\ 10\ mm}$ (%/10 mm)	88.7 to 88.1
Colour (Pt-Co units)	5 to 6
Sulphate (mg/L SO_4^-)	34.0 to 35.8
Chloride (mg/L Cl^-)	3.28 to 5.88

5.4 UV DOSE-INACTIVATION RELATIONSHIPS

UV dose-inactivation curves were determined by using data gathered from UV exposures performed on suspensions of MS2 phage in unaltered lake water collected during each experimental phase (Figure 5-1). MS2 phage was the only biodosimetric indicator used in this portion of the study. Data obtained from UV exposure of the phage in a collimated beam apparatus was modeled using linear regression, and was found to be statistically significant.

In the linear model, β_0 and β_1 were determined to be 0.0977 and 0.0446 ($p=4.5x10^{-14}$), respectively. The r^2 value for the model was calculated to be 1.00, and no tailing was detected for the UV doses examined (Figure A-3). The model yielded a positive y-intercept, which is consistent with phases 1 and 2 (as discussed in section 4.4) and is also reported in literature (Havelaar et al. 1990). The UV dose-inactivation relationship determined is comparable to values reported in literature (Table 5-4).

Table 5-4: Summary of UV dose-inactivation relationship of MS2 phage suspended in unaltered lake water and exposed to UV radiation in a collimated beam apparatus (phase 3), accompanied by the dose ranges reported in literature.

Log Inactivation				Source
1	2	3	4	
UV Dose (mJ/cm^2)				
20	43	65		Phase 3
4 to 25	13 to 50	21 to 75	29 to 100	Range from literature reviewed in Table 2-2

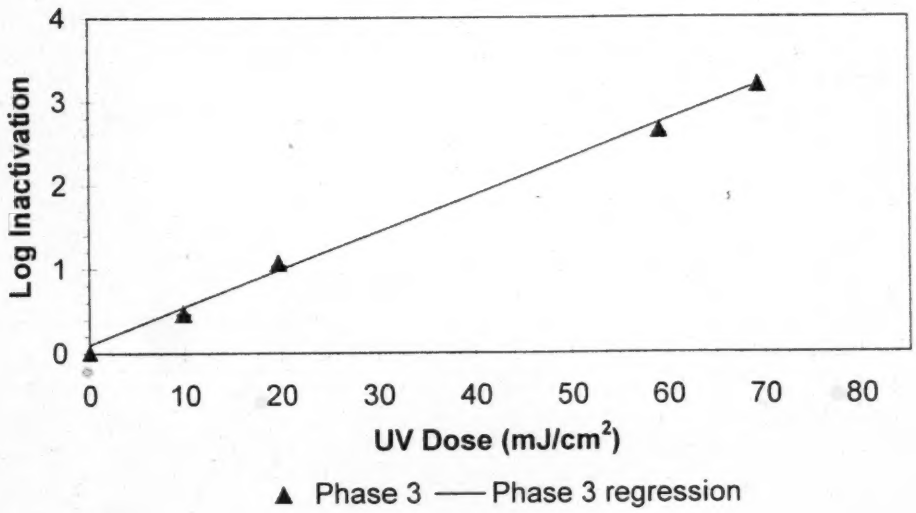

Figure 5-1: UV dose-inactivation relationship for MS2 phage suspended in unaltered lake water and exposed to UV radiation in a collimated beam apparatus (phase 3).

5.5 COMPOSITION OF TURBIDITY AND UV ABSORBING SUBSTANCES

This study would serve little purpose if the surrogate turbidity and UV absorbance additives were not adequately described. In order to characterize the turbidity added to the influent water, gravimetric, grain size distribution and absorbance spectrum analyses were performed on the lake bottom sediment suspension. The UV absorbance spectrum of the tea was determined and compared to that of unaltered lake water.

Gravimetric analysis provided information regarding the composition of dissolved and suspended solids in the lake bottom sediment suspension. A summary of the gravimetric testing results is given in Table 5-5. It is important to note that 95% of the total solids were retained on the 2 μm glass filter. The majority of the solids material in the lake sediment suspension was classified as suspended solids. This was not unexpected because the lake sediment used in UV reactor challenge tests was able to settle out in the non-quiescent conditions that exist near a water intake. Larger particles will naturally settle out of solution more readily, suggesting that lake sediment near a water intake would contain a high percentage of large particles. It was also determined that 92% of the solids were fixed solids, suggesting that only a small portion of the lake sediment injected into the feed water was organic.

The grain size analysis established that 45% of the total suspended matter was between 150 and 38 μm in diameter, while 54% of particles were smaller than 38 μm (Figure 5-2, Table D-1). This demonstrates that a large percentage of particles injected

Table 5-5: Summary of the gravimetric analysis performed on the diluted lake bottom sediment suspension injected into the feed water in phase 3.

Parameter	Diluted Lake Bottom Sediment		
	Average (mg/L)	± 95% C.I. (mg/L)	% of Total Solids
Total Solids	4.78	0.19	100.0
Total Fixed Solids	4.42	0.14	92.3
Total Volatile Solids	0.37	0.06	7.7
Total Filterable Solids	4.57	0.45	95.5
Filterable Fixed Solids	4.23	0.47	88.5
Filterable Volatile Solids	0.33	0.06	7.0
Total Dissolved Solids	0.34	0.07	7.2
Dissolved Fixed Solids	0.36	0.07	7.5
Dissolved Volatile Solids	-0.01	0.10	-0.3

into the feed water were several orders of magnitude larger than MS2 phage, which is typically has a diameter of approximately 0.026 μm (van Duin 1988). The large difference in the size of MS2 phage relative to the particulate suggests there may be potential for particles to shield MS2 from UV light in a reactor.

High water turbidity events in the Kelowna distribution system have been found to be due to the increased action of lake currents during storms, which potentially stir up sediment and transport highly turbid water to the water intakes. Therefore, turbidity composition in such events may closely resemble the lake bottom sediment. However, it is also possible that the material used to experimentally increase turbidity had a tendency towards larger particle sizes than would occur naturally. The presence of larger particles in the lake bottom sediment may increase the probability of organisms being partially protected from UV light due to particle shielding.

It is possible that the percentage of organic matter contributing to the turbidity in the manipulated feed water may not be representative of all natural turbidity events,

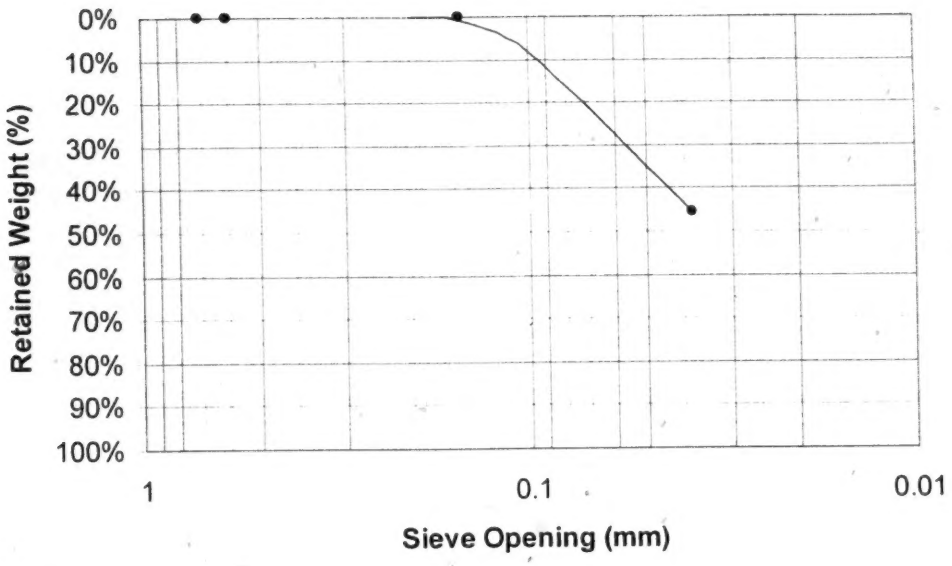

Figure 5-2: Grain size distribution of lake bottom sediment used to increase influent turbidity levels in phase 3.

because organic content in the upper regions of a lake changes temporally. In many lakes, the amount of organic material reaching the sediment is proportional to the intensity of photosynthesis occurring (Bronmark and Hansson 1998). While phase 3 was conducted in the winter, turbidity events could also occur during warmer period where photosynthesis intensity would increase, resulting in increased organic content of lake bottom sediment, and therefore in water at the intake. The increased action of lake currents during storm events could also potentially carry water from the upper regions of the lake to the intake to cause a high turbidity event. During periods of high photosynthetic intensity, such as would occur during summer, water from the upper

regions of the lake would likely have a higher organic content than in the winter. Gravimetric testing suggested little organic matter (8%) in the experimentally increased turbidity of the test water. Highly turbid water containing a larger percentage of organic particles such as algae or decaying organic matter may display slightly different behavior than what was observed in this study. For this reason, the lake bottom sediment used to increase turbidity in this study may not be representative of naturally occurring high turbidity events occurring during periods of higher photosynthesis intensity, when there is potentially a higher organic content in the lake water near the surface and in the sediment. However, analysis of unaltered lake water samples from naturally occurring high turbidity events are required to confidently assess what the true characteristics of the particles contributing to turbidity are and if there are any significant seasonal fluctuations in their composition.

The response of a UV absorbing substance to radiation over the germicidal UV spectrum is the primary issue in using it as a surrogate to simulate natural UV absorbance spikes. Figure 5-3 shows the UV absorbance of tea, lake sediment and unaltered lake water normalized to 254 nm. Lake sediment has little variation in UV absorbance as wavelength is changed. The tea tends to have higher absorbance below 240 nm and above 260 nm. However, when the additives are combined with the unaltered lake water, the wavelength dependant differences were reduced. Figure 5-4 shows the response of unaltered lake water combined with tea ($UVT_{254\ nm,\ 10\ mm}$ = 84%), and unaltered lake water combined with lake bottom sediment (turbidity = 5 ntu). Both lake water with tea added, and lake water with lake bottom sediment added, have similarly shaped UV

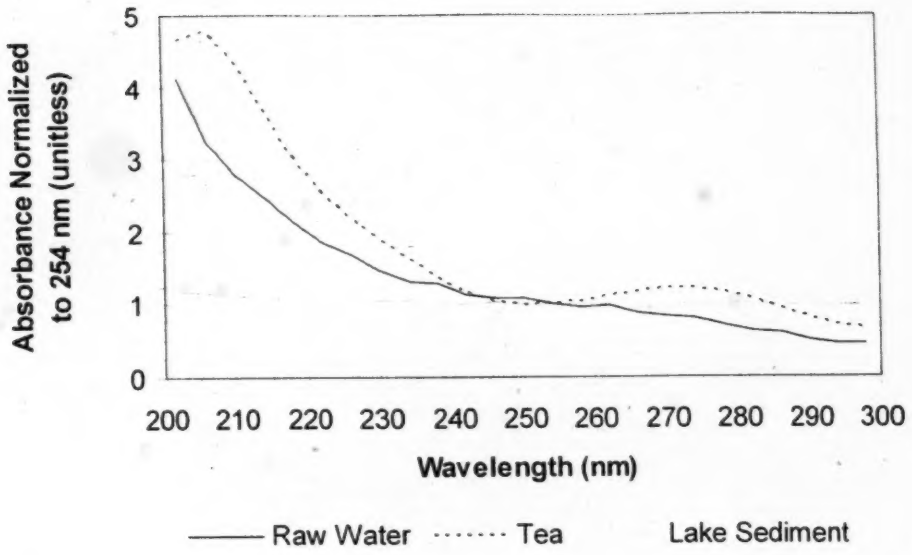

Figure 5-3: UV absorbance of tea and lake sediment suspensions added to the feed water in phase 3, relative to unaltered lake water.

spectra as the unaltered lake water (Figure 5-4). This suggests that both the tea and lake sediment are suitable surrogates for simulating natural UV absorbance and turbidity spikes. Before the practical application of results from this part of the study, it is recommended that further analysis on the turbidity and UV absorbing compounds present in the natural water be performed in order to verify that the additives used were representative.

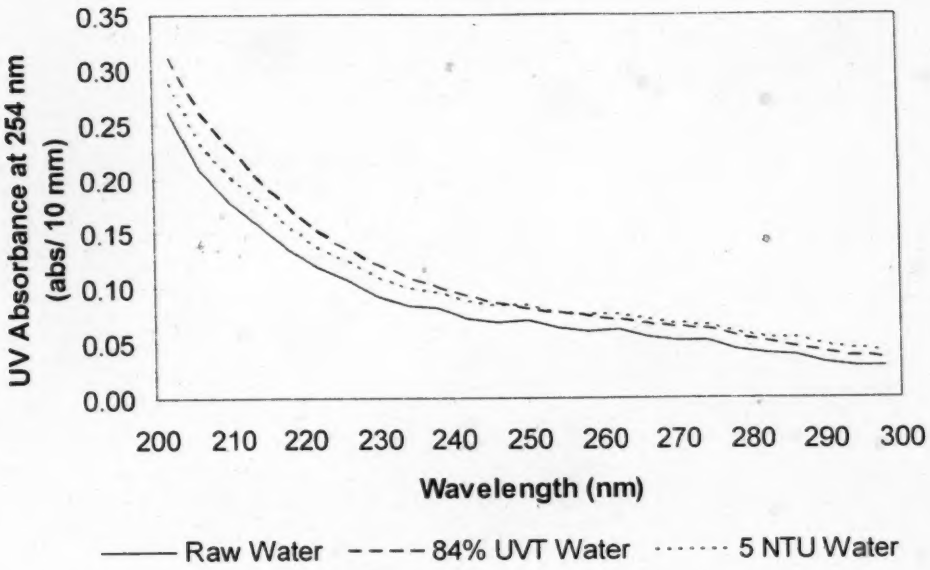

Figure 5-4: UV absorbance normalized to 254 nm, for unaltered lake water, 84% UVT water prepared by the addition of tea to unaltered lake water, and 5 NTU water prepared by the addition of lake bottom sediment to unaltered lake water.

5.5.1 Turbidity-UV Transmittance Relationship

The relationship between test water turbidity and $UVT_{254\ nm,\ 10\ mm}$ for phase 3 trials was examined, and is presented in Figure 5-5. Linear regression analysis resulted in a statistically significant model, with β_0 and β_1 values of 149 and -1.68 ($p=1.2x10^{-6}$), respectively. The r^2 for the model was calculated to be 0.98. The trial with average turbidity of 17.17 ntu was excluded from this model because the turbidity measurement

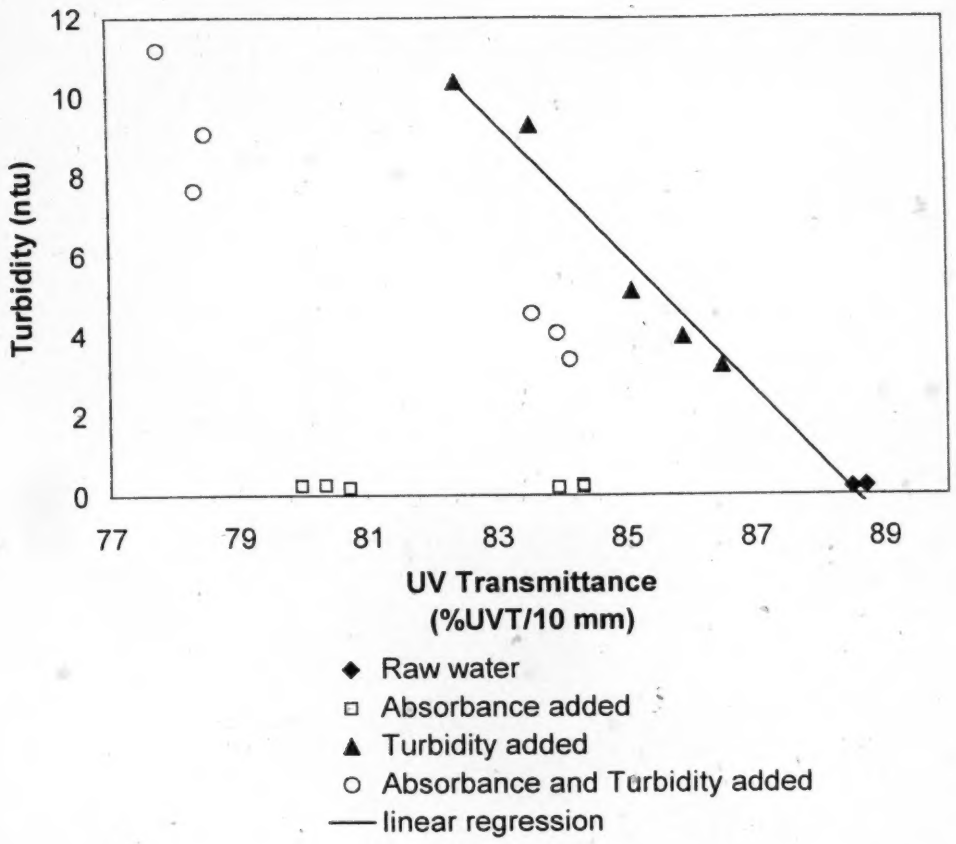

Figure 5-5: Turbidity as a function of UVT, calculated from challenge tests performed on the Sentinel™ UV reactor treating unaltered lake water, lake water with absorbance added, lake water with turbidity added, or lake water with absorbance and turbidity added simultaneously. The linear regression model carried out on data from trials performed using unaltered lake water and trials in which turbidity was added, is plotted alongside the data (phase 3).

was considered to be erroneous (Table D-2). This was based on comparisons of its $UVT_{254\ nm,\ 10\ mm}$ and log inactivation data to replicate trials, which had similar measured $UVT_{254\ nm,\ 10\ mm}$, but large differences in turbidity (Table D-2).

Water samples are often filtered before measuring UV absorbance, in order to minimize the influence of particle induced light scattering. For studies examining microbial reduction using UV radiation, UV absorbance is often determined using unfiltered samples. This study also determined UV absorbance using unfiltered water.

The most accurate spectrophotometers use an integrated sphere light receptor, which accounts for forward and side scattered light. The majority of spectrophotometers do not have integrated sphere receptors, and therefore do not adequately account for forward and side scattered light. Therefore, it is common for spectrophotometers to overestimate UV absorbance (Qualls et al. 1983). The equipment in the Kelowna lab, used to perform absorbance measurements on daily unaltered lake water samples and water samples from trials did not contain an integrated sphere measurement system and thus UV absorbance was potentially overestimated.

5.6 INFLUENCE OF TURBIDITY AND UV ABSORBANCE ON MS2 PHAGE INACTIVATION

UV absorbance and turbidity targets were readily achieved in phase 3. Detailed information from phase 3 challenge tests is given by Tables D-2 and D-3. It was possible to accurately and repeatedly achieve target water absorbance goals by addition of tea. Further, steady state conditions were confirmed for trials where tea was added to the influent by monitoring of the UV sensors and inline turbidimeter readings during each trial. As expected, the addition of tea caused minimal increase in turbidity (Figure 5-5).

Specifically, the maximum turbidity increase was only 0.06 ntu above the average turbidity observed in unaltered lake water trials (0.20 ntu). For these reasons, phase 3 trials provided excellent information on the effect of increasing the fluence rate gradient in the reactor. Average $UVT_{254\ nm,\ 10\ mm}$ at the medium setting was 84% (0.076 absorbance units/10 mm) with a standard deviation of 0.2 %, while the high setting yielded 80% (0.097 absorbance units/10mm) with a standard deviation of 0.4%. Log inactivation was reduced by 0.49 log inactivation units at the 84% $UVT_{254\ nm,\ 10\ mm}$ setting, and 0.77 log inactivation units at the 80% $UVT_{254\ nm,\ 10\ mm}$ setting, relative to trials performed using unaltered lake water as influent (Figure 5-6).

For trials where lake bottom sediment was added to the influent, steady state conditions were confirmed by monitoring of UV sensors, inline turbidity readings, and bench-top turbidimeter readings of influent and effluent water samples for each trial. The average turbidity was 4.10 ntu with a standard deviation of 0.94 ntu for trials performed at the medium turbidity setting. High turbidity trials resulted in an average turbidity of 12.28 ntu with a standard deviation of 4.27 ntu. However, one of the high turbidity trials greatly exceeded the target (17.17 ntu), and was excluded from the analysis as an outlier (Table D- 2). It is important to note that the trial with a measured turbidity of 17.17 ntu had a $UVT_{254\ nm,\ 10\ mm}$ of 83%, which was very close to the other two high level setting turbidity trials which had $UVT_{254\ nm,\ 10\ mm}$ values of 82% and 84%, respectively. This suggests an inaccurate measurement for either the turbidity or the $UVT_{254\ nm,\ 10\ mm}$ for this trial. Excluding the 17.17 ntu trial, the high setting turbidity trials had an average turbidity of 9.83 ntu with a standard deviation of 0.77 ntu. Average MS2 phage inactivation for trials performed at the medium and high turbidity settings were 0.25 and

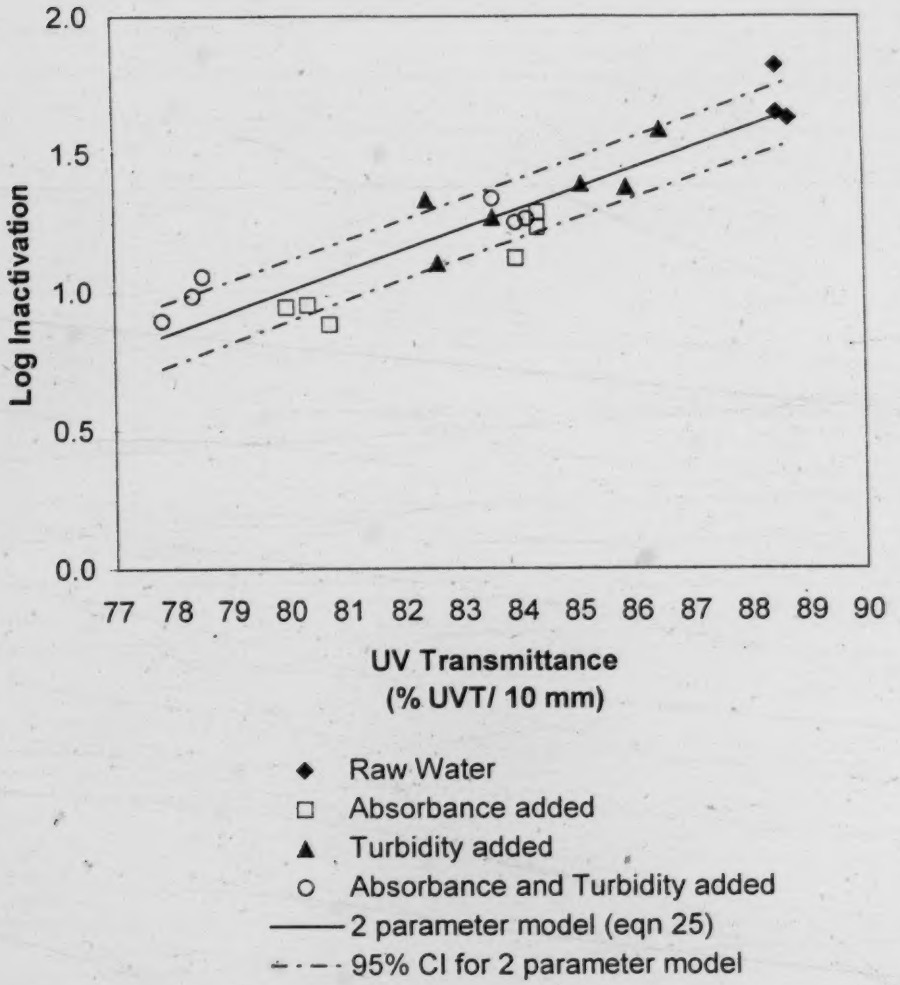

Figure 5-6: Log inactivation of MS2 phage as a function of UVT, calculated from challenge tests performed on the Sentinel™ UV reactor treating unaltered lake water, lake water with absorbance added, lake water with turbidity added, or lake water with absorbance and turbidity added simultaneously. The linear regression model (equation 25) and its associated 95 percent confidence interval are plotted alongside the data (phase 3).

0.47 log inactivation units less than was observed for trials performed using unaltered lake water (Figure 5-6).

Similar obstacles were encountered in accurately replicating target turbidity levels for trials involving the simultaneous addition of lake bottom sediment and tea, relative to trials involving the addition of lake bottom sediment alone. Trials performed at the medium and high settings resulted in a decrease in activation of 0.24 and 0.72 log inactivation units relative to trials performed using unaltered lake water (Figure 5-6).

Figure 5-6 shows the log inactivation plotted against $UVT_{254\ nm,\ 10\ mm}$ for all phase 3 trials. The significance of each factor was determined by performing multi-variable regression analysis on the data. The influence of turbidity, UV transmittance and the interaction between turbidity and UV transmittance were all considered. The models treated data from all trials as discrete data points and did not average values from replicate challenge test trials. In order to determine which regression model was superior, the statistical parameters r^2, residual mean square (RMS) and Mallows C_p were compared. The two best models determined were as follows:

$$\text{log inactivation} = -6.5 + (0.092)*UVT_{254\ nm,\ 10\ mm} + (0.32)*T - (0.0038)*UVT_{254\ nm,\ 10\ mm}*T \quad (24)$$

$$\text{log inactivation} = (-5.0) + (0.075)*UVT_{254\ nm,\ 10\ mm} \quad (25)$$

where T is the turbidity. In equation 24, $UVT_{254\ nm,\ 10\ mm}$ was highly significant ($p=1.51\times10^{-8}$), while turbidity ($p=0.0385$) and the $UVT_{254\ nm,\ 10\ mm}$ - turbidity interaction

(p=0.0428) were marginally significant. The model using UV transmittance as the only dependent variable had highly significant y-intercept ($p=1.07x10^{-7}$) and β_1 coefficient ($p=3.05x10^{-9}$). The four parameter model, given by equation 24, proved to be superior for r^2, RMS and Mallows C_p. Equation 24, suggests that increased turbidity actually aids in the UV microbial reduction process, which is contradictory to expectations. The positive turbidity coefficient and the marginally significant probabilities associated with the turbidity and $UVT_{254\ nm,\ 10\ mm}$ – turbidity coefficients implies that the model may closely match the limited number of data points, but does not make physical sense. For this reason, equation 25 was considered to be the more valid model for UV inactivation within the reactor for unaltered Kelowna water. The equation 25 model is plotted along with its 95% confidence intervals in Figure 5-6.

The multi-variable regression analysis does not clearly identify the effect that turbidity has on microbial reduction for operation of the UV reactor with unaltered lake water. Previous literature has shown turbidity to have additional impacts on microbial reduction other than the absorption of UV light (Oliver and Cosgrove 1975; Qualls et al. 1983; Parker and Darby 1995; Emerick et al. 2000). The primary questions raised by the phase 3 data were, (a) was the lake bottom sediment added to the influent acting like a simple UV absorbing substance, and (b) were solids association effects hindering microbe inactivation?

Emerick et al. (2000) hypothesized the existence of a critical particle size, below which a particle is not capable of shielding a particular organism. For a coliform bacteria exposed to UV light in secondary wastewater effluent, a critical particle size of 10 μm was identified (Emerick et al. 2000). Further, coliform bacteria are not typically found in

the most shielded areas of particles, resulting in microbe shielding being independent of particle size for particles larger than the critical size (Emerick et al. 2000). MS2 phage is several orders of magnitude smaller than coliform bacteria and intuitively should have a substantially smaller critical particle size. It then makes sense that, with 46% of particles in the water between 38 and 150 μm in diameter and a typical phage diameter of 0.026 μm, some degree of shielding from UV radiation may have occurred to the injected MS2 phage.

The explanation as to why the presence of particulate in UV reactor feed water did not impede microbial reduction relates to the characteristics of the particles, and the microorganisms being exposed to UV light. Particulate matter with a tendency to agglomerate or form flocs will inevitably harbor some amount of indicator organism within the newly formed flocs, partially protecting them from the applied UV light. Floc formation will also increase the average particle size in the reactor, thus increasing the shielding ability of the matter in suspension. Municipal secondary wastewater effluent has the potential to be flocculent in nature, because conventional treatment includes aeration preceding the secondary clarifier. This aeration treatment is intended to encourage microbiological growth and enhance floc formation (Viessman and Hammer 1993). This would tend to increase the probability of floc formation in secondary wastewater effluent. However, in drinking water treatment, matter suspended in unaltered surface water has the potential to be stable, requiring the addition of coagulant chemicals to achieve flocculation and subsequent solids separation from the water. Due to the potential of newly formed floc to encompass microorganisms and protect then from UV radiation, the tendency for the matter in suspension to form flocs should be considered

when applying the critical particle size theory proposed by Emerick et al. (2000). In this thesis no coagulants were present in the feed water. Natural stability of the lake sediment particles, combined with the turbulent flow regime within the UV treatment system may have been sufficient to keep turbidity particles discrete.

It was possible to statistically verify if a significant amount of MS2 phage was attaching to the lake bottom sediment added in challenge tests. This was done by comparing the MS2 phage influent concentration of trials run using unaltered lake water, and trials where lake bottom sediment was added to the influent. If MS2 phage was attaching to the particulate in the water, then the viable MS2 phage concentrations in influent water would be lower in trials where lake bottom sediment was added. The average MS2 phage concentrations measured in the influent samples from trials performed with and without lake bottom sediment were compared using a two sample t-test. No statistically significant difference in mean influent MS2 phage concentrations was observed for trials performed with and without lake bottom sediment ($p=0.24$). This suggests that MS2 phage injected into the influent were not attaching to the lake bottom sediment added to the feed water. Previous studies have reported that MS2 phage undergoes minimal adsorption to granular porous media (Jin and Yates 2002). Ionic strength and particle composition likely have a significant affect on the adsorption of MS2 phage on porous media. Adsorption to soil by MS2 phage has been found to be highly dependent on the organic content of the soil, even at low percentages (Gerba and Goyal 1981).

The critical particle size theory developed for coliform bacteria in secondary wastewater effluent cannot be directly applied to MS2 phage in potable water. Coliform

bacteria tend to actively grow in an aqueous environment containing basic nutrients, such as wastewater effluent or the lake water used in this experiment, which allows them to attach to a particle and potentially colonize areas deep within particles. MS2 phage is restricted to reproduction within an active *E. coli* cell. Enumeration of viable *E. coli* in the influent water suggested that low to undetectable concentrations of the organism were present (Tables E- 1 to E- 3). The low concentrations of *E. coli* present in the feed water for this experiment combined with the high concentrations of MS2 phage injected into the influent stream, ensured that the growth rate of MS2 phage in the test water was negligible. If a microorganism does not have the ability to attach to a particle and colonize the protective crevices and pores of that particle, theoretically, the critical particle size would increase. However, due to the large size difference between viruses and bacteria, viruses would tend to fit within many more shielded regions than bacteria (Emerick et al. 2000). The critical particle size for viruses is expected to be smaller than the 10 μm reported for coliform bacteria, because for a given particle there is more opportunity for a particle associated virus to be shielded from UV light (Emerick et al. 2000).

In theory, the degree of particle shielding and embedment within particles for MS2 phage in unfiltered surface water should be less than what was observed in the study performed by Emerick et al. (2000), analyzing inactivation of coliform bacteria by UV radiation in secondary wastewater effluent. Particles can exist in some lake waters for months or years as stable, discrete units, so coagulant chemicals are sometimes added to encourage floc formation and subsequent settling out of solution of the stable particulate (Letterman et al. 1999). The feed water used in this study originated from the middle of a

long, deep lake with a total retention time of over 50 years (Table 3-2). Therefore, it is likely that the water entering the intake at Kelowna had resided in the lake for a substantial period of time. Water collected at the intakes for the City of Kelowna's water treatment system typically has low turbidity, which suggests that the majority of particulate has settled out of solution. This would result in predominantly smaller, more stable particulate in suspension. Stable particulate in low concentrations would potentially have a lower tendency to form flocs, than water containing coagulant chemicals or secondary wastewater effluent. Additionally, the data from phase 3 suggests that MS2 phage did not have an affinity for absorption to particle surfaces as demonstrated by comparing influent concentrations of trials performed with and without injection of lake bottom sediment into the feed water. In theory, the particle size below which a particle is not capable of shielding a particular microbe from UV radiation should be larger in water without the tendency to form flocs, relative to trials performed in secondary wastewater effluent where floc formation is more probable.

The most probable reason that particle associated effects were not a major influence on microbe inactivation in this study was due the combination of non-floc forming turbidity, and a lack of affinity between the suspended particulate and the target microorganism.

5.7 INACTIVATION IN POWER-OFF PROCESS CONTROLS AND TRIP CONTROLS

A total of 12 power-off controls were performed in phase 3. Three controls were performed using unaltered lake water, three with tea added to the influent, three with lake bottom sediment added to the influent, and three with both tea and lake bottom sediment

simultaneously added to the influent. Detailed information on the phase 3 power-off controls can be found in Table D-2. The average log inactivation for all controls was approximately 0.022 with an associated standard error of 0.011. The controls do not prove to be statistically equal to zero, but considering the overall variability of the process, the difference is negligible. The 95% confidence band width is typically 0.20 to 0.22 log inactivation units (Figure 5-6), which is much larger than the range of values observed in the controls (Table D-2). The controls suggest there are no major factors causing loss of MS2 phage viability other than UV radiation, upon passage through the UV treatment system.

In phase 3, a trip control was performed using the MS2 phage concentrated stock solution. The purpose of the trip control was to confirm that transportation and handling of the indicators did not affect the test results. Practical considerations prevented the immediate determination of sample viability, and a decrease in viability was observed between the time when trials were run and when indicator viability was assessed. However, inactivation was determined by comparing the relative concentrations in influent and effluent samples, and the viability of influent and effluent water sample for a given trial were always tested concurrently. This ensured that any reduction in viability would have occurred equally in influent and effluent samples and thus would not have influenced the inactivation. Further, the power-off process controls returned average inactivation values of approximately zero, which indicates that viability loss due to transportation and handling was the same in influent and effluent samples and thus did not influence inactivation results.

5.8 SUMMARY OF EXPERIMENTS ADDING TURBIDITY AND UV ABSORBANCE TO FEED WATER

For the production of drinking water, future regulations are likely to require or recommend that filtered water be used in conjunction with UV microbial reduction technology. However, future regulations may permit some exceptions. This study examined the effect of increases of turbidity and UV absorbance on microbial reduction efficiency in a UV reactor treating an unfiltered lake water. The effects of inhibition of UV inactivation due to changes in water quality are important to identify because unfiltered water has a greater tendency to undergo large fluctuations in water quality. Investigation into the use of UV reactors to treat unfiltered water could enable the application of this technology in a wider range of scenarios. The following conclusions can be drawn from phase 3 of this study:

1. The $UVT_{254\ nm.\ 10\ mm}$ of the water had a significant effect on microbe inactivation in the reactor, as determined using regression analysis. Inactivation reductions due to increased turbidity level and the turbidity-UVT interaction were only marginally significant as determined using regression analysis. Additionally, results from regression analysis suggested that the presence of particulate increased MS2 phage inactivation in the UV reactor, relative to inactivation in the absence of particulate. An increase in microbial reduction due to the presence of particulate does not make physical sense. The majority of existing literature links the presence of particulate in water to a decrease in the microbial reduction achievable at a given UV dose. However,

most of these studies were performed using wastewater, where UVT values are much lower than what is encountered in drinking water treatment, and the microorganisms being inactivated are not the same as are typically used in drinking water treatment. Overall, the most probable explanation as to why the effect of particulate on microbial reduction varied from what is reported in literature relates to the characteristics of the particles contributing to turbidity, and the indicator organism used.

2. MS2 phage did not display a statistically significant tendency to attach to lake bottom sediment particulate, which was added to feed water to simulate a high turbidity event. If the virus was not attaching to particles then it is less likely that MS2 phage would be located deep within pores and crevices of particles where they would be protected from UV light. This partially accounts for why no particle associated effects were observed in this study.
3. The lake bottom sediment suspension used to artificially increase feed water turbidity in this study was determined to be 92% inorganic. The characteristics of the matter contributing to turbidity could potentially have an impact on microbe inactivation in a UV reactor. It is recommended to analyze water from naturally occurring high turbidity events at several different times of the year. This would help define what the true characteristics of the particles contributing to turbidity are and identify any temporal changes in their composition. Analyzing particles from a naturally occurring high turbidity event would also determine if the lake bottom sediment used in this study was similar to suspended material that enters distribution system water intakes

during these events. This could verify that lake sediment is an acceptable surrogate for particulate in such events. Site specific investigations should be considered for any location contemplating use of UV microbial reduction of drinking water using an unfiltered water supply in order to verify that the feed water can be successfully treated using UV technology.

6 CONCLUSIONS

A study was carried out investigating the microbial reduction of unfiltered lake water using a medium pressure UV model R-110 Sentinel reactor. The recent increase in usage of UV reactors for microbial reduction of potable water has encouraged research that investigates the practical issues of widespread application of this technology. For the production of drinking water, future regulations are likely to require or recommend that filtered water be used in conjunction with UV microbial reduction technology. This study also examined the effect of increases of turbidity and UV absorbance on microbial inactivation efficiency in a UV reactor treating an unfiltered lake water. The effects of inhibition of UV inactivation due to changes in water quality are important to identify because unfiltered water has a greater tendency to undergo large fluctuations in water quality. Investigation into the use of UV reactors to treat unfiltered water could enable the application of this technology in a wider range of scenarios. The main conclusions of this study are listed below.

1. More consistent microbial reduction of MS2 phage was achieved when two or more adjacent lamps were operated in the UV reactor. For trials involving MS2 phage, operation of the UV reactor with 2 or more adjacent lamps on resulted in an increased REFR, relative to operation with a single lamp on. The elevated REFR suggests a narrower dose distribution exists in the reactor for this operating condition, increasing the overall efficiency of the microbial

reduction process. With only 1 lamp in operation, the probability of MS2 phage passing through the reactor and receiving a low UV dose was higher.

2. The results from trials performed using *B. subtilis*, displayed a statistically significant increase in REFR as flow rate increased while running the reactor with 1 lamp in operation. This increase in REFR suggests the reactor's dose distribution narrowed as flow rate was increased.
3. MS2 phage and *B. subtilis* responded differently to running of the reactor with 1 lamp in operation. As flow rate was increased when 1 lamp was in operation, the REFR of MS2 phage decreased, while the REFR of *B. subtilis* increased. Based on the UV dose-inactivation relationships of the two indicators, this is opposite of what theory would predict. The exact cause of this departure from theory cannot be adequately explained without further experimentation.
4. MS2 phage was found to be the superior of the two biodosimetric indicators because it has a greater resistance to UV radiation, and it is easy to cultivate large titers of the organism over short periods of time. These traits allow for identification of a wide range of UV doses occurring in a reactor. The major limitation of MS2 phage as an indicator is that viability rapidly decreases over time and the phage must be enumerated quickly after testing.
5. MS2 phage did not display a statistically significant tendency to attach to lake bottom sediment particulate, which was added to feed water to simulate a high turbidity event. If the virus did not have a tendency to occupy the pores and crevices of particles where there is no direct pathway to UV light, this would

reduce the probability of the virus passing through the reactor and being partially protected from UV radiation due to the action of particulate.

6. Alteration of the $UVT_{254\ nm,\ 10\ mm}$ of the water had a significant influence on microbe inactivation of seeded MS2 phage in the reactor, as determined using regression analysis. This suggests that operation of the unit in Kelowna should focus on UV transmittance of the water more than turbidity, when adjusting operational settings to account for changes in feed water quality.
7. Inactivation reductions due to increased turbidity levels and the $UVT_{254\ nm,\ 10\ mm}$ - turbidity interaction were marginally significant as determined using regression analysis. The lack of observed particle associated effects is not predicted by the majority of existing literature. However, most of these studies were performed using secondary wastewater effluent, where UVT values are much lower than what is encountered in drinking water treatment, and the microorganisms being inactivated are not the same.

7 RECOMMENDATIONS

Although this study contributed a number of important findings relating to the viability of using a UV reactor for microbial reduction of unfiltered lake water, several issues require further investigation for a full understanding of the factors influencing microbial reduction within the Sentinel UV reactor. It is recommended that the following issues be studied further:

1. The correlation between tailing in the UV dose-inactivation relationship for pathogenic organisms such as *C. parvum*, and tailing observed for biodosimetric indicators such as MS2 phage and *B. subtilis*;
2. The influence of the time lag between generation of indicator organisms and the experimental determination of UV dose-inactivation of MS2 phage and *B. subtilis*, on inactivation relationships;
3. The interaction of various pathogens or biodosimetric indicators with particles, and the influence of that interaction on subsequent inactivation of the organisms by UV radiation;
4. The influence of particle size and the composition of particles in the water on inactivation of pathogens and biodosimetric indicators using UV radiation;
5. The temporal variation in composition of particles in Kelowna lake water and its subsequent effects on the inactivation of microbes and pathogens using UV radiation.

Based on the findings of the study, some basic recommendations can be made for the operation of the 304 mm internal diameter Sentinel™ medium pressure UV reactor treating unfiltered Lake Okanagan Water. These recommendations are listed below.

1. The unit should be operated with a minimum of two or more adjacent lamps in operation at all times;
2. The UV transmittance of feed water for the reactor should be tested frequently and if possible monitored continuously during operation of the UV reactor.

8 REFERENCES

Barbeau, B., L. Boulos, R. Desjardins and J. Coallier (1997). A Modified Method for the Enumeration of Aerobic Spore-Forming Bacteria. *Can. J. Microbiol.*, 43(10): 976-980.

Battigelli, D. A., M. D. Sobsey and D. C. Lobe (1993). The Inactivation of Hepatitus A Virus and Other Model Viruses by UV Irradiation. *Wat. Sci. Tech.*, 27(3-4): 339-342.

Bolton, J. R. (1999). *Ultraviolet Applications Handbook*. Ayr, ON: Bolton Photosciences Inc.

Bolton, J. R. (2000). Calculation of Ultraviolet Fluence Rate Distributions in an Annular Reactor: Significance of Refraction and Reflection. *Wat. Res.*, 34(13): 3315-3324.

Bronmark, C. and L. A. Hansson (1998). *The Biology of Lakes and Ponds*. Oxford, UK: Oxford University Press.

Bukhari, Z., T. M. Hargy, J. R. Bolton, B. Dussert and J. L. Clancy (1999). Medium Pressure UV for Oocyst Inactivation. *J. Am. Water Works Assoc.*, 91(3): 86-94.

Cabaj, A., R. Sommer and D. Schoenen (1996). Biodosimetry: Model Calculations for U.V. Water Disinfection Devices with Regard to Dose Distributions. *Wat. Res.*, 30(4): 1003-1009.

Cerf, O. (1977). A Review: Tailing of Survival Curves of Bacterial Spores. *J. Appl. Bacteriol.*, 42(1): 1-19.

Chang, J. C. H., S. F. Ossoff, D. C. Lobe, M. H. Dorfman, C. M. Dumais, R. G. Qualls and J. D. Johnson (1985). UV Inactivation of Pathogenic and Indicator Microorganisms. *Appl. Envir. Microbiol.*, 49(6): 1361-1365.

Clancy, J. L., T. M. Hargy, M. M. Marshall and J. E. Dyksen (1998). UV Light Inactivation of *Cryptosporidium* Oocysts. *J. Am. Water Works Assoc.*, 90(9): 92-102.

Cohn, P. D., M. C. Cox and P. S. Berger (1999). Health and Aesthetic Aspects of Water Quality. *Water Quality and Treatment: A Handbook of Community Water Supplies*. R. D. Letterman. New York, NY: McGraw-Hill, Inc.: 2.1-2.86.

Craik, S. A. (2001). Improving the Design of Ozone Contactors for Microorganism Reduction with a Static Mixer. PhD dissertation, University of Alberta, Edmonton, AB, 335.

Craik, S. A., G. R. Finch, J. R. Bolton and M. Belosevic (2000). Inactivation of *Giardia muris* Cysts Using Medium Pressure Ultraviolet Radiation in Filtered Drinking Water. *Wat. Res.*, 34(18): 4325-4332.

Craik, S. A., D. Weldon, G. R. Finch, J. R. Bolton and M. Belosevic (2001). Inactivation of *Cryptosporidium parvum* Oocysts Using Medium- and Low-Pressure Ultraviolet Radiation. *Wat. Res.*, 35(6): 1387-1398.

Doi, R. H. (1989). Sporulation and Germination. *Bacillus*. C. R. Harwood. New York: Plenum Press. 2: 169-216.

Draper, N. R. and H. Smith (1998). *Applied Regression Analysis*. New York, NY: John Wiley and Sons, Inc.

Emerick, R. W., F. J. Loge, T. Ginn and J. L. Darby (2000). Modeling the Inactivation of Particle-Associated Coliform Bacteria. *Wat. Environ. Res.*, 72(4): 432-438.

Gates, F. L. (1930). A Study of the Bactericidal Action of Ultraviolet Light. III. The Adsorption of Ultraviolet Light by Bacteria. *J. of Gen. Physiol.*, 14: 31-42.

Gerba, C. P. and S. M. Goyal (1981). Quantitative Assessment of the Adsorptive Behavior of Viruses to Soils. *Environ. Sci. Technol.*, 15(8): 940-944.

Giese, N. and J. Darby (2000). Sensitivity of Microorganisms to Different Wavelengths of UV Light: Implications on Modeling of Medium Pressure UV Systems. *Wat. Res.*, 34(16): 4007-4013.

Greenberg, A. E., L. S. Clesceri and A. D. Eaton, Eds. (1992). *Standard Methods for the Examination of Water and Wastewater*. Washington, D.C.: American Public Health Association, American Water Works Association, Water Environment Federation.

Haas, C. N. (1999). Disinfection. *Water Quality and Treatment: A Handbook of Community Water Supplies*. R. D. Letterman. New York, NY: McGraw-Hill, Inc.: 14.1-14.60.

Harm, W. (1980). *Biological Effects of Ultraviolet Radiation*. Cambridge, UK: Cambridge University Press.

Harris, G. D., V. D. Adams, W. M. Moore and D. L. Sorensen (1987). Potassium Ferrioxalate as Chemical Actinometer in Ultraviolet Reactors. *J. of Environ. Engin.*, 113(3): 612-627.

Havelaar, A. H., C. C. Meulemans, W. M. Pot-Hogeboom and J. Koster (1990). Inactivation of Bacteriophage MS2 in Wastewater Effluent with Monochromatic and Polychromatic Ultraviolet Light. *Wat. Res.*, 24(11): 1387-1393.

Havelaar, A. H., T. J. Nieuwstad, C. C. Meulemans and M. van Olphen (1991). F-Specific RNA Bacteriophages as model viruses in UV Disinfection of Wastewater. *Wat. Sci. Tech.*, 24(2): 347-352.

Hroncich, J. A. (1999). Source Water Quality Management: Surface Water. *Water Quality & Treatment: A Handbook of Community Water Supplies*. R. D. Letterman. New York, NY: McGraw-Hill, Inc.: 4.47-4.64.

Jagger, J. (1967). *Introduction to Research in Photobiology*. Englewood Cliffs, N.J.: Prentice-Hall Inc.

Jin, Y. and M. Yates (2002). *Virus Behavior in Saturated and Unsaturated Subsurface Media*. Denver, CO: AWWA Research Foundation and American Water Works Association.

Kobayashi, Y. (1989). Sporulation of *B. subtilis*. *Bacillus subtilis: Molecular Biology and Industrial Application*. B. Maruo and H. Yoshikawa. New York, NY: Elsevier Science Publishing Company, Inc.: 43-74.

Kolch, A. (1999). Disinfecting Drinking Water with UV Light. *Pollut. Engin.*, 31(10): 34-36.

Letterman, R. D., A. Amirtharajah and C. R. O'Melia (1999). Coagulation and Flocculation. *Water Quality and Treatment: A Handbook of Community Water Supplies*. R. D. Letterman. New York, NY: McGraw-Hill, Inc.: 6.1-6.66.

Leuker, G. (1999). Description and Application of Biodosimetry - a Testing Procedure for UV Systems. *Aqua*, 48(4): 154-160.

Lin, L.-S., C. T. Johnson and E. R. Blatchley III (1999). Inorganic Fouling at Quartz: Water Interfaces in Ultraviolet Photoreactors - I. Chemical Characterization. *Wat. Res.*, 33(15): 3321-3329.

Loge, F. J., R. W. Emerick, D. E. Thompson, D. C. Nelson and J. Darby (1999). Factors Influencing Ultraviolet Disinfection Performance Part I: Light Penetration to Wastewater Particles. *Wat. Environ. Res.*, 71(3): 377-381.

Mackey, E. D., T. M. Hargy, H. B. Wright, J. P. J. Malley and R. S. Cushing (2002). Comparing *Cryptosporidium* and MS2 Bioassays - Implications for UV Reactor Validation. *J. Am. Water Works Assoc.*, 94(2): 62-69.

Malley, J. P. J., J. P. Shaw and J. R. Ropp (1995). *Evaluation of By-Products Produced by Treatment of Groundwaters with Ultraviolet Irradiation.* Denver, CO: AWWA Research Foundation and American Water Works Association.

Meng, Q. S. and C. P. Gerba (1996). Comparative Inactivation of Enteric Adenovirus, Poliovirus and Coliphages by Ultraviolet Irradiation. *Wat. Res.*, 30(11): 2665-2668.

Morton, R. A. and R. H. Haynes (1969). Changes in the Ultraviolet Sensitivity of *Escherichia Coli* During Growth in Batch Cultures. *J. Bacteriol.*, 97(3): 1379-1385.

Nieuwstad, T. J. and A. H. Havelaar (1994). The Kinetics of Batch Ultraviolet Inactivation of Bacteriophage MS2 and Microbiological Calibration of an Ultraviolet Pilot Plant. *J. Environ. Sci. Health*, A29(9): 1993-2007.

Oliver, B. G. and E. G. Cosgrove (1975). The Disinfection of Sewage Treatement Plant Effluents Using Ultraviolet Light. *Can. J. Chem. Eng*, 53(2): 170-174.

Parker, J. A. and J. L. Darby (1995). Particle-Associated Coliform in Secondary Effluents: Shielding from Ultraviolet Light Disinfection. *Wat. Environ. Res.*, 67(7): 1065-1075.

Peldszus, S., R. Souza, J. Bolton, B. Dussert, F. Smith and S. Andrews (2000). Impact of Medium Pressure UV-Disinfection on the Formation of Low Molecular Weight Organic By-Products and Nitrite, and the Reduction of Bromate. AWWA Water Quality Technology Conference, Salt Lake City, UT: AWWA.

Petri, B. M. and D. A. Olsen (2002). Bioassay Validation of Computational Disinfection Models Used for UV Reactor Design and Scale-Up. WEF Disinfection 2002 Conference Proceedings, St. Petersburg, FL.

Prescott, L. M., J. P. Harley and D. A. Klein (1996). *Microbiology*. Dubuque, IA: Wm. C. Brown Publishers.

Qualls, R. G., M. H. Dorfman and J. D. Johnson (1989). Evaluation of the Efficiency of Ultraviolet Disinfection Systems. *Wat. Res.*, 23(3): 317-325.

Qualls, R. G., M. P. Flynn and J. D. Johnson (1983). The Role of Suspended Particles in Ultraviolet Disinfection. *J. WPCF*, 55(10): 1280-1285.

Qualls, R. G. and J. D. Johnson (1983). Bioassay and Dose Measurement in UV Disinfection. *Appl. Environ. Microbiol.*, 45(3): 872-877.

Qualls, R. G. and J. D. Johnson (1985). Modeling and Disinfection Efficiency of Ultraviolet Disinfection Systems. *Wat. Res.*, 19(8): 1039-1046.

Ransome, M. E., T. N. Whitmore and E. G. Carrington (1993). Effect of Disinfectants on the Viability of *Cryptosporidium parvum* Oocysts. *Water Supply*, 11(1): 75-89.

Rauth, A. M. (1965). The Physical State of Viral Nucleic Acid and the Sensitivity of Viruses to Ultraviolet Light. *Biophyisical J.*, 5(3): 257-273.

Reese, R. L. (2000). *University Physics*. Pacific Grove, CA: Brooks/Cole Publishing Company.

Rice, E. W. and J. C. Hoff (1981). Inactivation of *Giardia lamblia* Cysts by Ultraviolet Irradiation. *Applied and Environmental Microbiology*, 42(3): 546-547.

Sethi, V., P. Patniak, C. R. Biswas and E. W. Rice (1997). Evaluation of Optical Detection Methods for Waterborne Suspensions. *J. Am. Water Works Assoc.*, 89(2): 98-112.

Severin, B. F., M. T. Suidan and R. S. Engelbrecht (1983). Effects of Temperature on Ultraviolet Light Disinfection. *Environ. Sci. Technol.*, 17(12): 717-721.

Severin, B. F., M. T. Suidan and R. S. Engelbrecht (1983). Kinetic Modeling of U.V. Disinfection of Water. *Wat. Res.*, 17(11): 1669-1678.

Sommer, R. and A. Cabaj (1993). Evaluation of the Efficiency of a UV Plant for Drinking Water Disinfection. *Wat. Sci. Tech.*, 27(3-4): 357-362.

Sommer, R., A. Cabaj, W. Pribil and T. Haider (1997). Influence of Lamp Intensity and Water Transmittance on the UV Disinfection of Water. *Wat. Sci. Tech.*, 35(11-12): 113-118.

Sommer, R., A. Cabaj, D. Schoenen, J. Gebel, A. Kolch, A. H. Havelaar and F. M. Schets (1995). Comparison of Three Laboratory Devices for UV-Inactivation of Microorganisms. *Wat. Sci. Tech.*, 31(5-6): 147-156.

Tree, J. A., M. R. Adams and D. N. Lees (1997). Virus Inactivation During Disinfection of Wastewater By Chlorination and UV Irradiation and the Efficacy of F+ Bacteriophage as a Viral Indicator. *Wat. Sci. Tech.*, 35(11-12): 227-232.

van Duin, J. (1988). The Single-Stranded RNA Bacteriophages. *The Bacteriophages*. R. Calendar. New York: Plenum Press. 1: 117-168.

Viessman, W. J. and M. Hammer (1993). *Water Supply and Pollution Control*. New York, NY: Harper Collins College Publishers.

von Sonntag, C. and H. P. Schuchmann (1992). UV Disinfection of Drinking Water and By-Product Formation-Some Basic Considerations. *Aqua*, 41(2): 67-74.

Weaden, A. (2002). Water and Wastewater Operations, City of Kelowna Works and Utilities, Kelowna, B.C., Personal Communication.

Wiedenmann, A., B. Fischer, U. Straub, C.-H. Wang, B. Flehmig and D. Schoenen (1993). Disinfection of Hepatitis A Virus and MS2 Coliphage in Water by Ultraviolet Irradiation: Comparison of UV-Susceptibility. *Wat. Sci. Tech.*, 27(3-4): 335-338.

Wilson, B. R., P. F. Roessler, E. Van Dellen, M. Abbaszadegan and C. P. Gerba (1992). Coliphage MS-2 as a UV Water Disinfection Efficacy Test Surrogate for Bacterial and Viral Pathogens. Proceedings of The Water Quality Technology Conference, Toronto, ON.

Wright, H. B. (2001). Understanding Reduction Equivalent Dose with UV Disinfection Reactors. *IUVA News*, 3(6): 16-20.

Wright, H. B., W. L. Cairns and G. Sakamota (1999). *UV Dose Requirements and Reactor Validation*. London, ON: Trojan Technologies Inc.

Yip, R. W. and D. E. Konasewich (1972). Ultraviolet Sterilization of Water - Its Potential and Limitations. *Wat. Pollut. Contr.*, 14(4): 14-21.

APPENDIX A: INFORMATION RELATED TO COLLIMATED BEAM UV DOSE-INACTIVATION EXPERIMENTS

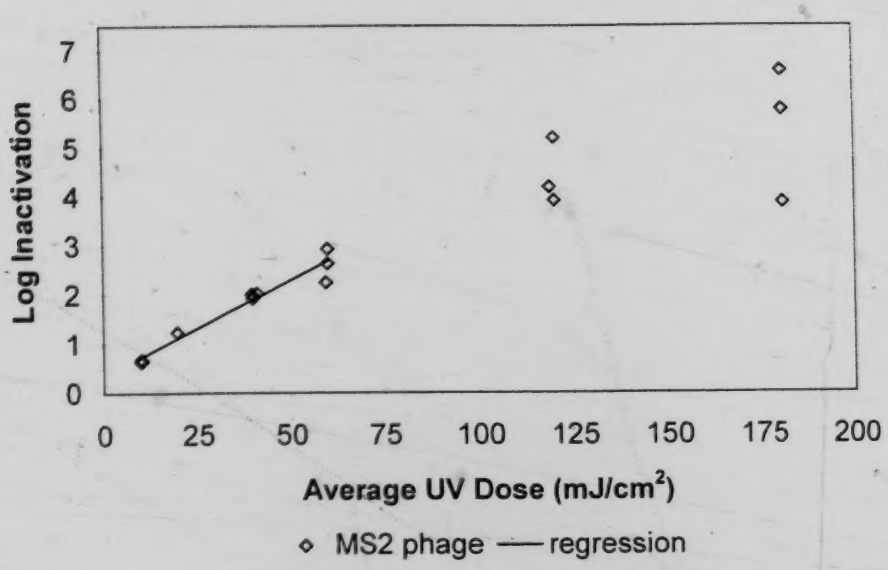

Figure A- 1: UV dose-inactivation relationship determined in collimated beam experiments for MS2 phage showing individual trial data points (phase 1).

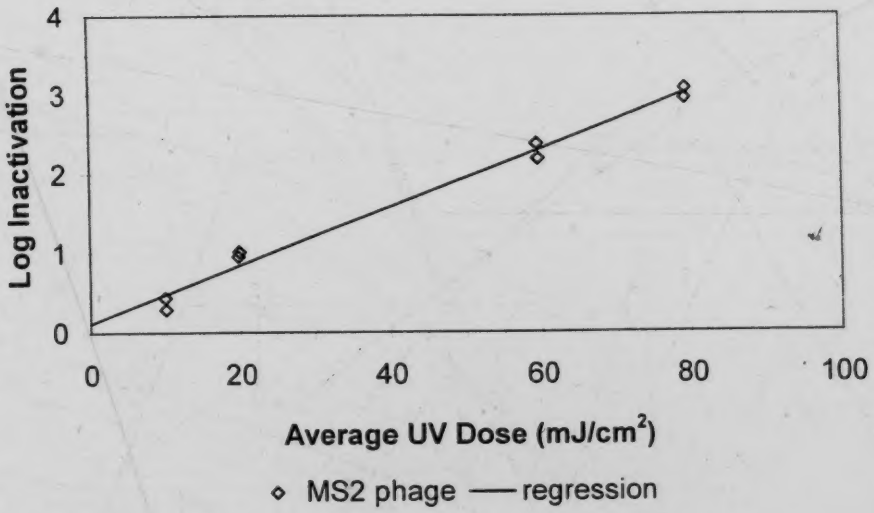

Figure A- 2: UV dose-inactivation relationship determined in collimated beam experiments for MS2 phage showing individual trial data points (phase 2).

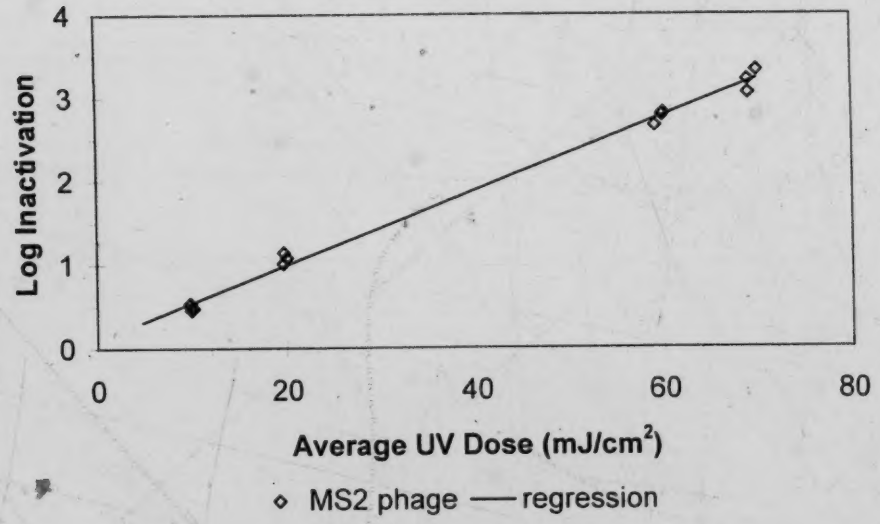

Figure A- 3: UV dose-inactivation relationship determined in collimated beam experiments for MS2 phage showing individual trial data points (phase 3).

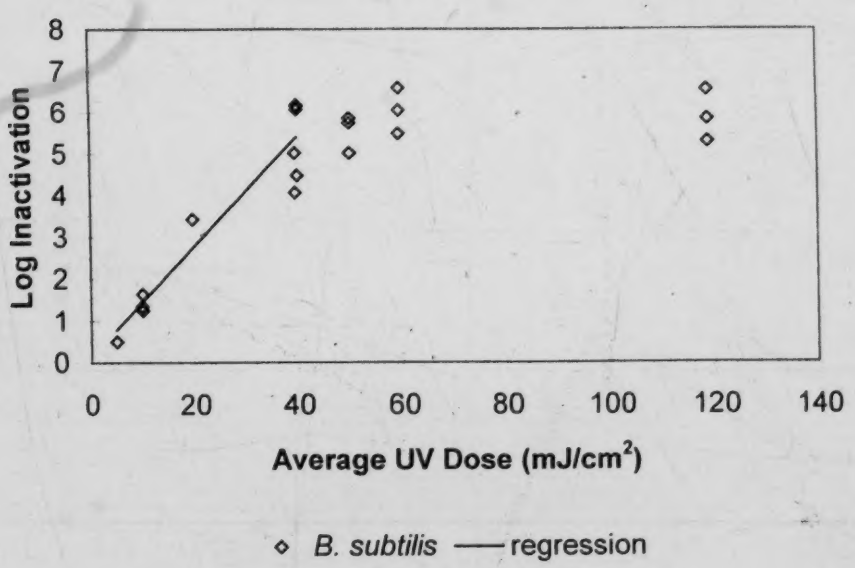

Figure A- 4: UV dose-inactivation relationship determined in collimated beam experiments for *B. subtilis* showing individual trial data points and tailing (phase 1).

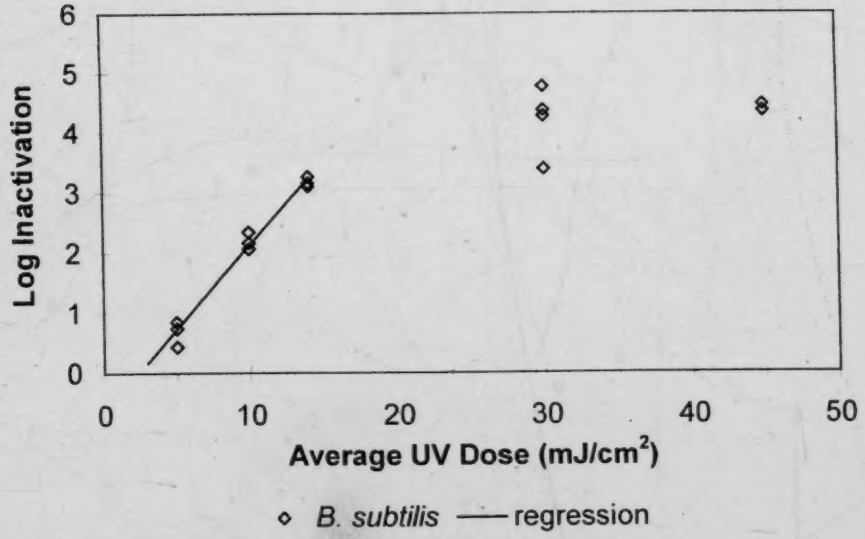

Figure A- 5: UV dose-inactivation relationship determined in collimated beam experiments for *B. subtilis* showing individual trial data points and tailing (phase 2).

Table A- 1: Inactivation of MS2 phage suspended in unaltered Lake Okanagan water and exposed to UV radiation in a collimated beam apparatus (phase 1).

Applied UV Dose (mJ/cm^2)	N_0 (pfu/mL)	N (pfu/mL)	- Log N/N_0	± 95% Conf. Interval
10.0	2.12E+07	4.48E+06	0.68	0.25
10.3	2.37E+07	5.38E+06	0.65	0.29
9.9	2.37E+07	5.48E+06	0.64	0.25
19.7	2.12E+07	1.23E+06	1.24	0.22
39.7	2.12E+07	2.13E+05	2.00	0.25
40.0	2.37E+07	2.92E+05	1.92	0.34
40.0	2.37E+07	2.77E+05	1.93	0.21
41.0	3.01E+07	2.87E+05	2.02	0.25
59.5	2.12E+07	1.23E+05	2.24	0.33
60.0	2.37E+07	5.58E+04	2.63	0.20
60.0	2.37E+07	3.15E+04	2.93	0.73
118.9	2.12E+07	1.38E+03	4.19	0.20
120.1	3.01E+07	3.63E+03	3.92	0.09
120.1	3.01E+07	1.93E+02	5.19	0.70
180.6	3.01E+07	4.07E+03	3.87	0.09
180.6	3.01E+07	5.33E+01	5.77	0.47
180.6	3.01E+07	8.33E+00	6.58	0.49

Table A- 2: Inactivation of MS2 phage suspended in unaltered Lake Okanagan water and exposed to UV radiation in a collimated beam apparatus (phase 2).

Applied UV Dose (mJ/cm^2)	N_0 (pfu/mL)	N (pfu/mL)	- Log N/N_0	± 95% Conf. Interval
10.0	3.68E+06	1.90E+06	0.29	0.26
9.9	3.68E+06	1.35E+06	0.43	0.16
19.8	3.68E+06	4.13E+05	0.95	0.12
19.9	3.68E+06	3.70E+05	1.01	0.37
59.4	3.68E+06	1.63E+04	2.36	0.37
59.5	3.68E+06	2.48E+04	2.18	0.31
79.3	3.68E+06	4.28E+03	2.93	0.19
79.4	3.68E+06	3.18E+03	3.06	0.21

Table A- 3: Inactivation of MS2 phage suspended in unaltered Lake Okanagan water and exposed to UV radiation in a collimated beam apparatus (phase 3).

Applied UV Dose (mJ/cm^2)	N_0 (pfu/mL)	N (pfu/mL)	- Log N/N_0	± 95% Conf. Interval
9.9	1.07E+07	3.73E+06	0.46	0.14
9.9	1.07E+07	3.45E+06	0.49	0.46
9.8	1.13E+07	3.32E+06	0.53	0.14
10.1	1.13E+07	3.77E+06	0.48	0.24
19.8	1.07E+07	7.82E+05	1.13	0.15
19.7	1.07E+07	1.05E+06	1.01	0.21
20.1	1.13E+07	9.52E+05	1.07	0.18
59.2	1.07E+07	2.40E+04	2.65	0.26
60.1	1.13E+07	1.75E+04	2.81	0.18
60.0	1.13E+07	1.87E+04	2.78	0.06
69.1	1.07E+07	6.63E+03	3.21	0.21
69.1	1.07E+07	9.60E+03	3.05	0.17
70.0	1.13E+07	5.40E+03	3.32	0.25

Table A- 4: Inactivation of *B. subtilis* spores suspended in unaltered Lake Okanagan water and exposed to UV radiation in a collimated beam apparatus (phase 1).

Applied UV Dose (mJ/cm^2)	N_0 (cfu/mL)	N (cfu/mL)	- Log N/N_0	± 95% Conf. Interval
4.9	2.32E+06	7.53E+05	0.50	0.30
10.0	2.32E+06	5.91E+04	1.62	0.51
10.0	1.17E+06	6.83E+04	1.24	0.17
9.9	1.26E+06	5.91E+04	1.34	0.53
19.8	2.32E+06	9.92E+02	3.41	0.66
39.6	2.32E+06	3.71E+02	4.06	1.84
40.0	1.17E+06	4.03E+01	4.46	0.31
39.6	1.26E+06	1.30E+01	5.01	0.72
40.0	7.54E+06	1.31E+01	6.17	2.32
40.0	7.54E+06	7.90E+00	6.14	1.55
40.0	7.54E+06	1.36E+01	6.06	1.96
50.0	7.54E+06	7.43E+01	5.00	0.36
50.0	7.54E+06	1.08E+01	5.84	1.08
50.0	7.54E+06	2.11E+01	5.74	1.55
59.4	2.32E+06	9.85E+00	5.48	1.00
59.6	1.26E+06	3.52E-01	6.57	0.66
59.5	1.26E+06	1.13E+00	6.05	1.64
118.9	2.32E+06	1.22E+01	5.28	0.99
118.9	1.26E+06	2.25E+00	5.84	1.10
118.9	1.26E+06	4.93E-01	6.54	1.23

Table A- 5: Inactivation of *B. subtilis* spores suspended in unaltered Lake Okanagan water and exposed to UV radiation in a collimated beam apparatus (phase 2).

Applied UV Dose (mJ/cm^2)	N_0 (cfu/mL)	N (cfu/mL)	- Log N/N_0	± 95% Conf. Interval
5.0	2.13E+06	3.12E+05	0.85	0.44
5.0	2.13E+06	3.88E+05	0.74	0.31
5.0	1.46E+06	4.88E+05	0.44	0.19
9.9	2.13E+06	1.91E+04	2.06	0.44
9.9	2.13E+06	9.70E+03	2.34	0.20
10.0	1.46E+06	9.46E+03	2.16	0.44
14.0	1.46E+06	9.39E+02	3.16	0.32
14.0	1.46E+06	7.67E+02	3.26	0.61
14.0	1.46E+06	1.11E+03	3.11	0.64
30.2	2.13E+06	8.70E+02	3.39	0.15
29.7	2.13E+06	9.47E+01	4.36	0.41
29.9	1.46E+06	7.27E+01	4.27	0.44
30.0	1.46E+06	2.33E+01	4.77	0.49
44.5	2.13E+06	9.51E+01	4.35	0.20
44.5	2.13E+06	7.51E+01	4.46	0.17

Table A- 6: Summary of linear regression models performed on data from collimated beam experiments.

Phase	β_0	β_0 P-value	β_1	β_1 P-value	r^2
MS2 phage					
1	0.333	1.77E-02	0.0390	2.50E-07	0.954
2	0.115	2.19E-01	0.0365	5.51E-07	0.988
3	0.0977	4.27E-02	0.0446	4.49E-14	0.995
B. subtilis					
1	0.128	7.85E-01	0.131	1.05E-05	0.895
2	-0.675	3.15E-03	0.279	3.05E-07	0.980

APPENDIX B: INFORMATION RELATED TO UV REACTOR TRIALS PERFORMED USING MS2 PHAGE (CHAPTER 4 DATA)

Table B- 1: Summary of trials examining number of lamps in operation and flow rate using MS2 phage (phase 1).

Trial	Flow (L/min)	# Lamps in Operation	Absorbance at 254 nm (abs/ 10 mm)	UVT at 254 nm (%/ 10 mm)	Log Inactivation	RED (mJ/cm^2)	REFR (mW/cm^2)
6	378.5	0	0.063	86.5	-0.04		
12	368.7	0	0.063	86.5	N/A		
21	1852.6	0	0.062	86.7	0.10		
24	1854.5	0	0.063	86.5	N/A		
4	377.8	4	0.063	86.5	4.96	> 60	> 6.8
10	374.4	4	0.062	86.7	4.91	> 60	> 6.8
5	377.8	1	0.063	86.5	1.20	22	7.5
11	372.5	1	0.062	86.7	1.54	31	10.4
19	1776.1	4	0.063	86.5	2.07	45	19.8
22	1861.7	4	0.062	86.7	1.99	42	19.7
20	1854.5	1	0.063	86.5	0.73	10	16.9
23	1857.9	1	0.063	86.5	0.32	0	-0.6

Table B- 2: Summary of trials examining number of lamps in operation and flow rate using MS2 phage (phase 2).

Trial	Flow (L/min)	# Lamps in Operation	Absorbance at 254 nm (abs/ 10 mm)	UVT at 254 nm (%/ 10 mm)	Log Inactivation	RED (mJ/cm^2)	REFR (mW/cm^2)
11	372.3	0	0.056	87.9	0.10		
16	746.7	0	0.056	87.9	0.29		
36	1107.2	0	0.053	88.5	0.13		
9	374.4	2	0.056	87.9	2.63	69	12
30	375.8	2	0.056	87.9	2.63	69	12
32	381.2	2	0.053	88.5	2.77	73	12
10	374.4	1	0.056	87.9	1.55	39	13
31	377.9	1	0.056	87.9	1.09	27	9
33	375.9	1	0.053	88.5	1.20	30	10
14	739.7	2	0.056	87.9	1.81	46	15
26	746.7	2	0.055	88.1	1.28	32	11
39	748.8	2	0.054	88.3	1.85	48	16
15	746.7	1	0.056	87.9	0.42	8	6
27	745.3	1	0.056	87.9	0.08	-1	-1
40	743.1	1	0.054	88.3	0.20	2	1
20	1102.3	2	0.056	87.9	1.09	27	13
34	1109.1	2	0.053	88.5	0.39	8	4
41	1121.2	2	0.054	88.3	1.02	25	13
21	1105.8	1	0.055	88.1	0.12	0	0
35	1107.2	1	0.053	88.5	0.02	-3	-3
42	1110.6	1	0.054	88.3	0.34	6	6

Table B- 3: Summary of inactivation data and associated error for trials using MS2 phage (phase 1).

Trial	Average N_0 (pfu/mL)	Average N (pfu/mL)	Log Inactivation	Standard Error (log N_0)	Standard Error (log N)	± 95% C.I. (log N/N_0)
4	6.45E+04	< 1.43E+00	4.52	0.02	N/A	N/A
5	5.75E+04	3.69E+03	1.20	0.01	0.03	0.08
6	5.58E+04	6.19E+04	-0.04	0.03	0.02	0.18
10	5.92E+04	1.11E+00	4.91	0.04	0.00	0.18
11	3.88E+04	1.20E+03	1.54	0.00	0.06	0.14
19	1.78E+05	1.57E+03	2.07	0.03	0.04	0.24
20	2.27E+05	4.26E+04	0.73	0.02	0.02	0.11
21	1.02E+05	8.29E+04	0.10	0.04	0.04	0.26
22	5.48E+04	6.06E+02	1.99	0.02	0.05	0.19
23	5.67E+04	2.72E+04	0.32	0.03	0.02	0.18

Table B- 4: Summary of inactivation data and associated error for trials using MS2 phage (phase 2).

Trial	Average N_0 (pfu/mL)	Average N (pfu/mL)	Log Inactivation	Standard Error (log N_0)	Standard Error (log N)	± 95% C.I. (log N/N_0)
9	6.08E+03	1.42E+01	2.63	0.0294	0.0266	0.195
10	2.00E+04	5.66E+02	1.55	0.0000	0.0115	0.027
11	1.55E+04	1.22E+04	0.10	0.0479	0.0385	0.313
14	2.02E+04	3.13E+02	1.81	0.0435	0.0146	0.225
15	2.35E+03	9.05E+02	0.42	0.0478	0.0300	0.283
16	5.78E+03	3.02E+03	0.29	0.0193	0.0324	0.166
20	6.08E+03	4.99E+02	1.09	0.0000	0.0095	0.030
21	4.88E+03	3.66E+03	0.12	0.0195	0.0360	0.184
26	4.00E+03	2.11E+02	1.28	0.0000	0.0117	0.037
27	2.72E+03	2.28E+03	0.08	0.0388	0.0160	0.212
30	1.77E+04	4.14E+01	2.63	0.0159	0.0253	0.139
31	4.73E+03	3.80E+02	1.09	0.0217	0.0080	0.119
32	1.43E+04	2.43E+01	2.77	0.0000	0.0150	0.042
33	9.65E+03	6.11E+02	1.20	0.0068	0.0264	0.154
34	1.06E+03	4.30E+02	0.39	0.0061	0.0087	0.047
35	6.58E+03	6.36E+03	0.02	0.0481	0.0259	0.678
36	8.37E+03	6.13E+03	0.13	0.0091	0.0058	0.055
39	2.52E+04	3.57E+02	1.85	0.0000	0.0105	0.029
40	4.93E+03	3.16E+03	0.20	0.0052	0.0270	0.097
41	1.78E+04	1.69E+03	1.02	0.0061	0.0251	0.142
42	9.93E+03	4.62E+03	0.34	0.0110	0.0161	0.098

APPENDIX C: INFORMATION RELATING TO UV REACTOR TRIALS PERFORMED USING *B. SUBTILIS* (CHAPTER 4 DATA)

Table C- 1: Summary of trials examining the effects of flow rate and number of lamps in operation using *B. subtilis* spores (phase 1).

Trial	Flow (L/min)	# Lamps in Operation	Absorbance at 254 nm (abs/ 10 mm)	UVT at 254 nm (%/ 10 mm)	Log Inactivation	RED (mJ/cm^2)	REFR (mW/cm^2)
3	379.3	0	0.063	86.5	0.02		
9	377.8	0	0.063	86.5	0.15		
15	1844.2	0	0.063	86.5	-0.11		
18	1857.9	0	0.063	86.5	-0.03		
1	379.3	4	0.063	86.5	> 5.60[a]	> 40	> 3.4
7	371.0	4	0.063	86.5	> 5.64[a]	> 40	> 3.3
2	381.2	1	0.062	86.7	3.09	23	7.7
8	374.4	1	0.063	86.5	3.51	26	8.7
13	1840.8	4	0.063	86.5	4.29	32	14.5
16	1857.9	4	0.063	86.5	4.52	33	15.5
14	1852.6	1	0.063	86.5	0.95	6	10.4
17	1859.4	1	0.064	86.3	0.77	5	8.2

[a] plate counts beyond quantitation

Table C- 2: Summary of trials examining the effects of flow rate and number of lamps in operation using *B. subtilis* spores (phase 2).

Trial	Flow (L/min)	# Lamps in Operation	Absorbance at 254 nm (abs/ 10 mm)	UVT at 254 nm (%/ 10 mm)	Log Inactivation	RED (mJ/cm^2)	REFR (mW/cm^2)
3	386.1	0	0.057	87.7	-0.37		
6	1114.1	0	0.057	87.7	-0.02		
19	748.8	0	0.056	87.9	-0.04		
1	382.7	2	0.057	87.7	> 6.04[a]	> 14	> 2.4
12	377.9	2	0.056	87.9	> 5.68[a]	> 14	> 2.4
28	379.2	2	0.056	87.9	> 5.74[a]	> 14	> 2.4
2	377.9	1	0.057	87.7	3.24	14	5
13	381.3	1	0.056	87.9	2.96	13	4
29	375.8	1	0.056	87.9	3.88	> 14	> 4.7
7	741.8	2	0.057	87.7	disturbed		
17	746.7	2	0.056	87.9	4.54	> 14	> 5.0
24	750.2	2	0.056	87.9	4.61	> 14	> 5.1
8	753.6	1	0.057	87.7	2.33	11	7
18	743.2	1	0.056	87.9	2.38	11	7
25	748.8	1	0.056	87.9	2.13	10	7
4	1109.3	2	0.057	87.7	disturbed		
22	1109.3	2	0.056	[illegible]	3.11	14	7
37	1109.1	2	0.053	88.5	3.70	> 14	> 7.0
5	1110.3	1	0.057	87.7	1.51	8	8
23	1098.9	1	0.056	87.9	1.67	8	8
38	1110.6	1	0.054	88.3	1.70	9	9

[a] plate counts beyond quantitation

Table C- 3: Summary of inactivation data and associated error for trials using *B. subtilis* spores (phase 1).

Trial	Average N_0 (cfu/mL)	Average N (cfu/mL)	Log Inactivation	Standard Error (log N_0)	Standard Error (log N)	± 95% C.I. (log N/N_0)
1	3.44E+03	0.00E+00	> 5.60[a]	0.05	N/A	N/A
2	1.16E+03	8.39E-01	3.09	0.16	0.05	0.90
3	1.30E+03	1.25E+03	0.04	0.15	0.17	1.36
7	3.22E+03	0.00E+00	> 5.64[a]	0.06	N/A	N/A
8	4.93E+03	1.54E+00	3.51	0.02	0.04	0.25
9	4.84E+03	3.26E+03	0.15	0.10	0.03	0.55
13	1.42E+03	6.90E-02	4.29	0.16	0.12	1.20
14	2.54E+03	2.72E+02	0.95	0.11	0.02	0.58
15	1.81E+03	2.31E+03	-0.11	0.09	0.08	0.73
16	3.33E+03	1.01E-01	4.52	0.05	0.07	0.53
17	2.67E+03	4.56E+02	0.77	0.03	0.05	0.33
18	3.89E+03	4.15E+03	-0.03	0.04	0.04	0.35

[a] plate counts beyond quantitation

Table C- 4: Summary of inactivation data and associated error for trials using *B. subtilis* spores (phase 2).

Trial	Average N_0 (cfu/mL)	Average N (cfu/mL)	Log Inactivation	Standard Error (log N_0)	Standard Error (log N)	± 95% C.I. (log N/N_0)
1	2.85E+03	2.62E-03	> 6.04[a]	0.08	N/A	N/A
2	1.79E+03	1.07E+00	3.24	0.00	0.07	0.32
3	1.88E+03	3.96E+03	-0.37	0.14	0.04	0.76
4	3.37E+03	disturbed	N/A	0.03	N/A	N/A
5	3.15E+03	9.56E+01	1.51	0.06	0.00	0.26
6	3.30E+03	3.50E+03	-0.02	0.03	0.05	0.32
7	3.95E+03	disturbed	N/A	0.09	N/A	N/A
8	3.11E+03	1.43E+01	2.33	0.07	0.01	0.35
12	4.33E+03	9.09E-03	> 5.68[a]	0.06	N/A	N/A
13	5.47E+02	5.98E-01	2.96	0.05	0.02	0.31
17	2.44E+03	7.36E-02	4.54	0.02	0.10	0.50
18	4.30E+03	1.80E+01	2.38	0.04	0.01	0.21
19	3.60E+03	4.07E+03	-0.04	0.03	0.08	0.45
22	2.18E+03	1.71E+00	3.11	0.04	0.05	0.37
23	4.60E+03	9.89E+01	1.67	0.02	0.03	0.25
24	4.03E+03	9.96E-02	4.61	0.06	0.07	0.55
25	3.07E+03	2.29E+01	2.13	0.02	0.04	0.27
28	5.03E+03	0.00E+00	> 5.74[a]	0.06	N/A	N/A
29	2.75E+03	3.60E-01	3.88	0.01	0.03	0.22
37	3.87E+03	7.66E-01	3.70	0.05	0.04	0.39
38	4.80E+03	9.70E+01	1.70	0.01	0.05	0.24

[a] plate counts beyond quantitation

APPENDIX D: INFORMATION FROM UV REACTOR TRIALS INVOLVING MANIPULATED TURBIDITY AND UV ABSORBANCE LEVELS (CHAPTER 5 DATA)

Table D- 1: Summary of grain size distribution analysis performed on lake bottom sediment added to feed water to increase influent turbidity levels in phase 3.

Sieve Number	Sieve Opening (mm)	Retained Weight (g)	Cumulative Retained Weight (g)	Cumulative Retained Weight (%)
# 25 (710 mm)	0.710	0.0025	0.0025	0.02%
# 30 (600 mm)	0.600	0.0038	0.0063	0.05%
# 100 (150 mm)	0.150	0.0053	0.0116	0.08%
# 400 (38 mm)	0.038	6.2900	6.3016	45.59%
Pan		7.5200	13.8216	100.00%

Table D- 2: Summary of MS2 phage trials examining the influence of turbidity and UVT on log inactivation measured in challenge tests performed on the Sentinel™ UV reactor (phase 3).

Trial	Additives	Flow (L/min)	# Lamps in Operation	Average Turbidity (ntu)	Absorbance at 254 nm (abs/ 10 mm)	UVT at 254 nm (%/ 10 mm)	Log Inactivation	RED (mJ/cm^2)	REFR (mW/cm^2)
7	R	1075	0		0.053	88.5	0.06		
16	R	1060	0		0.053	88.5	0.02		
24	R	1030	0		0.055	88.1	0.11		
2	U	1067	0		0.073	84.5	0.00		
11	U	1056	0		0.075	84.1	-0.02		
12	U	1067	0		0.096	80.2	-0.01		
15	T	1060	0	10.40	0.084	82.4	-0.01		
20	T	1056	0	4.59	0.067	85.7	0.04		
23	T	1030	0	9.44	0.078	83.6	-0.01		
26	UT	1064	0	3.82	0.078	83.6	0.04		
28	UT	1064	0	3.86	0.077	83.8	0.00		
30	UT	1071	0	7.75	0.102	79.1	0.03		
4	R	1071	2	0.21	0.052	88.7	1.63	34	8.7
10	R	1067	2	0.19	0.053	88.5	1.82	39	9.8
17	R	1064	2	0.19	0.053	88.5	1.65	35	8.8
1	U	1075	2	0.22	0.074	84.3	1.29	27	6.8
6	U	1086	2	0.26	0.074	84.3	1.23	25	6.6
8	U	1071	2	0.20	0.076	83.9	1.12	23	5.8
3	U	1075	2	0.18	0.093	80.7	0.88	18	4.5
5	U	1086	2	0.26	0.095	80.4	0.95	19	4.9
9	U	1067	2	0.25	0.097	80.0	0.94	19	4.8

Note: Additives: R = unaltered lake water; U = UV absorbing agent added; T = Turbidity added; and UT = UV absorbing agent and turbidity added.

Table D- 2 (continued)

Trial	Additives	Flow (L/min)	# Lamps in Operation	Average Turbidity (ntu)	Absorbance at 254 nm (abs/ 10 mm)	UVT at 254 nm (%/ 10 mm)	Log Inactivation	RED (mJ/cm^2)	REFR (mW/cm^2)
13	T	1052	2	5.10	0.07	85.1	1.39	29	7.2
18	T	1060	2	3.24	0.063	86.5	1.59	33	8.4
19	T	1049	2	3.97	0.066	85.9	1.38	29	7.1
14	T	1060	2	17.17	0.083	82.6	1.10	23	5.7
21	T	1033	2	10.38	0.084	82.4	1.33	28	6.8
22	T	1033	2	9.28	0.078	83.6	1.27	26	6.4
25	UT	1060	2	4.55	0.078	83.6	1.34	28	7.0
27	UT	1060	2	4.05	0.076	83.9	1.25	26	6.5
31	UT	1060	2	3.38	0.075	84.1	1.26	26	6.6
29	UT	1064	2	7.63	0.106	78.3	0.98	20	5.0
32	UT	1060	2	11.18	0.109	77.8	0.89	18	4.5
33	UT	1060	2	9.06	0.105	78.5	1.05	21	5.4

Note: Additives: R = unaltered lake water; U = UV absorbing agent added; T = Turbidity added; and UT = UV absorbing agent and turbidity added

Table D- 3: Summary of inactivation data and associated error for MS2 phage trials examining the influence of turbidity on UV reactor performance (phase 3).

Trial	Additives	Average N_0 (pfu/mL)	Average N (pfu/mL)	Log Inactivation	Standard Error (log N_0)	Standard Error (log N)	± 95% C.I. (log N/N_0)
1	U	8.32E+05	4.35E+04	1.29	0.0162	0.036	0.163
2	U	6.43E+05	6.48E+05	0.00	0.0224	0.026	0.164
3	U	5.33E+05	7.02E+04	0.88	0.0328	0.029	0.221
4	R	5.05E+05	1.18E+04	1.63	0.0608	0.028	0.333
5	U	7.57E+05	8.48E+04	0.95	0.0035	0.019	0.065
6	U	1.11E+06	6.55E+04	1.23	0.0040	0.027	0.091
7	R	5.85E+05	5.08E+05	0.06	0.0182	0.016	0.121
8	U	4.93E+05	3.75E+04	1.12	0.0167	0.016	0.114
9	U	7.48E+05	8.58E+04	0.94	0.0128	0.021	0.110
10	R	6.67E+05	1.02E+04	1.82	0.0126	0.016	0.097
11	U	7.53E+05	7.90E+05	-0.02	0.0310	0.013	0.166
12	U	9.88E+05	1.02E+06	-0.01	0.0190	0.013	0.115
13	T	6.18E+05	2.54E+04	1.39	0.0214	0.030	0.168
14	T	4.28E+05	3.41E+04	1.10	0.0253	0.025	0.174
15	T	6.58E+05	6.81E+05	-0.01	0.0078	0.017	0.078
16	R	4.42E+05	4.18E+05	0.02	0.0172	0.018	0.132
17	R	4.05E+05	9.04E+03	1.65	0.0311	0.015	0.174
18	T	7.88E+05	2.04E+04	1.59	0.0446	0.031	0.272
19	T	4.42E+05	1.86E+04	1.38	0.0343	0.027	0.217
20	T	7.00E+05	6.36E+05	0.04	0.0300	0.029	0.204
21	T	6.45E+05	3.03E+04	1.33	0.0134	0.022	0.114
22	T	5.97E+05	3.24E+04	1.27	0.0138	0.023	0.120
23	T	3.22E+05	3.26E+05	-0.01	0.0198	0.011	0.114
24	R	3.18E+05	2.54E+05	0.11	0.0618	0.088	0.547
25	UT	1.21E+06	5.62E+04	1.34	0.0174	0.029	0.151
26	UT	7.28E+05	6.74E+05	0.04	0.0224	0.033	0.181
27	UT	7.98E+05	4.50E+04	1.25	0.0276	0.020	0.171
28	UT	7.90E+05	7.59E+05	0.00	0.0771	0.011	0.361
29	UT	6.25E+05	6.50E+04	0.98	0.0450	0.030	0.276
30	UT	8.00E+05	7.51E+05	0.03	0.0296	0.021	0.181
31	UT	7.22E+05	3.98E+04	1.26	0.0089	0.030	0.114
32	UT	8.93E+05	1.14E+05	0.89	0.0233	0.019	0.148
33	UT	9.87E+05	8.73E+04	1.05	0.0255	0.017	0.154

Note: Additives: R = unaltered lake water; U = UV absorbing agent added;
T = Turbidity added; and UT = UV absorbing agent and turbidity added

APPENDIX E: WATER QUALITY ANALYSIS RESULTS FOR UV REACTOR TRIALS

Table E- 1: Detailed summary of water quality analysis (phase 1).

Parameter/Date	17-Jul-01		18-Jul-01		18-Jul-01	
Flow (L/min)	380		380		1900	
# Lamps on	4		1		4	
	Influent	Effluent	Influent	Effluent	Influent	Effluent
pH	8.60	8.60	8.45	8.45	8.46	8.50
Alkalinity-Total (mg/L as $CaCO_3$)	113	112	110	112	110	111
Hardness-Total (mg/L as $CaCO_3$)	122	120	120	119	120	122
Turbidity (ntu)	0.379	0.339	0.314	0.313	0.342	0.306
UV absorbance (at 254nm)	0.062	0.062	0.062	0.062	0.06	0.059
Colour (Pt-Co units)	10	10	9	9	8	7
Sulphate (mg/L SO_4^-)	34.9	33.7	34.2	33.8	34.6	35.4
Chloride (mg/L Cl^-)	3.68	3.20	3.90	3.72	3.71	3.79
Total Coliform (cfu/ 100 mL)	28.8	0	12.4	0	27.1	0
E. Coli (cfu/ 100 mL)	1	0	1	0	0	0
Enterococcus (cfu/ 100 mL)	0	0	0	0	1	0
Heterotrophic (cfu/ 100 mL)	322.5	22	-	-	120	20

Table E- 1 (continued)

Parameter/Date	19-Jul-01		19-Jul-01	
Flow (L/min)	1900		1900	
# Lamps on	1		4	
	Influent	Effluent	Influent	Effluent
pH	8.50	8.50	8.40	8.40
Alkalinity-Total (mg/L as $CaCO_3$)	110	110	110	112
Hardness-Total (mg/L as $CaCO_3$)	121	120	120	122
Turbidity (ntu)	0.312	0.282	0.317	0.32
UV absorbance (at 254nm)	0.059	0.059	0.059	0.058
Colour (Pt-Co units)	8	7	8	8
Sulphate (mg/L SO_4^-)	34.2	34.7	34.7	33.9
Chloride (mg/L Cl^-)	3.93	3.63	3.73	3.51
Total Coliform (cfu/ 100 mL)	4.2	1	8.7	0
E. Coli (cfu/ 100 mL)	0	0	0	0
Enterococcus (cfu/ 100 mL)	0	0	1	1
Heterotrophic (cfu/ 100 mL)	740	360	>740	300

Table E- 2: Detailed summary of water quality analysis (phase 2).

Parameter/Date	25-Sep-01		26-Sep-01		27-Sep-01	
Flow (L/min)	380		380		1140	
# Lamps on	0		2		2	
	Influent	Effluent	Influent	Effluent	Influent	Effluent
pH	8.52	8.52	8.50	8.50	8.52	8.52
Alkalinity-Total (mg/L as $CaCO_3$)	110	112	111	110	110	110
Hardness-Total (mg/L as $CaCO_3$)	120	121	120	120	120	120
Turbidity (ntu)	0.512	0.547	0.368	0.429	0.407	0.343
UV absorbance (at 254nm)	0.058	0.057	0.057	0.056	0.056	0.056
Colour (Pt-Co units)	8	8	7	7	7	7
Sulphate (mg/L SO_4^-)	32.8	34.4	33.3	34.1	33.2	32.5
Chloride (mg/L Cl^-)	5.39	5.41	5.35	5.31	5.24	5.35
Total Coliform (cfu/ 100 mL)	-	-	35.4	0	37.4	0
E. Coli (cfu/ 100 mL)	-	-	0	0	0	0
Enterococcus (cfu/ 100 mL)	-	-	0	0	0	0

Table E- 2 (continued)

Parameter/Date	27-Sep-01		1-Oct-01		1-Oct-01	
Flow (L/min)	380		1140		1140	
# Lamps on	1		2		1	
	Influent	Effluent	Influent	Effluent	Influent	Effluent
pH	-	-	-	-	8.54	8.55
Alkalinity-Total (mg/L as $CaCO_3$)	-	-	-	-	114	114
Hardness-Total (mg/L as $CaCO_3$)	-	-	-	-	122	122
Turbidity (ntu)	-	-	-	-	0.481	0.521
UV absorbance (at 254nm)	-	-	-	-	0.055	0.054
Colour (Pt-Co units)	-	-	-	-	9	9
Sulphate (mg/L SO_4^-)	-	-	-	-	34	33.3
Chloride (mg/L Cl^-)	-	-	-	-	5.26	5.25
Total Coliform (cfu/ 100 mL)	49.5	0	37.3	0	-	-
E. Coli (cfu/ 100 mL)	8.6	0	1	0	-	-
Enterococcus (cfu/ 100 mL)	-	-	-	-	-	-

Table E- 3: Detailed summary of water quality analysis (phase 3).

Parameter/Date	27-Feb-02		28-Feb-02		1-Mar-02	
Flow (L/min)	1140		1140		1140	
# Lamps on	2		2		2	
Sample info:	raw water		raw water		raw water	
	Influent	Effluent	Influent	Effluent	Influent	Effluent
pH	8.00	7.99	8.01	8.00	8.18	8.17
Alkalinity-Total (mg/L as $CaCO_3$)	108	110	113	110	109	109
Hardness-Total (mg/L as $CaCO_3$)	122	124	122	121	120	121
Turbidity (ntu)	0.382	0.488	0.342	0.332	0.258	0.249
UV absorbance (at 254nm)	0.053	0.052	0.053	0.054	0.055	0.054
Colour (Pt-Co units)	5	5	6	6	6	6
Sulphate (mg/L SO_4^-)	35.7	35.3	34	34.6	35.8	34.8
Chloride (mg/L Cl^-)	3.78	3.28	3.68	3.78	5.88	5.74
Total Coliform (cfu/ 100 mL)	3.1	0	-	-	-	-
E. Coli (cfu/ 100 mL)	0	0	-	-	-	-

Table E- 3 (continued)

Parameter/Date	27-Feb-02		28-Feb-02		28-Feb-02	
Flow (L/min)	1140		1140		1140	
# Lamps on	2		0		0	
Sample info:	High absorbance water		trial 15 (T) water		Trial 20 (T) water	
	Influent	Effluent	Influent	Effluent	Influent	Effluent
pH	7.98	7.98	8.06	-	7.95	8.01
Alkalinity-Total (mg/L as $CaCO_3$)	111	113	115	-	115	112
Hardness-Total (mg/L as $CaCO_3$)	118	140	120	-	126	140
Turbidity (ntu)	0.584	0.57	-	-	1.97	-
UV absorbance (at 254nm)	0.095	0.095	0.07	-	0.62	0.061
Colour (Pt-Co units)	26	26	41	-	23	35
Sulphate (mg/L SO_4^-)	35	36.5	36.0	-	34.7	35.0
Chloride (mg/L Cl^-)	3.34	3.72	4.12	-	3.86	3.97

Table E- 3 (continued)

Parameter/Date	1-Mar-01		1-Mar-01	
Flow (L/min)	1140		1140	
# Lamps on	2		2	
Sample info:	Trial 27 (UT) water		Trial 29 (UT) water	
	Influent	Effluent	Influent	Effluent
pH	8.10	8.07	8.06	8.08
Alkalinity-Total (mg/L as $CaCO_3$)	111	110	110	109
Hardness-Total (mg/L as $CaCO_3$)	122	122	121	115
Turbidity (ntu)	4.02	4.07	7.38	7.88
UV absorbance (at 254nm)	0.076	-	0.106	-
Colour (Pt-Co units)	43	44	78	82
Sulphate (mg/L SO_4^-)	35.4	36	35.4	33.9
Chloride (mg/L Cl^-)	6.04	6.05	6.51	6.47

APPENDIX F: DETAILED SCHEMATIC OF UV TREATMENT SYSTEM

Figure F- 1: Detailed drawing of the UV treatment system installed in the City of Kelowna.

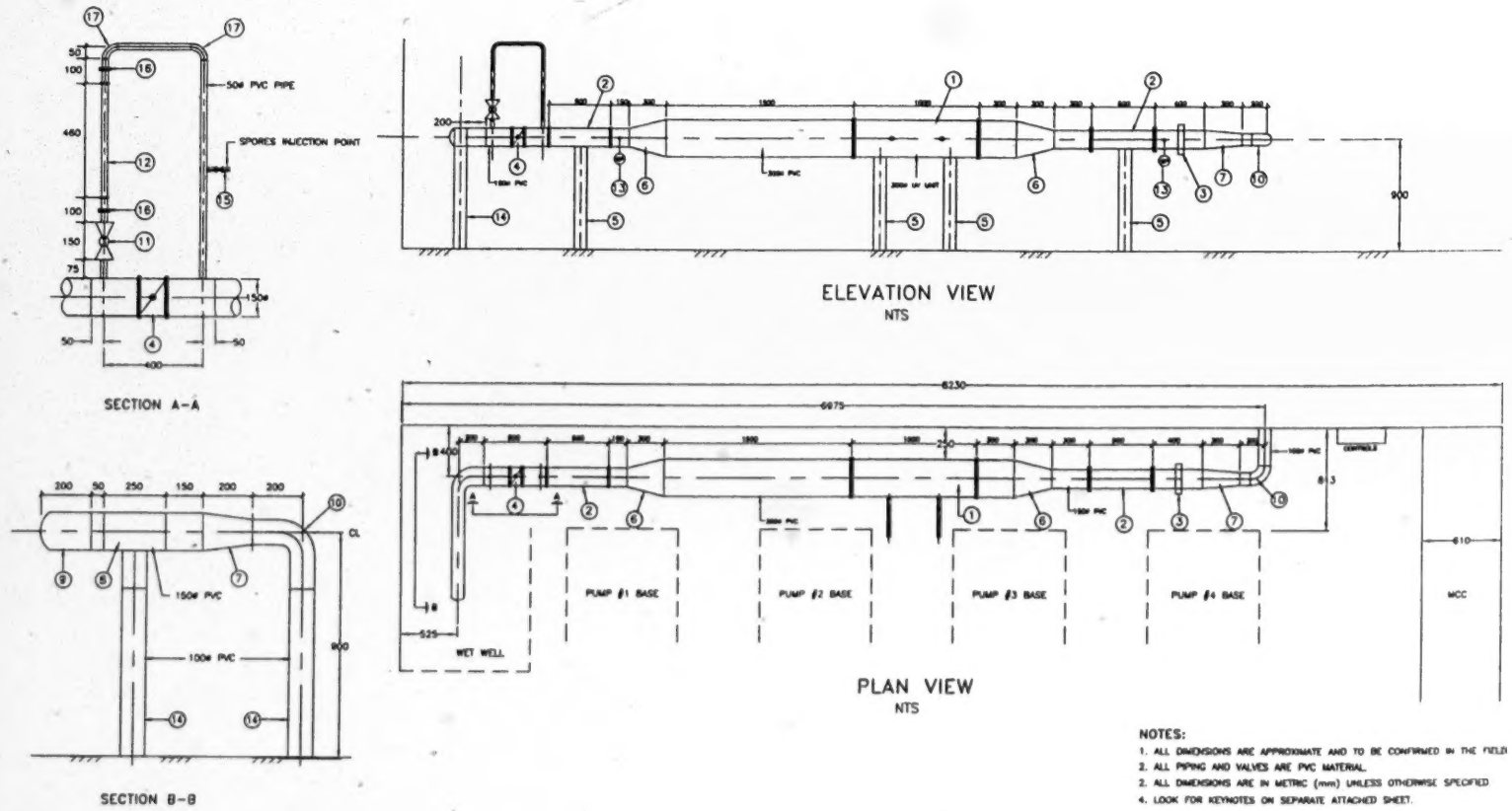

Adapted from EPCOR drawing KEL-UV-001

Note:

1. 300 mm, Calgon Carbon Corporation, model R-110, Sentinel™ UV disinfection unit
2. 150 mm static mixer – Statiflo motionless mixer, series 400, schedule 80 PVC, 1035 kPa FF flanges, two elements
3. Clamp on flow meter
4. 150 mm, manual butterfly valve
5. Pipe support
6. 300 mm x 150 mm reducer
7. 150 mm x 100 mm reducer
8. 150 mm x 100 mm tee
9. 150 mm, 90° elbow
10. 100 mm, 90° elbow
11. 50 mm ball valve
12. 50 mm rotameter, FABCO model no. F-453100LH, 20 to 380 L/min capacity
13. 15 mm sampling port with isolation ball valve
14. 100 mm, submersible pump discharge piping
15. 15 mm indicator organism injection port with isolation ball valve
16. 50 mm coupling
17. 25 mm, 90° elbow